

Subconcussion Exposure in Sport and
the Effects on Spontaneous Brain Activity
and Functional Brain Connectivity

Bryson Brugh Reynolds

Nashville, TN

B.S. Psychology

Middle Tennessee State University, 2010

A Dissertation presented to the Graduate Faculty
of the University of Virginia in Candidacy
for the Degree of Doctor of Philosophy

Neuroscience Graduate Program

University of Virginia

August, 2016

ABSTRACT

As concerns about long term effects of concussions in contact and collision sports have grown, similar concerns have started to extend to the repetitive subconcussive head impacts that athletes experience in sport. While the quantity and severity of subconcussive head impact has been studied in football for over a decade, little research has been done to quantify these head impacts in other contact and collision sports. Even less is known about the effects that subconcussive head impacts have on the brains of athletes. This dissertation contains a review of the biomechanical and neuroimaging literature related to head impact in sports. We present a quantification of the relative burden of head impact in college football, men's soccer, and men's lacrosse players. Using wearable accelerometers, it was determined that college football received the highest quantity of moderate and severe head impacts, and had the highest average impact severity. We also address whether the burden of head impacts in college football may have spatially heterogeneous effects on functional connectivity in the brains of college football players. Subconcussive head impacts may not be entirely benign, but their effects on brain connectivity are still controversial. Using mass-univariate and multivariate analyses, the results indicate that the subconcussive head impact load in college football seems to be sufficient to affect local functional connectivity and low-frequency fluctuations in the brain, and that these effects are be spatially heterogeneous. In total, this dissertation presents novel comparison of subconcussive head impact in different college men's sports, and indicates that the subconcussive burden in college football may be sufficient to produce spatially heterogeneous changes in the brain.

TABLE OF CONTENTS

Abstract	ii
Table of Contents	iii
Dedication	v
List of Abbreviations	vi
Introduction	1
Chapter I: Background	
<i>Background for Biomechanics</i>	8
<i>Background for Magnetic Resonance Imaging</i>	14
Chapter II: Quantification of Head Impact in Contact and Collision Sports	
<i>Introduction</i>	23
<i>Methods</i>	24
<i>Results</i>	30
<i>Table 1. Summary for Each Subject’s Captured Athletic Events</i>	35
<i>Figure 1. Average Quantity and Severity of Impacts</i>	37
<i>Figure 2. Impacts per Practice at Multiple Thresholds</i>	38
<i>Figure 3. Impacts per Game at Multiple Thresholds</i>	39
<i>Figure 4. Impact Burden per Athletic Exposure</i>	40
<i>Table 2. Ratio of Mean Impacts per Practice at Multiple Thresholds</i>	41
<i>Table 3. Ratio of Mean Impacts per Game at Multiple Thresholds</i>	46
<i>Table 4. Summary for each subject’s captured athletic events – All Games Included</i>	50
<i>Figure 5. Average Quantity and Severity of Impacts per Game – All Games Included</i>	52
<i>Figure 6. Impacts per Game with Respect to Multiple Thresholds – All Games Included</i>	53
<i>Figure 7. Impact Burden per Game – All Games Included</i>	54
<i>Table 5. Ratio of Mean Impacts per Game at Multiple Thresholds – All Games Included</i>	55
<i>Discussion</i>	59

Chapter III: Effects of Subconcussion on the Functional Activity and Connectivity in the Brain

<i>Introduction</i>	67
<i>Methods</i>	71
<i>Results</i>	78
<i>Figure 8. Analysis Framework</i>	81
<i>Table 6. SVM Accuracies and P-values</i>	82
<i>Figure 9. SVM Confusion Matrix and Prediction Graph</i>	83
<i>Figure 10. Histogram for Ranking Distance Permutation</i>	84
<i>Table 7. Ranking Distance for Each Group's comparison of T_{ROI} and W_{ROI}</i> <i>Rankings</i>	85
<i>Figure 11. Region Average Metric Difference Maps for $fALFF$ and $ReHo$</i>	86
<i>Figure 12. College Football $ALFF$, $fALFF$, $ReHo$, and DC Trends for Each</i> <i>Region</i>	87
<i>Figure 13. Control Group's $ALFF$ and $fALFF$ Trends for Each Region</i>	88
<i>Table 8. Ranking Distance for Comparisons Between College Football's</i> <i>Metrics</i>	89
<i>Table 9. Ranking Distance for Comparisons Between Groups for $ALFF$ and</i> <i>$fALFF$</i>	89
<i>Table 10. Region Rankings for College Football Players' $ALFF$</i>	90
<i>Table 11. Region Rankings for College Football Players' $fALFF$</i>	92
<i>Table 12. Region Rankings for College Football Players' $ReHo$</i>	94
<i>Table 13. Region Rankings for College Football Players' DC</i>	96
<i>Table 14. Region Rankings for the Control Group's $ALFF$</i>	98
<i>Table 15. Region Rankings for the Control Group's $fALFF$</i>	100
<i>Discussion</i>	102
Chapter IV: Conclusions and Future Directions	110
Acknowledgements	115
References	116

DEDICATION

This dissertation, like nearly all worthwhile endeavors, is not the product of a single person. I would first like to thank my advisor, Dr. Jason Druzgal, for pushing me to produce and achieve more than I thought I could have done. While it was not always enjoyable, it was always worth the effort. I would also like to thank the other lab members who have aided in this research and been companions on this journey: Jasmine Manalel, Todd Chatlos, Riley North, Jamie Blair, Christina Gancayo, Erich Henry, Amanda Staunton, and Sauson Soldozy. I would also like to thank our research collaborators for providing assistance and feedback at critical junctures in pursuing this research: Howard Goodkin, Donna Broshek, Max Wintermark, and Jim Patrie. Without your support and guidance, this research would not have been possible. I thank my dissertation committee, Kevin Lee, Howard Goodkin, Jamie Morris, and John Lach, for their thorough critical evaluation of my research in progress and for providing advice on how to consistently improve my work.

The Neuroscience Graduate Program here at UVa has been incredibly supportive and provided essential assistance. The program directors, Bettina Winkler and Manoj Patel, have shown genuine care and concern, and the program coordinators, Tracy Mourton and Nadia Badr Cempre, have provided support and shown patience for my seemingly endless questions and concerns. The other NGP graduate students have been an unending source of encouragement. To be in the company of such brilliant people and to know that they are going through the same graduate school gauntlet as me is immensely comforting.

On a personal note, I would like to thank my parents, Roxie Reynolds and Brugh Reynolds, and my siblings, Derek Ward, Elijah Reynolds, and Beth Thielman, for their support and encouragement. I would like to thank my son, Parker, for arriving half-way through this graduate school journey. While the added sleep deprivation was not entirely welcome, he has been a constant source of joy that has brightened my life in times of stress. Lastly, I want to thank my wife. She is the most wonderful person I have met in my life, and I am so incredibly lucky to have her as my wife. Throughout this process, she has been my best friend, my counselor, my banker, my personal assistant, my role model, and the most amazing mother to Parker. I am absolutely certain that I would not have made it to graduate school, much less all the way through, without her constant love and support. I do not have the literary skill to truly express in words what she means to me and has done for me. This dissertation and everything in my life is dedicated to her, Erica Elizabeth Reynolds.

LIST OF ABBREVIATIONS

AE – athletic exposure

ALFF – amplitude of low-frequency fluctuations

CF – college football

CTE – chronic traumatic encephalopathy

DC – degree centrality

fALFF – fractional amplitude of low-frequency fluctuations

fMRI – functional magnetic resonance imaging

MC – male controls

MRI – magnetic resonance imaging

mTBI – mild traumatic brain injury

NCAA – National Collegiate Athletic Association

NFL – National Football League

OS – other sports (including soccer and lacrosse)

PRLA – peak resultant linear acceleration

PRRA – peak resultant rotational acceleration

ReHo – regional homogeneity

RoM – ratio of means

RMSE – root mean square error

rs-fMRI – resting state functional magnetic resonance imaging

RSN – resting state network

SRC – sports-related concussion

SVM – support vector machine

TBI – traumatic brain injury

INTRODUCTION

In 2005, Dr. Bennet Omalu published the first case of chronic traumatic encephalopathy (CTE) in a former National Football League (NFL) player¹⁴¹. CTE is a neurodegenerative tauopathy, previously termed dementia pugilistica or “punch drunk,” and it was thought to be restricted to boxers and not other athletes^{121,127,141}. Since then, concerns about the effects of repetitive head impacts in sports have been discussed everywhere from local school board meetings to the White House. Much of the concern has been driven by evidence that repetitive head impacts might have short-term and long-term effects on brain function and physiology. While much of the discussion has focused on sports-related concussions (SRC), the vast majority of head impacts are subconcussive, i.e. they do not result in any acute signs or symptoms. Even in the absence of a clinical concussion, there are growing concerns that multiple subconcussive hits to the head might cause damage to the brain.

One way to study subconcussive head impacts is to quantify the number and severity of head impacts in sports, using biomechanical sensors on the athletes. Most of this research has focused on American football, due to its popularity and high level head impact exposure. Chapter II of this dissertation expands the quantification of head impact to the college sports of soccer and lacrosse, and compares the burden of head impact in these sports to the well-studied sport of college football. A central goal of this research is to expand the quantification of head impact beyond football and determine the relative head impact burden of athletes in soccer and lacrosse compared to football.

The biomechanical research on head impact in football has focused on answering questions about the relative impact burden of different player positions^{23,26,45,131,163},

playing level^{40,49,163,206}, and event-types^{26,45,49}. These findings in football have led to practice and rule changes to reduce football players' burden of head impact. Expanding quantification of head impact to soccer and lacrosse could deepen the understanding of subconcussive burden in these sports, which in the future could provide data for athletes, coaches, and sport regulatory agencies to, if necessary, make changes aimed at reducing head impact. To begin this expansion into other sports, Lynall et al. (2016) collected head impact data from women's soccer that showed that practices result in fewer head impacts than in games¹¹⁵ and McCuen et al. (2015) showed that high school girls' soccer players sustain fewer impacts than college women's soccer players¹²⁶.

Biomechanical impact data in football has been primarily collected using the head impact telemetry (HIT) system⁵⁶, which consists of six accelerometers spring mounted inside the padding of a football helmet. For studies using this device in college football the mean/median number of head impacts per player per season ranged from 257 to 1354, the peak resultant linear acceleration (PRLA) per impact ranged from 20.5g to 32.0g, and the peak resultant rotational acceleration (PRRA) per impact ranged from 1355rad/s² to 2213rad/s²^{26,45,56,131,162,163}. As previously mentioned, these studies also addressed differences in player positions^{23,26,45,131,163}, playing level^{40,49,163,206}, and event-types^{26,45,49}.

The biomechanical research on head impacts in sport has been primarily driven by concerns about the long-term effects of multiple concussions. Most of this research either has been focused on determining the biomechanical threshold for concussive injury^{57,66,70,73,160} or has used the burden of head impact as a biomechanical proxy for relative concussion risk^{25,26,125,131,155}. The high incidence of concussion in football^{67,78,98,105,166} and the development of a helmet-based accelerometer system more

than a decade ago⁵⁶ have combined to make football the primary focus of the biomechanical head impact research up to this point.

At the same time, there has been increased interest in the effects of subconcussive impacts separate from their relationship to concussion^{20,22,49,50,74}. Other sports like soccer and lacrosse also have relatively high rates of concussion incidence^{67,78,98,105,166}, leading some to wonder if the overall burden of head impact may also be high in these sports. The recent development of biomechanical sensors that can be used in non-helmeted sports^{47,115,126} has enabled the quantification of head impact in soccer and lacrosse. We can now directly test if the burden of subconcussive head impact in soccer and lacrosse is commensurate to their high rates of concussion.

There has been no live-action biomechanical data collected in college men's soccer or lacrosse to determine if the impact burden in these sports is similar to football. For soccer, the level of subconcussive head impact burden has been inferred from studies using a helmet-based accelerometer in a laboratory setting¹³⁷, video analysis and biomechanical reconstruction²⁰⁵, and a modified helmet-based accelerometer in a controlled scrimmage⁷⁵. Similarly, the impact burden in lacrosse has been inferred from biomechanical reconstructions⁴³, and video capture of live lacrosse play^{30,104}. To perform an adequate comparison between the sports, data should be collected, cleaned, and processed in the same manner. Currently, the differences in the device settings and methodological differences in data cleaning, preprocessing, and analysis make it difficult to compare findings across studies⁹⁵.

Chapter II of this dissertation presents data collected from college football, men's soccer and men's lacrosse players, and compares quantity and severity values between

the sports. The hypothesis was that college football receives a higher number of impacts and a higher average impact severity than soccer and/or lacrosse. Results showed that college football players experienced the most or second-most impacts per athletic event depending on event-type and severity of impact. Football also resulted in the highest average peak resultant linear and rotational acceleration per impact, and highest cumulative linear and rotational acceleration per athletic event. For average peak resultant linear and rotational acceleration per individual impact, college football was followed by college lacrosse and then college soccer, with similar trends in both practices and games. While the absolute accuracy of the sensor used in this study needs further validation, the results strongly suggest that college football players experience a categorically higher burden of head impact compared to soccer and lacrosse.

Repetitive head impacts in sports have been linked to long-term cognitive and clinical effects, particularly in retired football players who have sustained high levels of subconcussive impact and who have often had multiple concussions over their careers. Lehman et al. (2012) found that while retired NFL players have lower overall mortality compared to the general population, the players had 3.9 and 4.3 times higher mortality rates for Alzheimer's disease and Amyotrophic Lateral Sclerosis (ALS)¹⁰¹. Additionally, there is a growing body of evidence that a history of repetitive brain trauma is a necessary component for developing CTE: a neurodegenerative tauopathy with emotional, cognitive, and motor symptoms^{27,127,140,181}. Concussion has received much of the blame for these effects, but it is still unknown what role subconcussive impacts play in the development of these outcomes.

While the idea of subconcussive head impacts affecting change in the brain is still controversial, there is substantial research that links subconcussive impacts to clinical, cognitive, and/or physiological effects. In the short term, subconcussive head impacts have been shown to increase susceptibility to concussion by lowering an athlete's tolerance to a subsequent concussive impact^{13,203}, and/or by a separate mechanism where concussive symptoms are the direct result of multiple subconcussive impacts^{10,14}. Subconcussive impacts have also been shown to affect cognitive performance, even in the absence of a diagnosed concussion, with Hwang et al. (2016) showing decreases in balance performance 24 hours after heading ten soccer balls⁸². Multiple studies have shown decreased task performance and have found changes in task-related brain activity using task-based functional magnetic resonance imaging (fMRI) after exposure to subconcussive impacts^{20,157,187}. Researchers have also shown subconcussion effects in resting-state fMRI (rs-fMRI) connectivity, particularly default mode network connectivity^{1,89}. Subconcussion has also been implicated in changes to brain structure, with studies showing correlations between measures of head impact and white matter structural metrics^{50,51,106}. In spite of these findings, many clinicians and researchers still consider subconcussive head impacts to be of little to no clinical relevance. Research that provides further clarity on the subconcussive impact load in sports and on the physiological mechanisms underlying these effects should increase confidence in the ability of subconcussion to produce relevant effects.

In concussion, a patient can present with any number or combination of concussion's symptoms and signs¹⁶ and heterogeneity in clinical presentation may indicate an underlying spatial heterogeneity in the brain¹⁵⁸. We believe that

subconcussion is likely to exhibit a similar spatial heterogeneity of effect as concussion. Functional MRI has shown some ability to detect changes related to subconcussion, but the locations of statistically significant changes have been inconsistent^{1,20,89,157,187}, possibly due to heterogeneity in affected areas across participants. If subconcussion does produce different spatial effects across participants, arbitrarily choosing a single task or resting state network may reduce the chances of finding a significant result. However, metrics of spontaneous brain activity and functional brain connectivity can be calculated for every grey matter voxel in the brain, allowing for analyses that survey changes across the brain without a priori selection of a subset of brain regions. These metrics have been successfully used to identify changes that occur in the brain after a concussion^{129,222-224}, and could therefore also provide a way to compare the effects of concussion to those from subconcussion. While most fMRI research relies on mass-univariate analysis methods, they perform poorly when faced with spatial heterogeneity across participants. Conversely, multivariate analysis methods are more resilient to spatial heterogeneity and may be more effective at detecting the changes that occur in response to subconcussive impacts.

Chapter III of this dissertation presents preseason and postseason rs-fMRI data collected from college football, men's soccer, and men's lacrosse players, and a group of college-age controls. Amplitude of low-frequency fluctuations (ALFF) and fractional ALFF (fALFF) were used as measures of spontaneous neural activity in the brain. Regional homogeneity (ReHo) and degree centrality (DC) were used as measures of local and global brain connectivity, respectively. ALFF, fALFF, ReHo, and DC were analyzed using mass-univariate and multivariate analyses. The hypothesis is that exposure to

repetitive subconcussive head impacts can produce spatially heterogeneous effects on brain function. To test this hypothesis, rs-fMRI data was acquired from college football players, soccer players, lacrosse players, and controls at preseason and postseason time points. For each participant at each time point, voxel-wise measures of spontaneous brain activity (ALFF/fALFF) and local (ReHo) and long-range (DC) functional connectivity were calculated. A combination of standard voxel-wise analysis and paired support vector machine (SVM) classification studied the effects of subconcussion on spontaneous brain activity and functional brain connectivity. Results from the voxel-wise analyses demonstrated no changes, but SVM classification showed changes in college football players' ALFF, fALFF, and ReHo values. Multivariate analyses also indicated changes in the control group's ALFF and fALFF values, but subsequent analysis indicated that the changes in the college football players ALFF and fALFF values demonstrated different trends than controls. This research does not directly link subconcussive impacts to these changes, but the results suggest that the effects of subconcussion may be on the same spectrum as sports-related concussion.

CHAPTER 1: BACKGROUND

BACKGROUND FOR BIOMECHANICS

One way to study concussion and subconcussion is by measuring the biomechanical properties of head impacts in sport. The most common sport in which to study this is football, because football has a high incidence of concussion, and players sustain significant numbers of subconcussive impacts^{8,105,162,220}. Early biomechanical research in football studied the effectiveness of a helmet to prevent skull fractures, subdural hematomas, and other life-threatening traumatic brain injuries. Since helmets were first introduced into football in the early 1960's, there has been concern that wearing a helmet might make the players feel invincible and exacerbate their aggressive play. In support of this, Clarke et al. (1998) showed that the incidence of head and neck fatality rose after the mass implementation of helmets in football³⁹. While fatalities have dropped considerably since then, many experts think that as football players have become bigger and faster they also hit harder than their predecessors.

In response to concerns about the short-term and long-term effects of SRC, the NFL formed a committee on mild traumatic brain injury (mTBI)¹⁴⁶. In 2003, the NFL mTBI Committee started publishing a series of experiments studying the biomechanical properties of concussion by reconstructing concussive and non-concussive impacts from video analysis^{147-149,194-198}. It represents a significant conflict of interest for the NFL to commission research on concussions and the studies have received criticism regarding many of their conclusions¹³⁹. However, these studies proved useful to prime future research and resulted in some interesting observations about concussions. For example, football players will frequently line up their head, neck, and torso while in the act of

tackling and lead with their helmeted head to deliver maximum force by increasing the effective weight behind their impact and distributing the force they experience¹⁹⁴. This is one reason why, in open field tackles, the striking player sustains concussion at a much lower rate than the player who is struck, and why tackling is responsible for 67.7% of concussions in football^{149,194}. While these observations resulted in rule changes regarding helmet-to-helmet impacts in the NCAA and the NFL (for example, the elimination of “spearing”), video reconstruction was insufficient to characterize the biomechanical causes of concussion.

In 2005, Duma et al. published the first study to use the head impact telemetry (HIT) system to analyze impacts sustained by college football players. The HIT system is a helmet-based accelerometers system that is used to measure the acceleration of an athlete's head as they participate in live-action practice and game events⁵⁶. The accelerometers are spring-mounted inside the padding of the helmet as to maintain contact with the player's head during an impact, to ensure that the sensors measure the acceleration of the head as opposed to the acceleration of the helmet¹¹⁸. This technology was quickly implemented by several research teams and has become a significant source of data on the biomechanics of head impact in football. The HIT system's integration into required equipment allowed quantification of head impact in football to be easily deployed to teams across the country, leading to a rapid expansion of live play biomechanical impact data in football.

Soon it became evident that not all football players experience impacts in the same location, severity, or quantity, and differences could be seen in between practices and games, player positions, and levels of competition. For instance, football players

experience twice the number of impacts during a game as they do during practice, and game impacts are on average more severe^{26,45}. When it comes to differences in playing position, linemen receive 1.5-2 times the number of impacts as other positions. However, skill players (quarterback, offensive back, defensive back, etc.) receive more high impact hits (>60G) than linemen, and running backs sustain the highest impacts overall^{23,26,45,131,163}. In regard to playing level differences, college players have higher average impact severities and sustain more high impact hits (>60g) than high school players in similar positions¹⁶³. For youth football, high impact hits are infrequent, but do still occur^{40,49,206}. In contrast to higher levels of competition, youth football players experience more impacts during practice than during games, and nearly all of their high severity hits occur during practice⁴⁹. These findings have led to changes in practice regulations, heads-up tackling interventions, and a movement to raise the minimum age for tackling in youth football.

In addition to these findings, many research groups tried to identify a biomechanical threshold for concussion^{23,25,142,149,160,220}. Many thresholds for concussion have been proposed: developed from data from the HIT system, impact reconstruction, or computer simulations. The published peak resultant linear acceleration (PRLA) thresholds range from 70-106g^{23,25,72,149,220}; and the peak resultant rotational acceleration (PRRA) thresholds range from 4,500-7,900 radians per second² (rad/s²)^{23,142,160,220}. At first glance, these thresholds seem reasonable with the distribution of head accelerations in football impacts highly positively skewed with only 3-4% of impacts exceeding 80G¹³¹ and since the average concussive PRLA and PRRA values are similar at 81-105g and 5312-7230rad/s^{222,25,56,73,149,197,220}. However, concussions occur at varying impact

magnitudes and impacts that exceed these values rarely result in a diagnosed concussion⁷³, and it has been reported that less than 0.5% of >80g impacts result in a diagnosed concussion^{56,73,131,163}. This has led to speculation that players may have a unique threshold based on their own physiological characteristics^{23,70}.

Part of the difficulty in defining an accurate threshold may be due to subconcussive impacts. There is evidence to support that the accumulation of subconcussive impacts makes an athlete more susceptible to sustain a concussion, or that repetitive impacts cause injury in the absence of single severe impact^{22,131,155}. To this point, Beckwith et al. (2012 and 2013) noted that several athletes developed concussive symptoms hours after they sustained a significant impact, whereas concussion symptoms usually immediately succeed the concussive impact^{13,14}. Concussed athletes were separated into two groups: those who were diagnosed immediately and those with a delayed diagnosis. Altogether, both groups had more impacts on days with a concussion diagnosis than on days without an injury, indicating that the increased number of impacts may have played a role making the athletes more susceptible to concussion. Furthermore, they found that players with an immediate diagnosis sustained a higher peak PRLA than those with a delayed diagnosis, 112g versus 103g, and players with a delayed diagnosis received more impacts above the 50th percentile of impact severity on the day and week preceding the concussion than those who were immediately diagnosed^{13,14}. This discrepancy in injury presentation indicates that subconcussive impacts modify susceptibility to subsequent concussion, and/or that multiple subconcussive impacts can result in a concussion in the absence of a single concussive impact. With more players receiving a delayed diagnosis than an immediate diagnosis, with a reported ratio of 4:3,

this pathway to concussion may actually be more common than concussion resulting from a single impact^{13,14}. This research suggests that subconcussive head impacts may not be benign events, but may cause subclinical damage that can accumulate.

While this research has revealed many important aspects concerning the biomechanical properties of concussion, answers to many important questions remain elusive, for example the biomechanical threshold for concussion. Part of the reason for this may be due to some of the inherent limitations in this research. First, in recent years there have been several concerns raised about the accuracy of the HIT system. The first concern is with the methods used to validate the HIT system. The initial HIT system was only validated for impacts up to 50g, but used to record impacts in excess of 100g¹¹⁸. The second generation HIT system was validated with higher impacts, but the helmet that was used to validate the HIT system was too small for proper fit on the headform, leading to a tight fit that is not reflective of the way that football players wear their helmets^{12,47,84,161}. Taking these and other issues into account, validation studies have shown the root mean square errors (RMSE) for the HIT system are 11%-198% for PRLA and 27%-208% for PRRA, and varies with impact location^{13,47,84}. These issues do not invalidate the studies using the HIT system, and every biomechanical sensor deployed in live play athletic events has non-trivial error rates^{47,208}. However, these issues should be considered when designing future biomechanical studies and when interpreting data from these sensors.

While football receives the most attention for head impacts and concussion, there is growing recognition that these issues may also be present in other contact and collision sports, like soccer and lacrosse. Soccer is the most popular sport in the world and lacrosse is one of the most rapidly growing contact sports in the United States, and have the third

and fourth highest concussion rates in men's collegiate sports, respectively⁷⁸. Soccer and lacrosse players have a higher concussion incidence than their counterparts in basketball, field hockey, wrestling, track & field, and baseball^{42,105,119,211}. It is unknown if the number or average severity of subconcussive head impacts follows the same incidence pattern as concussion, and frequency and severity of subconcussive head impact has not been directly measured in men's collegiate soccer and lacrosse. Some studies have attempted to quantify the severity of head impact in soccer and lacrosse, but much like the early research into head impact in football, most of these measurements have occurred outside live play situations. For soccer, helmet-based accelerometers have measured header acceleration in a laboratory setting¹³⁷, video analysis and biomechanical reconstruction have studied head impacts caused by player contact with instrumented dummies²⁰⁵, and a modified helmet-based accelerometer has recorded head impacts in controlled scrimmages⁷⁵. For lacrosse, researchers have attempted to infer similar data from laboratory-based biomechanical reconstructions⁴³ or video capture of live lacrosse play^{30,104}. Recent advancements in biomechanical sensor miniaturization has produced accelerometers that can be worn unobtrusively to quantify head impact during live play in either helmeted or un-helmeted sports. This research uses one of these sensors: the xPatch from X2 Biosystems (Seattle, WA). The xPatch is worn on the skin covering the mastoid process and it contains a triaxial high impact linear accelerometer and a triaxial gyroscope to capture biomechanical impact data similar to the HIT system.

The quantification of head impact in football developed a greater understanding the risks and led to rule changes that have made football safer. Now, with a biomechanical impact sensor that is not helmet-based, other unhelmeted sports can

experience the same rapid expansion of knowledge that occurred with the HIT system in football. There are many open questions regarding subconcussive head impact exposure in soccer and lacrosse. The main focus of this research is: how does the quantity and severity of head impact compare between college football, soccer, and lacrosse players? With the concerns about the long-term detrimental effects of head impacts in football spreading to other contact and collision sports like soccer and lacrosse, it is important to understand the relative levels of subconcussive exposure in these sports. Each of these sports have a top five concussion incidence, but it is unknown if the level of subconcussive impact exposure these sports is also similarly high. This research attempts to quantify head impact in college football, soccer, and lacrosse and compare the number and average severity of impacts that occur in their respective practices and games. We hypothesize that the number of head impacts and their average severity will be higher for lacrosse than for soccer, but both will be substantially lower than college football. This would indicate that concussion incidence is not a good proxy measure for subconcussive impact exposure, and when it comes to subconcussive head impact in these sports, college football is exceptional.

BACKGROUND FOR MAGNETIC RESONANCE IMAGING

Neuroimaging is often used as an objective measure of neural change, damage, or degeneration in several neurological processes, diseases, and disorders. While many patients receive a computed tomography (CT) or magnetic resonance imaging (MRI) scan when they present with an mTBI, the scan's primary purpose is to eliminate the possibility of a more serious injury, for example intracranial hemorrhage or cerebral

contusion. CT and structural MRI have shown little efficacy in the evaluation of a concussion, because these techniques are only able to detect gross structural changes⁵². However, other neuroimaging techniques are better suited to directly investigate the underlying physiological effects of SRC and subconcussion. These techniques are able to detect subtle changes in brain function or structure, which makes them better suited to detect the type of changes that might occur in response to SRC and subconcussion.

Functional MRI. One such neuroimaging technique is functional magnetic resonance imaging (fMRI), which is a non-invasive imaging technique that probes neural function in the brain. Functional MRI is usually a blood oxygen level dependent (BOLD) imaging technique that uses the increase of oxygenated hemoglobin that occurs shortly after neural firing as a proxy for neural activation. When neurons fire, astrocytes detect the local release of neurotransmitters and signal the blood vessels to increase blood flow to the area, which creates a local surplus of oxygen. This excess oxygen increases the T2* magnetic resonance (MR) signal from the area^{63,111,117}. Historically, the functional deficits arising from SRC have been more readily found than structural changes, and if subconcussive impacts result in a similar functional disruption that is similar to concussion, then fMRI may also be well suited for the study of subconcussion.

The majority of fMRI research is task-based, which involves a research participant performing a specific task while fMRI data is collected. This technique measures the activation of the brain caused by performing the experimental task and results in an activation map specific to the task. These activation maps can be statistically compared between groups performing identical tasks, to identify differences in cognitive processing between the groups. The most common task in concussion and subconcussion

fMRI research is an n-back task. During the n-back task the participant is presented with a series of stimuli (letters, numbers, pictures, etc.) and is asked to respond if the current item was presented previously. The n-back task usually involves trials of 1-back, 2-back, and 3-back. For example, in the 2-back trial the participant would respond if the stimuli matched a stimuli presented 2 items previously (A-B-R-D-R). N-back tasks assess aspects of attention, working memory, and executive function, which is why it is often used as an assay for general cognitive functioning. When performing an n-back task or a similar broad task, mTBI patients have been found to experience an increase in the area of fMRI activation and/or an increase in the magnitude of activation^{36,37,60,85,99,123,124,145,175,177,218}. However, some researchers found decreases in the area of fMRI activation and/or a decrease in the magnitude of activation in those with an mTBI or SRC when compared to a control group^{33,34,36,37,60,69,184}. It is unknown whether this discrepancy in results is due to methodological differences or real differences in the populations under study.

In order to study the effects of subconcussion, Talavage et al. (2010) collected neuropsychological testing (ImPACT) and n-back fMRI data from high school football players. Before the season they collected data from all participants, and each week during the season they recollected data from 1-3 players. Using this protocol, they were able to collect in-season data from athletes who received a concussion and from more who did not. Using the neuropsychological tests, they identified players who were not diagnosed with a concussion but demonstrated functional impairment. They showed that the non-concussed but functionally impaired athletes exhibited a reduction of activation in areas associated with working memory, indicating a functional impairment in this area¹⁸⁷. A

follow up study, demonstrated that the undiagnosed yet functionally impaired athletes received 450 more impacts than those who were not functionally impaired²⁰. This indicates that subconcussive impacts result in functional impairment that separate from concussion and is not being detected by the current clinical evaluations. It also suggests that fMRI may be more sensitive to the cognitive effects of subconcussive impact than current evaluation measures.

One limitation of task-based fMRI studies is that minor changes to the task make comparisons between studies ineffectual. While many of these studies used n-back tasks, there were differences in their design; the studies used auditory or visual presentation of letters, numbers, or pictures. These minor variations in the specific task make it difficult to determine whether the differences between studies are related to the differences in methodology or whether they reflect the heterogeneity of the underlying processes²⁸. Additionally, task-based fMRI is only able to probe areas associated with the specific task. A functional method that is easily replicable across research groups and that probes more than one functional network would be better suited for the study of subconcussion.

Resting-state fMRI. Resting-state functional MRI (rs-fMRI) is a task independent method of BOLD fMRI, which lacks some of the issues of task-based fMRI. Resting-state fMRI experiments capture spontaneous low frequency (0.01-0.10 Hz) fluctuations in the BOLD signal that occurs in the absence of a task or stimulus¹⁷⁸. Biswal et al. (1995) was the first to determine the neural significance of these fluctuations and identify resting-state networks (RSN): disparate functional regions that fluctuate with temporal synchronicity¹⁰⁰. Several RSNs have been identified: default mode network (DMN)⁷¹, somatosensory network¹⁷, visual network^{11,114,151,176,212}, language network¹⁸⁹, dorsal

attention network^{62,151,167,189}, ventral attention network⁶², frontoparietal control network¹⁹⁹, and the cingulo-opercular network^{55,151}. The benefits of rs-fMRI over task-based fMRI is that, collectively, these RSNs geographically cover the majority of the cortex, assessing global features of brain function, and the absence of a task allows this technique to easily replicable across research groups. Resting-state fMRI only requires that the patient remain still and awake, thus allowing a researcher or clinician to collect data that probes the functional connectivity of various networks with one simple scan. While rs-fMRI research is still burgeoning, studies have shown high test-retest reliability in rs-fMRI data^{18,38,168,188},

Patients with mTBI and SRC show abnormal connectivity in a few resting-state networks^{88,122,136,173,174,182,188,217,225}. Participants with mTBI or SRC have shown increased RSN connectivity^{173,188}, decreased RSN connectivity^{88,136}, or both increased and decreased RSN connectivity^{122,182,217}. In studying the effects of subconcussive impacts, Johnson et al. (2014) collected rs-fMRI data from 24 college rugby players 24 hours before and after a full contact rugby game, and found changes in the functional connectivity of the DMN. Similarly, Abbas and Shenk et al. (2016) found increases and decreases in DMN connectivity in high school football players when comparing in-season and postseason time points to a preseason baseline. Without the variability of a task, the heterogeneity of these results in mTBI, SRC, and subconcussion may suggest that head impacts produce heterogeneous effects across subjects. While the DMN is a popular RSN in which to probe functional connectivity of the brain, focusing on a single RSN limits the ability of rs-fMRI to probe the functional connectivity of the entire brain.

Metrics of spontaneous brain activity and functional brain connectivity. Another way to probe resting-state functional activity and connectivity in the entire brain is with the use of metrics that summarize the spontaneous brain activity and functional connectivity for each and every cortical voxel. Four such metrics are amplitude of low-frequency fluctuations (ALFF), fractional ALFF (fALFF), degree centrality (DC), regional homogeneity (ReHo). ALFF is a measure of the power spectrum in the range representing spontaneous neural activity (0.01-0.10Hz), and fALFF is the ratio of that power spectrum to that of the entire frequency range^{216,227}. ALFF and fALFF have been used to study several disease states, including: autism⁸³, depression^{87,107,170} Tourette syndrome⁴⁶, and various dementia disorders^{81,152,226}. Regional homogeneity (ReHo) is the Kendall's coefficient of concordance⁹³ of a given voxel and the 26 surrounding voxels in three-dimensional space:

$$W = \frac{12 \sum (R_i)^2 - n(\bar{R})^2}{K^2(n^3 - n)}$$

where W is the strength of concordance, with a value of 1 indicating perfect agreement and a value of 0 indicating no agreement, K is the number of voxels in the cluster ($K = 27$), n is the number of time points in the resting-state sequence ($n = 470$), R_i represents the sum rank of the i th time point (1 – 470), and \bar{R} is the mean of the R_i 's ($\frac{(n+1)K}{2}$)²¹⁵. ReHo is a measure of local functional connectivity. ReHo has been used to study several disease states, including: autism spectrum disorder^{48,144,171}, attention deficit hyperactivity disorder^{3,201} schizophrenia^{108,214}, depression^{79,103}, and various dementia disorders^{58,110,152,217}. Degree centrality (DC) is the sum of the Pearson correlation coefficients between each voxel and all other voxels, measuring of global functional

connectivity in the brain²⁹. DC has been used to study several disease states, including: autism⁵³, attention deficit hyperactivity disorder^{53,209}, epilepsy¹⁰⁹, psychosis¹¹³, and various dementia disorders^{2,6,152}.

A few recent studies have used these metrics of spontaneous brain activity and functional connectivity to study the effects of mTBI and concussion. Zhou et al. (2014) found lower fALFF in the frontal, temporal and occipital cortices when they compared mTBI patients weeks after their injury (mean: 23 days) to a healthy control group²²⁴. Using ALFF and fALFF, Zhan et al. (2016) found decreases in one region, and increases in three other regions when they compared mTBI patients days after their injury (mean: 3.6 days) to a healthy control group²²². To study local and global connectivity after SRC, Meier, Bellgowan, and Mayer (2016) measured ReHo and DC brain at multiple time points (mean days after injury: T1=1.7, T2=8.4, T3=32.4) and compared those measures to those found in a healthy athlete (HA) control group. Concussed athletes had increased ReHo in eight regions and decreased ReHo three regions at one-month post injury, and no changes in DC at any time point relative to the athlete control group¹²⁹. No published studies have used these metrics of functional activity and connectivity to study the effects of subconcussion.

While ALFF, fALFF, ReHo, and DC metrics measure spontaneous brain activity and functional connectivity across the entire cortex, traditional mass-univariate analyses may not be adequate to account for the heterogeneity of effects in subconcussion. Mass-univariate, or voxel-wise, analyses perform an independent statistical test for each voxel, requiring spatial homogeneity across participants. Many neurological processes and disorders have a similar spatial effects across the population, for example the n-back task

activates premotor and prefrontal regions, Parkinson's disease results in neural death in the substantia nigra, and temporal lobe epilepsy results in neural death in the hippocampus. This spatial homogeneity across participants makes voxel-wise analyses well-suited to detect relevant differences in group analyses. However, if subconcussion affects different brain regions in different participants, a voxel-wise approach might have insufficient statistical power to detect these changes.

Some fMRI researchers have started using multivariate analyses as a complement to standard mass univariate analyses¹¹⁶. Multivariate analyses are often performed as a supervised learning classifier, using a training set of data to create an algorithm that discriminates between two known groups, before testing classifier accuracy on novel data¹¹⁶. The resulting algorithms differentially weight voxels across the brain that might collectively discriminate between multiple groups of interest. This general approach is more robust in detecting changes that are spatially heterogeneous or spatially distributed across a group. Linear support vector machine (SVM) classification is an increasingly common technique in fMRI that tries to create a hyperplane decision boundary that separates the two groups' feature sets with the maximum possible margin^{41,192}. For fMRI data, the strength of linear SVM lies in its ability to deal with high dimensionality data and resistance to overtraining^{61,130}.

This study uses measures of spontaneous brain activity (ALFF/fALFF), local connectivity (ReHo), and global connectivity (DC) calculated from rs-fMRI scans collected from college football players, other college sport athletes, and college-age controls at preseason and postseason time points. To investigate the effects of subconcussion, which may be heterogeneous, both voxel-wise and SVM classification

will be performed to determine if changes are occurring in these metrics over the course of the season. To determine which regional trends are driving overall changes, the regional effects of the resulting t-statistic and SVM weight maps will be compared using a measure of ranking distance. We hypothesize that:

1) college football players will experience a mixture of increases and decreases in ALFF, fALFF and ReHo, similar to what is seen in response to concussion, 2) multivariate analyses will be more sensitive than mass-univariate analyses to the changes, due to underlying spatial heterogeneity on the effects, and 3) other college sport athletes may experience similar changes but to a lesser extent than college football, and college-age controls will not experience any longitudinal changes. If these hypotheses are correct, it would indicate that the increased subconcussive exposure in college football is producing spatially heterogeneous neural changes over the course of the single season. This method could also be used to monitor the functional effects of other physiological processes disorders with heterogeneity across patients, which is difficult with current methods.

CHAPTER II: QUANTIFICATION OF HEAD IMPACT IN CONTACT AND COLLISION SPORTS

INTRODUCTION

Despite unknown significance, concern about the detrimental effects of subconcussion has fueled a movement to quantify head impacts in contact and collision sports. There are dozens of studies analyzing head impact in American football, both using laboratory simulations/recreations^{64,148,149,194,197,205,220} and live play biomechanical measurements^{14,20,26,40,44-45,49,56-57,65,70,73,76,120,125,131,162-163,191,207}. A much smaller number of studies have quantified head impact in soccer and lacrosse, primarily using self-report questionnaires¹⁰⁶, video analysis^{30,104,205}, and/or laboratory simulations/recreations^{9,43,75,137,153}. No published studies present live play biomechanical data in lacrosse and although a couple of studies have reported head impact measured during live play in soccer^{115,126}. No studies have quantified subconcussion in multiple sports with the same biomechanical sensor and directly compared the sports' quantity and severity of head impacts.

Recent advances in biomechanical sensor technology have miniaturized accelerometers enough to be unobtrusively attached to the mastoid process with an adhesive patch, expanding the number of sports where head impact can be measured during live play. The present study compares biomechanical sensor data collected during one season for each of the following sports teams: college football, high school football, college men's lacrosse, and college men's soccer. These sports each have a comparatively high concussion incidence^{42,54,67,78,228}, with football typically near the top of all male sports. However, the relative amount of subconcussive head impact in these

sports is unknown, although football is widely assumed to have the highest subconcussive burden of all non-combat sports. The collected data are used to quantitatively investigate head impact differences between these teams during practices and games.

METHODS

Participants. During 2013 and 2014, 16 college football players, 15 high school football players, 15 college men's lacrosse players, and 15 college men's soccer players (mean (SD) age: 20.1 (1.3) years, 16.5 (1.2) years, 20.1 (1.1) years, and 20.2 (1.3) years, respectively) wore head impact sensors during official practices and games of their respective sport. College participants were volunteers from Division I teams and high school football players were from a small private high school. No athlete had a history of developmental or neurological disorder, or moderate to severe traumatic brain injury.

Standard protocol approvals, registrations, and patient consents. The University of Virginia Institutional Review Board for Health Science Research approved the research protocol. All participants gave written informed consent; if participant was under 18 years old at the time of enrollment, a parent or legal guardian also gave written informed consent.

Biomechanical measurements. Study participants wore the xPatch impact sensing skin patch (X2 Biosystems, Seattle, WA) on the skin covering their mastoid process (left or right side was decided by the athlete) (Figure 1A). Impact to the body or head can result in head acceleration; however, for simplicity we will henceforth refer to impacts that result in acceleration of the head as "head impacts." The sensor was to be worn during all

official team practices and games (soccer players only wore sensors for home games), although the athletes maintained the right to refuse at each event. The xPatch contains a triaxial high impact linear accelerometer and a triaxial gyroscope to capture six degrees of freedom for linear and rotational accelerations (one kilohertz sampling rate). If an accelerometer exceeded a predetermined 10g linear acceleration threshold, 100ms of data (10ms pre-trigger and 90ms post-trigger) from each accelerometer and gyroscope were recorded to onboard memory. Raw accelerometer data were then transformed to calculate peak resultant linear acceleration (PRLA) and peak resultant rotational acceleration (PRRA) at the head center of gravity by X2 Biosystems' Injury Monitoring System using a rigid body transformation for PRLA and a five point stencil for PRRA. False impacts are removed by X2 Biosystems' proprietary algorithm, which compares the waveform of each impact to a reference waveform using cross-correlation. Impacts with peak resultant linear acceleration less than 10g were removed. Impact data were then time filtered to include only impacts that occurred during a practice or game. Impact burden measures, PRLA sum and PRRA sum, were calculated per athletic exposure (a single practice or game event) by multiplying each impact by its linear or rotational severity and then summing them over each athletic event (ex. impacts of 10g, 10g, 20g, and 30g result in a PRLA sum of 70g), as in Broglio et al., 2011²². Studies investigating the biomechanical validity of the xPatch have found appreciable error in the measurement of PRLA and PRRA in individual impacts^{47,126,208}, discussed further in the limitations section. However, comparing relative values between two conditions with large numbers of impacts per condition has been demonstrated to provide reliable composite results¹²⁶.

Individual impact severity values reported by any head impact sensor should be considered approximate.

Game Data. All players participate in practices but not all players participate in every game. To account for this issue, athletes needed to meet a minimum playing time threshold for a game to include that player's data in the game analysis. Due to differences in substitution patterns and structure of the playing time for each sport, the thresholds are necessarily different. To be counted as a game player, a college football athlete needed to participate in at least one play, a college lacrosse player needed to play more than 33% of the game, and a soccer player needed to play more than 45 minutes in the game for the event to be included in the analysis. Detailed records of playing time were not available for high school football players, but on the small team under study, most players played at least some part of the game; therefore all recorded high school football games were analyzed. Additional supplementary analyses were performed that included all recorded game events, without any minimum playing time threshold for inclusion, to investigate whether the inclusion criteria substantially biased the results.

Statistical Methods.

Data summarization: Categorical scaled data were summarized by frequencies and percentages, while continuous scale data were summarized either by the mean and standard deviation, or the geometric mean, the median, and range of the empirical distribution.

Impacts per practice event: A negative binomial generalized estimate equation (GEE) model was utilized to compare the number of impacts per practice that the players experienced between college football, high school football, college lacrosse, and college

soccer. With regard to model specification, the GEE model only included a single indicator variable, which distinguished players from different teams. Since each player participated in several practices, each player's impact data was considered a cluster of potentially non-independent observations in the GEE analysis. The sandwich variance-covariance estimator of Huber and White^{80,202} was utilized to estimate the GEE model variance-covariance matrix. With respect to hypothesis testing, the GEE version of the Wald test was used to test the null hypothesis that mean number of impacts per practice was the same for all teams, and a two-sided $p \leq 0.05$ decision rule was used as the null hypothesis test rejection criterion.

Analysis of PRLA per impact: Average peak resultant linear acceleration (PRLA) per impact per practice event was analyzed on the natural logarithmic scale via a Gaussian GEE model. The natural logarithmic transformation was applied in order to rescale the data to a scale in which the measurement distributions were more symmetric in shape (i.e. bell shaped). With regard to model specification, the GEE model included one indicator variable that distinguished players from different teams. Since each player participated in several practices, each player's PRLA data was considered a cluster of potentially non-independent observations in the GEE analysis. The sandwich variance-covariance estimator of Huber and White^{80,202} was utilized to estimate the GEE model variance-covariance matrix. With respect to team differences in geometric mean PRLA per impact per practice, we tested the null hypothesis that the geometric mean is the same for players from different teams. A two-sided $p \leq 0.05$ rejection rule was used as the null hypothesis criterion.

Analysis of PRRA per impact: Average peak resultant rotational acceleration (PRRA) per impact per practice event was analyzed on the natural logarithmic scale in exactly the same way as the PRLA per impact data.

Analysis of PRLA threshold: A negative binomial GEE model was utilized to analyze the number of impacts per practice in which a player experienced an impact with PRLA greater than 10g, 20g, 30g, 40g, 50g, 60g, 70g, 80g, 90g, and 100g. With regard to the GEE model specification, two indicator variables were utilized, one to distinguish between players from different teams, and one to distinguish between the 10 different PRLA thresholds. A set of indicator variables for team by PRLA threshold interaction was also a component of the model specification. To account for *intra-player* measurement correlation, the GEE model variance covariance matrix was specified in the unstructured form; i.e. a variance-covariance matrix form that places no restriction of the variance-covariance structure. With regard to hypothesis testing, the GEE version of the Wald test was utilized to test the global hypothesis that for practice events the number of impacts per PRLA threshold was uniformly (i.e. across all PRLA thresholds) the same for the players from different teams. Wald tests were additionally used to examine on a per PRLA threshold bases, team differences in the mean number of impacts per practice event in which the PRLA was greater than the defined threshold. A Bonferroni correction was applied to all pairwise tests as a means to restrict the simultaneous type I error rate to be ≤ 0.05 .

Analysis of PRRA threshold: A negative binomial GEE model was utilized to analyze the number of impacts per practice event in which the athletes experience a peak resultant rotational acceleration greater than 0rad/s^2 , 2000rad/s^2 , 4000rad/s^2 , 6000rad/s^2 ,

8000rad/s², 10000rad/s², 12000rad/s², and 14000rad/s². The GEE analysis was conducted in exactly the same way as the analysis PRLA threshold.

Analysis of cumulative impact burden per practice event: Impact burden measures, PRLA sum and PRRA sum, were calculated per athletic exposure (a single practice or game event) by summing each impact linearly weighted by its severity as a measure of “cumulative impact burden²².” There is currently no widely accepted metric specifically for the quantification of cumulative impact burden. Many studies that try to quantify impact burden use the summation of a metric that was developed for individual impacts^{22,50,57,126,185,191}. This study chooses to use PRLA sum and PRRA sum, for their ease of calculation, and to match similar studies with the same accelerometer^{25,126}. The GEE version of the Cox proportionate hazard model was used to compare the empirical cumulative distribution for PRLA sum per practice between players from different teams as well as to compare the empirical cumulative distribution of PRRA between players from different teams. This approach was utilized so that the *intra-player* measurement correlation would be accounted for in the null hypothesis test that the underlying PRLA sum per practice cumulative distribution is the same for players from different teams.

Analyses of team differences in game events: Team differences in the number of impacts experienced by the players during games, and team differences in the impact forces experienced by the players during games were analyzed in the same way as the practice impact frequency data and practice impact force practice data. The only major differences were that this set of analyses focused on game event as opposed to practice events and this set of analyses focused only on the athletes who had game data that met the aforementioned inclusion criteria. To account for differences that were possibly caused

by different game inclusion criteria for the teams, additional analyses were performed with the same inclusion criteria used for all teams: the athlete wore the sensor during the game event. Hereafter, this analysis will be referred to as: “all games included” analysis. Supplemental table S1 contains a detailed account the “all games included” athletic exposures.

Software package: SAS version 9.4 (SAS Institute Inc., Cary, NC) was used to conduct the statistical analyses. Graphic displays were created with statistical software of Spotfire S plus (TIBCO Inc., Palo Alto, CA).

RESULTS

Participants. Results include data from 788 practices and 102 games from college football, 369 practices and 104 games from high school football, 943 practices and 37 games from college men’s lacrosse, and 480 practices and 28 games from college men’s soccer. Table 1 contains a detailed account of all captured athletic exposures.

Number of impacts per event. For practices, college football (CF) resulted in the most impacts per athlete per event, followed by college soccer (CS), followed by high school football (HF), and then college lacrosse (CL) (mean impacts/practice: 13.2; 95% CI: [10.3, 16.9], 7.4; 95% CI [5.1, 10.9], 5.3; 95% CI [3.3, 8.5], and 3.1; 95% CI [2.4, 4.0], respectively). However for games, CS > CF > HF > CL (mean impacts/game: 31.1; 95% CI: [15.3, 63.0], 24.2; 95% CI [17.4, 33.8], 14.3; 95% CI [9.2, 22.3], and 11.5; 95% CI [8.3, 16.0], respectively). Pairwise comparisons show Bonferroni-corrected significant differences in the ratio of means (RoM) for number of head impacts per event for HF:CF practices (RoM: 0.41, p=0.012), CL:CF practices (RoM: 0.24, p<0.001), CL:CS practices

(RoM: 0.42, $p=0.001$), and CL:CF games (RoM: 0.47, $p=0.010$) (Figure 1B). Analysis with all games included did not add or remove any significant team differences in number of impacts per game (Supplemental Figure 1A).

Geometric mean PRLA per event. For practices, CF resulted in the highest geometric mean peak resultant linear acceleration (PRLA) per athlete per event, followed by HF, followed by CL, and then CS (geometric mean PRLA/practice: 26.8g; 95% CI: [25.0, 28.7], 25.2g; 95% CI [23.4, 27.2], 21.3g; 95% CI [19.9, 22.8], and 18.5g; 95% CI [17.2, 19.9], respectively). The same order held true for games, CF > HF > CL > CS (geometric mean PRLA/game: 29.3g; 95% CI: [26.0, 32.9], 27.1g; 95% CI [25.2, 29.1], 21.1g; 95% CI [18.6, 24.0], and 17.6g; 95% CI [15.7, 19.8], respectively). Pairwise comparisons show Bonferroni-corrected significant differences in the ratio of geometric mean PRLA per event for CL:CF practices (RoM: 0.80, $p<0.001$), CS:CF practices (RoM: 0.69, $p<0.001$), CS:HF practices (RoM: 0.74, $p<0.001$), CS:CL practices (RoM: 0.87, $p<0.001$), CL:HF practices (RoM: 0.85, $p<0.001$), CL:CF games (RoM: 0.72, $p=0.003$), CS:CF games (RoM: 0.60, $p<0.001$), CS:HF games (RoM: 0.65, $p<0.001$), and CL:HF games (RoM: 0.78, $p=0.009$) (Figure 1C). Analysis with all games included resulted in lost significance between CL:CF (RoM: 0.84, $p=0.259$) and CL:HF (RoM: 0.89, $p=0.682$) games and increased effects between CS:CL (RoM: 0.74, $p=0.004$) games in geometric mean PRLA per game (Supplemental Figure 1B).

Geometric mean PRRA per event. For practices, CF resulted in the highest geometric mean peak resultant rotational acceleration (PRRA) per athlete per event, followed by HF, followed by CL, and then CS (geometric mean PRRA/practice: 5140.0; 95% CI: [4676.4, 5649.5], 4327.1; 95% CI [3817.9, 4811.2], 3817.9; 95% CI [3470.1, 4200.5],

and 2960.4; 95% CI [2674.2, 3277.2], respectively). The same order held true for games, CF > HF > CL > CS (geometric mean PRRA/game: 5805.8; 95% CI [5030.9, 6700.0], 4796.6; 95% CI [4056.2, 5672.1], 3603.1; 95% CI [2756.6, 4709.4], and 2713.8; 95% CI [2617.9, 2813.2], respectively). Pairwise comparisons showed Bonferroni-corrected significant differences in the ratio of geometric mean PRRA per event for all practices HF:CF (RoM: 0.84, $p < 0.001$), CL:CF (RoM: 0.74, $p < 0.001$), CS:CF (RoM: 0.58, $p < 0.001$), CS:HF (RoM: 0.68, $p < 0.001$), CS:CL (RoM: 0.78, $p < 0.001$), CL:HF (RoM: 0.88, $p = 0.036$), and CL:CF games (RoM: 0.62, $p = 0.018$), CS:CF games (RoM: 0.47, $p < 0.001$), and CS:HF games (RoM: 0.56, $p < 0.001$) (Figure 1D).

Analysis with all games included resulted in lost significance between CL:CF games (RoM: 0.74, $p = 0.052$) and increased effects between CS:CL games (RoM: 0.72, $p = 0.011$) in geometric mean PRRA per game (Supplemental Figure 1C).

Number of impacts above thresholds. For practices, the distributions for number of impacts per athlete per event, with respect to multiple linear and rotational acceleration thresholds, differed between CF, HF, CS, and CL ($p < 0.001$ for all pair-wise comparisons) (Figures 2A-B). Threshold by threshold post hoc pair-wise ratio of means comparisons showed sport differences in the mean number of impacts per practice at several linear and rotational acceleration thresholds after Bonferroni correction (Figures 2C-D and supplemental table S2). Compared to CF practices, trends across multiple PRLA and PRRA thresholds have practices for HF at ~26%, CS at ~18%, and CL at ~11% the number of CF impacts, with the percentage generally dropping as the thresholds increase. For games, the distributions for number of impacts per athlete per event, with respect to multiple linear and rotational acceleration thresholds, differed between CF, HF, CS, and

CL ($p \leq 0.017$ for all pair-wise comparisons) (Figures 3A-B). Threshold by threshold post hoc pair-wise ratio of means comparisons showed sport differences in the mean number of impacts per game at several linear and rotational acceleration thresholds after Bonferroni correction (Figures 3C-D and supplemental table S3). Compared to CF games, trends across multiple PRLA and PRRA thresholds have games for HF at ~54%, CS at ~42%, and CL at ~20% the number of CF impacts, with the percentage generally decreasing as the thresholds increase. Analysis with all games included resulted in lost significance between HF:CF games ($p=0.332$) in the distributions for number of impacts per athlete per event, with respect to multiple linear acceleration thresholds (Supplemental Figure S2A). Analysis with all games included did not add or remove any significant team differences in the distributions for number of impacts per athlete per event, with respect to multiple rotational acceleration thresholds. (Supplemental Figure S2B). Threshold by threshold post hoc pair-wise ratio of means comparisons showed changes in sport differences in the mean number of impacts per game at some linear and rotational acceleration thresholds after Bonferroni correction (Supplemental Figures S2C-D and supplemental table S4).

Cumulative impact load per event. The Kaplan Meier forms of the cumulative distributions for impact burden (a summation of the impacts which are each weighted by severity) per athletic exposure are shown in Figures 4A-B with regard to linear acceleration, and in Figures 4C-D with regard to rotational acceleration. During practice, linear acceleration cumulative distributions differed between all pairwise comparisons (Bonferroni corrected $p \leq 0.05$) with the exception of the comparison of HF-to-CS, with the median of the linear acceleration distribution being greatest for CF (277.3g; 95% CI

[249.4, 309.6]), followed by HF (63.1g; 95% CI [56.0, 73.5]) and CS (84.9g; 95% CI [73.0, 94.9]), and then CL (41.6g; 95% CI [36.8, 46.9]) (Figure 4A). During games, linear acceleration cumulative distributions differed for comparisons of CF-to-CS, CF-to-CL, CS-to-CL, and HF-CL (Bonferroni corrected $p \leq 0.05$), but not between any other pairwise comparisons, with CL resulting in the lowest linear acceleration distribution (median: CF-567g; 95% CI [453, 691], CS-410g; 95% CI [261, 471], HF-202g; 95% CI [128, 302], CL-101g; 95% CI [55, 144]) (Figure 4B). Analysis with all games included resulted in lost significance between CF-to-CS games in cumulative linear impact load per event (Supplemental Figure S3A). During practice, rotational acceleration cumulative distributions also differed between all pairwise comparisons (Bonferroni corrected $p \leq 0.05$) with the exception of the comparison of HF-to-CS, again with the median of the rotational acceleration distribution being greatest for CF (53,800rad/s²; 95% CI [47,200, 61,700]), followed by HF (11,200rad/s²; 95% CI [9,200, 13,400]) and CS (13,900rad/s²; 95% CI [11,800, 16,300]), and then CL (7,600rad/s²; 95% CI [6,800, 8,600]) (Figure 4C). During games, rotational acceleration cumulative distributions differed for comparisons of CL-to-CS, CL-to-HF, and CL-to-CF (Bonferroni corrected $p \leq 0.05$), but not between any other pairwise comparisons, again with CL resulting in the lowest rotational acceleration distribution median (median: CF-111,800rad/s²; 95% CI [90,200, 139,700], CS-61,700rad/s²; 95% CI [33,300, 68,600], HF-41,800rad/s²; 95% CI [29,300, 59,700], CL-40,200rad/s²; 95% CI [27,300, 55,000]) (Figure 4D). Analysis with all games included did not add or remove any significant team differences in cumulative linear impact load per event (Supplemental Figure S3B).

Table 1. Summary for each subject's captured athletic events.

For each athlete the following information is provided: player position, number of captured events for each event type, mean number of impacts for each event type, geometric mean peak resultant linear acceleration (PRLA) per impact per event and peak resultant rotational acceleration (PRRA) per impact per event.

Participant Number	Position	Practice Summary				Game Summary			
		Number of Events	Mean Hits per Practice	Geometric Mean PRLA per Hit per Practice (g)	Geometric Mean PRRA per Hit per Practice (rad/s ²)	Number of Events	Mean Hits per Game	Geometric Mean PRLA per Hit per Practice (g)	Geometric Mean PRRA per Hit per Game (rad/s ²)
CF1	FB	57	9.5	34.8	6411.6	12	13.6	35	7165.6
CF2	FB	61	13.8	29.1	5098.3	8	12.3	33.1	6250.8
CF3	SS	48	18.3	32.7	6708.6	9	32.2	32.5	7148.4
CF4	DT	63	18.2	25.6	5408.3	3	10	20.8	4439.1
CF5	WR	56	5.6	24	4794.5	10	19.6	27.2	5203
CF6	LB	32	15.2	23.8	4267.5	7	23.7	27.4	5084.8
CF7	FS	23	8.2	25.1	5206.1	-	-	-	-
CF8	DE	58	13.4	27.5	5471.7	11	15.3	32.4	5878.3
CF9	WR	60	9.4	17.8	2593.3	8	33	17.1	3084.7
CF10	DT	41	23.2	25.8	4890.9	4	36	27.2	5253.6
CF11	T	29	15.6	23.5	4698.1	1	23	31.6	4427.4
CF12	TE	50	6.5	21.5	4617.9	8	20.3	26.2	5341.6
CF13	DT	63	27.1	32.3	6432.8	11	55.5	33.5	7519.2
CF14	LS	39	4.2	22.1	5056.5	1	1	15.2	3644.7
CF15	CB	60	8.8	29.7	5128.7	-	-	-	-
CF16	LB	48	10.7	45.7	9239.5	9	17.4	35.1	7087.9
Mean (SD) or GM†		47.0 (12.9)	13.8 (12.3)	27.2†	5212.9†	7.3 (3.6)	24.2 (13.2)	29.3 †	5805.8 †
Median		50.5	12	25.7	5113.5	8	19.9	29.5	5297.6
Range		[22, 61]	[4.2, 27.1]	[17.8, 45.7]	[2593.3, 9239.5]	[1, 12]	[1, 55.5]	[15.2, 35.1]	[3084.7, 7519.2]
HF1	WR and CB	14	3.6	24.9	4136.7	3	13.3	29.8	6335.1
HF2	WR and FS	20	2.2	29.1	4443.8	5	2.6	29.8	6708.8
HF3	WR and CB	28	1.6	26.3	4743.5	10	16.2	30.2	5484.4
HF4	QB	31	1.1	26.3	3309.3	10	3.3	22.4	3105.7
HF5	DL	24	1.4	30.4	7022.9	8	3.3	33.9	9023.3
HF6	OL and LB	20	6.2	25.8	4403.1	6	31	26.3	3745.7
HF7	WR and CB	22	2.7	24.7	4506.8	5	2.4	21.7	2723.4
HF8	WR	26	4.7	31	6433.7	10	4.3	29.7	5765.6
HF9	WR	33	3.2	21.6	2568.3	9	38.1	25.6	4736.6
HF10	G	38	8.2	21.9	4761.9	9	17.6	25.4	4896.5
HF11	OL and DT	19	5.3	23	4316.6	6	28	33.2	6224.4

HF12	C	29	16.8	27.1	5590.3	6	27.3	25.6	4134.9
HF13	LB	21	1.8	20.4	2942.1	5	5.2	26.5	4890.2
HF14	OL and DL	23	6.1	23.1	4085.9	7	2.6	24.8	2947.1
HF15	RB and WR	21	3.3	23.4	3441.8	7	14.6	25.8	5357.9
Mean (SD) or GM†		24.6 (6.2)	4.8 (7.5)	24.9†	4307.8†	7.1 (2.2)	14.3 (11.9)	27.1 †	4796.6 †
Median		23	3.3	24.9	4403.1	7	13.3	26.3	4896.5
Range		[14, 38]	[1.1, 16.8]	[20.4, 31.0]	[2568.3, 7022.93]	[3, 10]	[2.4, 38.1]	[21.7, 33.9]	[2723.4, 9023.3]
CL1	Midfield	47	2.6	21.8	3959.3	4	13.3	26.3	4377.4
CL2	Attack	60	2.5	27.2	4883	-	-	-	-
CL3	Midfield	73	3.3	22.4	4099.8	-	-	-	-
CL4	Attack	77	3.8	23.5	4614	11	12.1	23.2	4591.8
CL5	Attack	20	7	26.4	5996.7	-	-	-	-
CL6	Midfield	63	2	15.7	2222.8	-	-	-	-
CL7	Midfield	63	2	24.6	4323.6	-	-	-	-
CL8	Midfield	63	3.9	21.5	4052.7	-	-	-	-
CL9	Midfield	66	1.4	18.7	3212.8	11	6.4	20.4	3627.4
CL10	Midfield	74	3	20.5	4201.7	-	-	-	-
CL11	Midfield	59	1.4	21.7	4015	-	-	-	-
CL12	Midfield	81	5.9	14.8	1938.5	-	-	-	-
CL13	Midfield	74	5.5	17.3	2796.1	11	15.4	17.7	2438.5
CL14	Defense	67	2.1	31.2	5806.9	-	-	-	-
CL15	Defense	56	1.3	24.9	4594.8	-	-	-	-
Mean (SD) or GM†		24.6 (6.2)	3.1 (4.4)	21.3†	3751.9†	9.3 (3.5)	5.5 (6.1)	24.6†	4350.7†
Median		23	2.6	21.8	4099.8	11	2.4	24.7	4365
Range		[14, 38]	[1.3, 7.0]	[14.8, 31.2]	[1938.5, 5996.7]	[4, 11]	[0, 10.8]	[14.4, 33.3]	[947.2, 6687.6]
CS1	Goalkeeper	18	14.4	24.3	4843.1	-	-	-	-
CS2	Defense	13	8.2	20.3	3373.7	-	-	-	-
CS3	Defense	11	1.1	34.3	5974.3	-	-	-	-
CS4	Midfield	16	5.1	19.2	3264.5	-	-	-	-
CS5	Midfield	8	3.1	24.4	4096	-	-	-	-
CS6	Defense	50	5.5	16.3	2290.3	7	20.9	18.1	2589.8
CS7	Midfield	52	6.5	15.2	2115.1	-	-	-	-
CS8	Forward	43	6.2	17.1	2625.5	7	18	19.9	2726.6
CS9	Midfield	49	3.4	18.6	3354.8	-	-	-	-
CS10	Defense	46	5.7	18.4	2759.8	5	17	19.7	2825.6
CS11	Defense	50	19.8	15.7	2795	7	71	15.1	2817
CS12	Goalkeeper	30	7	19.5	3544.7	-	-	-	-
CS13	Defense	27	5.7	17.3	2852	-	-	-	-
CS14	Goalkeeper	35	5	15.9	2366.2	-	-	-	-
CS15	Goalkeeper	32	7.7	18.3	3337.2	2	8.5	13.7	2494.1

Mean (SD) or GM†	32.0 (15.9)	7.4 (9.6)	17.8†	2862.1†	5.6 (2.2)	31.1 (23.2)	17.6 †	2713.8 †
Median	32	5.7	18.4	3264.5	7	18	18.1	2726.6
Range	[8, 52]	[1.1, 19.8]	[15.2, 34.3]	[2115.1, 5974.3]	[5, 7]	[8.5, 71.0]	[13.7, 19.9]	[2494.1, 2825.6]

Figure 1.

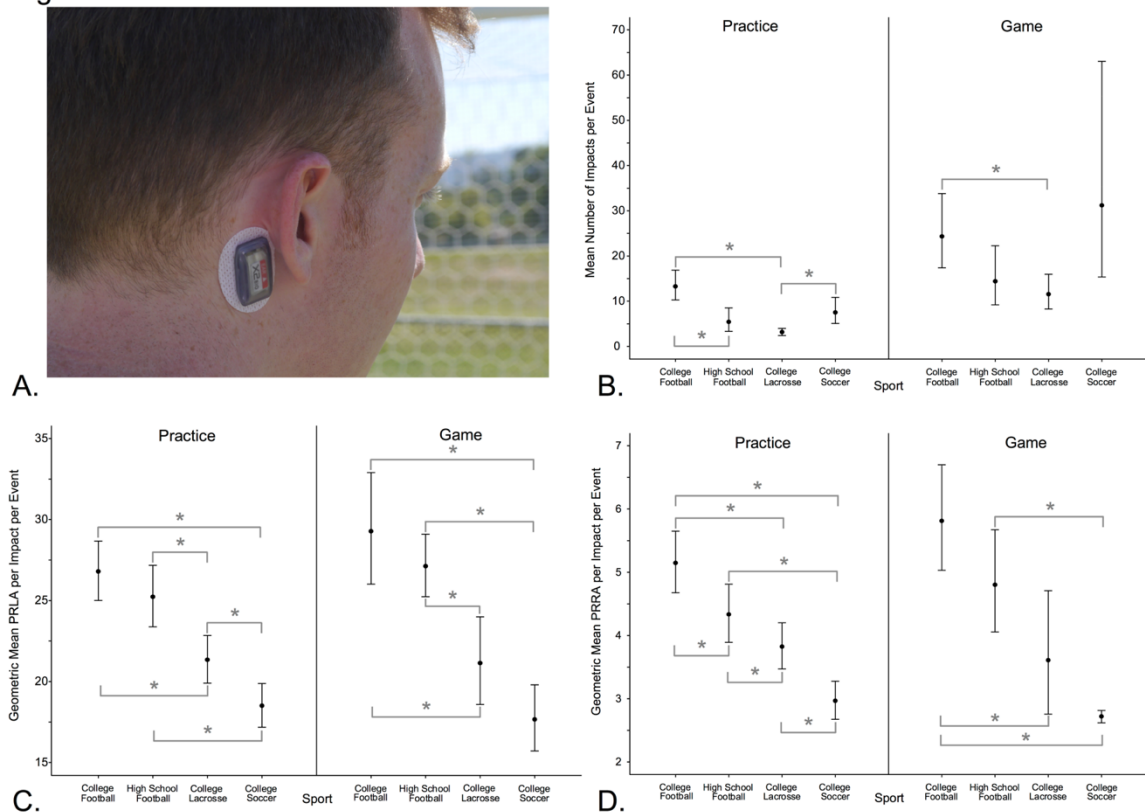


Figure 1. Average Quantity and Severity of Impacts. Picture of an athlete wearing the xPatch (A). Graph showing impact rates per athletic event, according to sport and event type (B). Geometric mean PRLA (g) (C) and PRRA ($\text{rad/s}^2 / 1000$) (D) per individual impact. Black circles identify the mean impact rate or geometric mean peak acceleration per impact, and vertical lines identify the 95% confidence interval. Brackets with an asterisk indicate that the indicated sports' differed at the $p \leq 0.05$ Bonferroni corrected level of statistical significance for that measure.

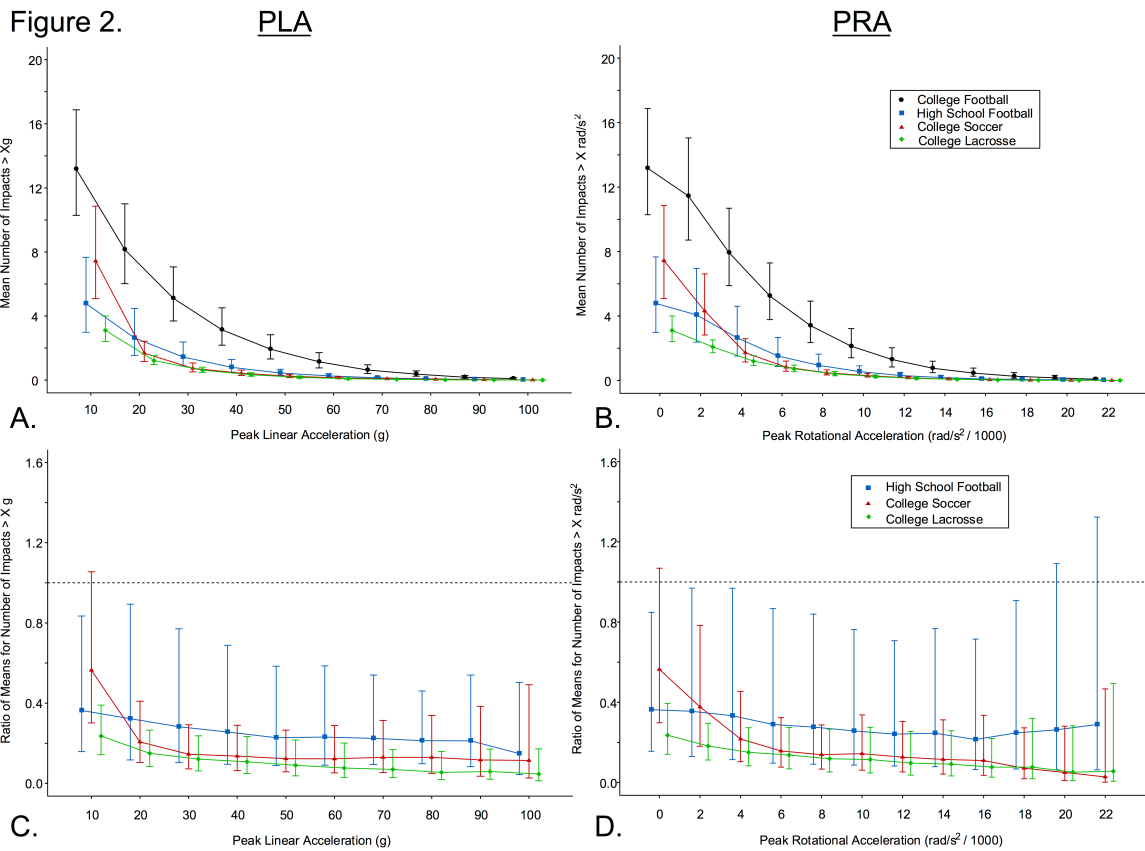


Figure 2. Impacts per Practice at Multiple Thresholds. Graphs of the mean number of impacts greater than the PRLA (A) or PRRA (B) threshold for CF, HF, CL, and CS practices. Vertical lines identify the 95% confidence interval for the mean number of impacts per practice greater than threshold. Graphs showing the ratio of means for comparing the mean number of impacts greater than the PRLA (C) or PRRA (D) threshold between CF practices and HF, CL, and CS practices. Data points identify the mean impact rate ratio (e.g., HF:CF practices) and vertical lines identify the Bonferroni corrected 95% confidence interval. Dotted line identifies the line of equality (i.e. ratio equals 1).

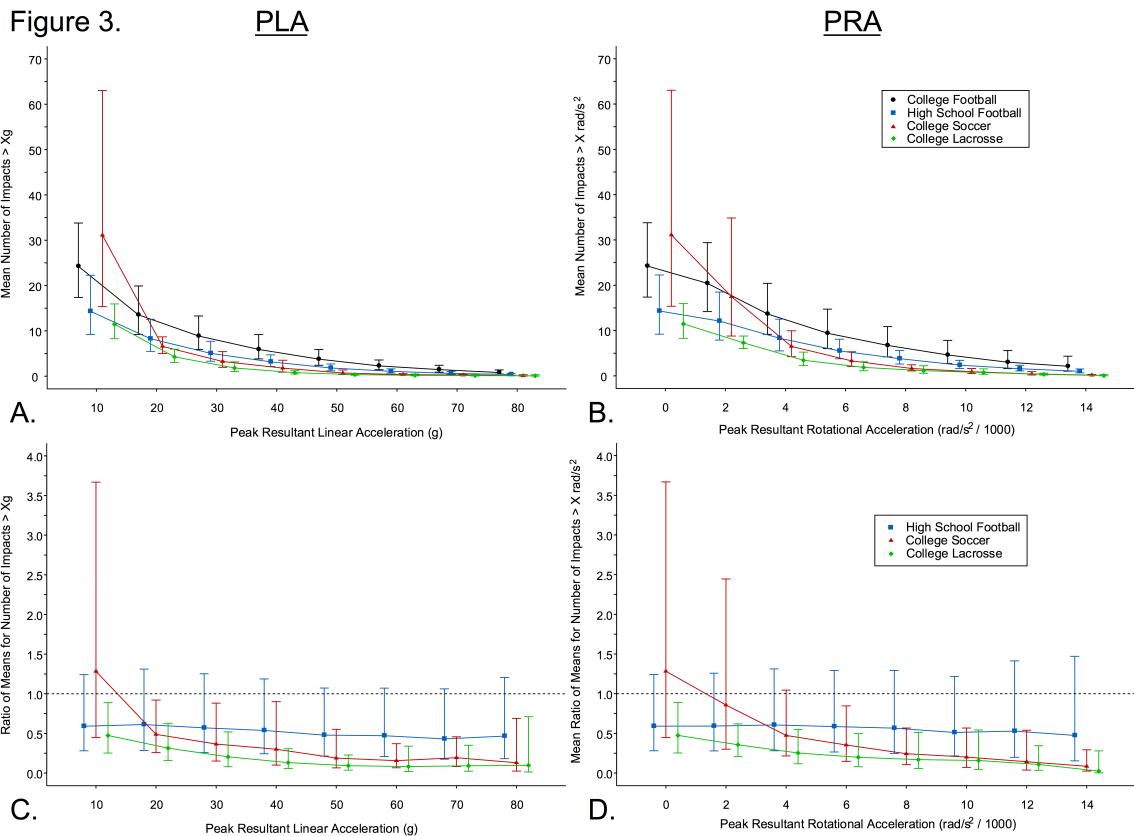


Figure 3. Impacts per Game at Multiple Thresholds. Graphs of the mean number of impacts greater than the PRLA (A) or PRRA (B) threshold for CF, HF, CL, and CS games. Vertical lines identify the 95% confidence interval for the mean number of impacts per game greater than threshold. Graphs showing the ratio of means for comparing the mean number of impacts greater than the PRLA (C) or PRRA (D) threshold between CF games and HF, CL, and CS games. Data points identify the mean impact rate ratio (e.g., HF:CF games) and vertical lines identify the Bonferroni corrected 95% confidence interval. Dotted line identifies the line of equality (i.e. ratio equals 1).

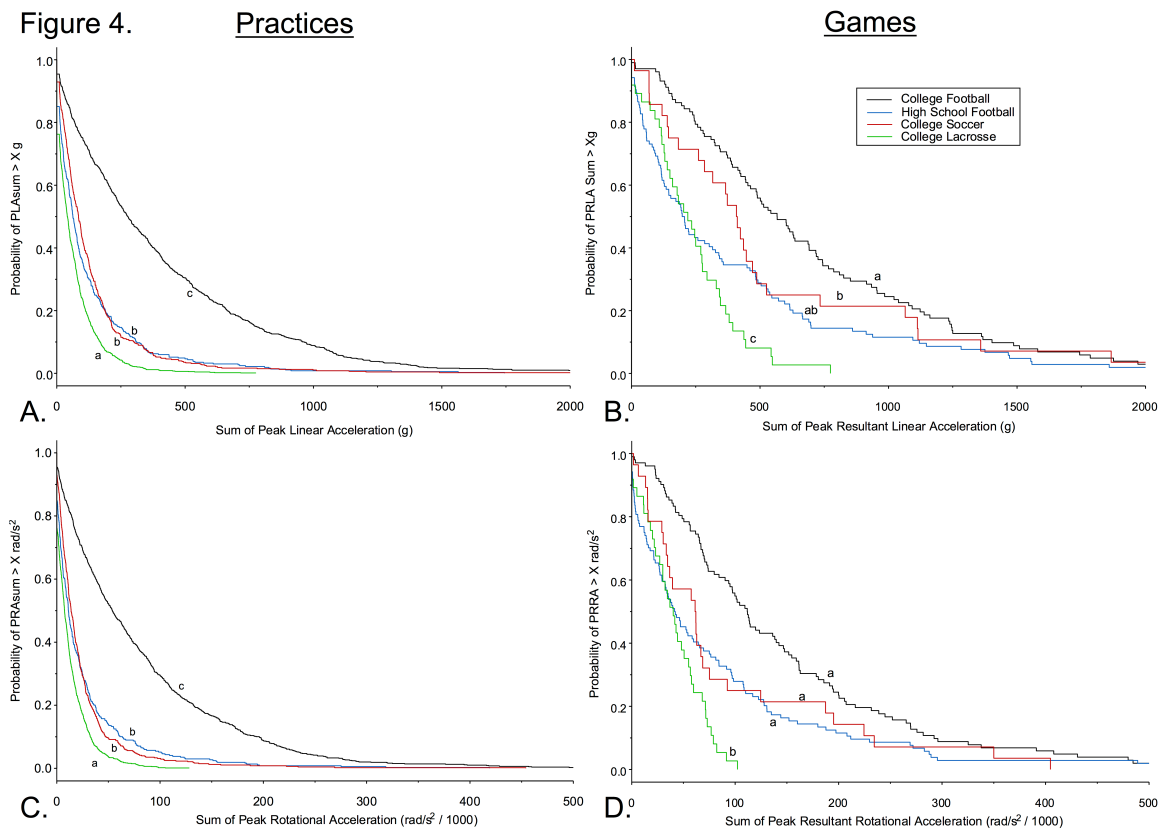


Figure 4. Impact Burden per Athletic Exposure. Graphs showing cumulative distributions per event for the PRLA sum during practices (A) and games (B) and PRRA sum during practices (C) and games (D). The cumulative distribution is expressed as cumulative probability for observing a single athletic exposure PRLA or PRRA sum greater than X. Curves with different lowercase letters (a–c) differed at the $p \leq 0.05$ Bonferroni corrected level of statistical significance.

Table 2. Ratio of Mean Impacts per Practice at Multiple Thresholds. Ratio of mean impacts per practice at multiple PRLA and PRRA thresholds. For each pairwise team comparison and each PRLA or PRRA threshold the following information is provided: ratio of mean impacts per practice, uncorrected and Bonferroni corrected 95% confidence limits (95% CL), uncorrected and Bonferroni corrected p-values. For each PRLA and PRRA pairwise global test degrees of freedom (DF), Wald statistic, and p-values are also provided.

High School Football vs. College Football

Threshold (g)	Ratio of Mean Impacts per Practice	Lower 95% CL	Upper 95% CL	Uncorrected p-value	Bonferroni Lower 95% CL	Bonferroni Upper 95% CL	Bonferroni p-value
10	0.36	0.20	0.65	0.001	0.16	0.83	0.006
20	0.32	0.16	0.66	0.002	0.12	0.89	0.018
30	0.28	0.14	0.57	<0.001	0.10	0.77	0.004
40	0.26	0.13	0.51	<0.001	0.10	0.69	0.001
50	0.23	0.12	0.44	<0.001	0.09	0.58	<0.001
60	0.23	0.12	0.44	<0.001	0.09	0.59	<0.001
70	0.22	0.12	0.41	<0.001	0.09	0.54	<0.001
80	0.21	0.12	0.37	<0.001	0.10	0.46	<0.001
90	0.21	0.11	0.41	<0.001	0.08	0.54	<0.001
100	0.15	0.06	0.35	<0.001	0.04	0.50	<0.001
Global Test: HF vs CF		DF = 10			Wald Statistic = 78.5		p < 0.001
Threshold (rad/s ²)	Ratio of Mean Impacts per Practice	Lower 95% CL	Upper 95% CL	Uncorrected p-value	Bonferroni Lower 95% CL	Bonferroni Upper 95% CL	Bonferroni p-value
0	0.36	0.20	0.65	0.001	0.16	0.85	0.008
2000	0.36	0.18	0.71	0.003	0.13	0.97	0.038
4000	0.33	0.16	0.69	0.003	0.11	0.97	0.038
6000	0.29	0.14	0.61	0.001	0.10	0.87	0.014
8000	0.28	0.13	0.59	0.001	0.09	0.84	0.011
10000	0.26	0.12	0.54	<0.001	0.09	0.76	0.004
12000	0.24	0.12	0.50	<0.001	0.08	0.71	0.002
14000	0.25	0.11	0.54	<0.001	0.08	0.77	0.005
16000	0.21	0.09	0.49	<0.001	0.06	0.72	0.003
18000	0.25	0.10	0.60	0.002	0.07	0.91	0.025
20000	0.26	0.10	0.70	0.007	0.06	1.09	0.086
22000	0.29	0.10	0.82	0.019	0.06	1.32	0.234
Global Test: HF vs CF		DF = 12			Wald Statistic = 158.3		p < 0.001

College Lacrosse vs. College Football

Threshold	Ratio of Mean	Lower	Upper	Uncorrected	Bonferroni	Bonferroni	Bonferroni
-----------	---------------	-------	-------	-------------	------------	------------	------------

(g)	Impacts per Practice	95% CL	95% CL	p-value	Lower 95% CL	Upper 95% CL	p-value
10	0.24	0.17	0.34	<0.001	0.14	0.39	<0.001
20	0.15	0.10	0.22	<0.001	0.08	0.27	<0.001
30	0.12	0.08	0.19	<0.001	0.06	0.24	<0.001
40	0.11	0.06	0.18	<0.001	0.05	0.23	<0.001
50	0.09	0.05	0.17	<0.001	0.04	0.22	<0.001
60	0.08	0.04	0.15	<0.001	0.03	0.20	<0.001
70	0.07	0.04	0.13	<0.001	0.03	0.17	<0.001
80	0.05	0.03	0.12	<0.001	0.02	0.16	<0.001
90	0.06	0.03	0.12	<0.001	0.02	0.17	<0.001
100	0.05	0.02	0.12	<0.001	0.01	0.17	<0.001
Global Test: CL vs CF		DF = 10		Wald Statistic = 331.7		p < 0.001	
Threshold (rad/s ²)	Ratio of Mean Impacts per Practice	Lower 95% CL	Upper 95% CL	Uncorrected p-value	Bonferroni Lower 95% CL	Bonferroni Upper 95% CL	Bonferroni p-value
0	0.24	0.17	0.34	<0.001	0.14	0.39	<0.001
2000	0.18	0.13	0.25	<0.001	0.11	0.30	<0.001
4000	0.15	0.10	0.23	<0.001	0.08	0.27	<0.001
6000	0.14	0.08	0.22	<0.001	0.07	0.27	<0.001
8000	0.12	0.07	0.21	<0.001	0.05	0.27	<0.001
10000	0.11	0.06	0.21	<0.001	0.05	0.28	<0.001
12000	0.10	0.05	0.19	<0.001	0.04	0.25	<0.001
14000	0.09	0.05	0.19	<0.001	0.03	0.26	<0.001
16000	0.08	0.04	0.16	<0.001	0.03	0.22	<0.001
18000	0.08	0.03	0.20	<0.001	0.02	0.32	<0.001
20000	0.05	0.02	0.17	<0.001	0.01	0.28	<0.001
22000	0.06	0.01	0.25	<0.001	0.01	0.49	0.002
Global Test: CL vs CF		DF = 12		Wald Statistic = 151.4		p < 0.001	

College Soccer vs. College Football

Threshold (g)	Ratio of Mean Impacts per Practice	Lower 95% CL	Upper 95% CL	Uncorrected p-value	Bonferroni Lower 95% CL	Bonferroni Upper 95% CL	Bonferroni p-value
10	0.56	0.36	0.87	0.010	0.30	1.06	0.103
20	0.21	0.13	0.33	<0.001	0.10	0.41	<0.001
30	0.14	0.09	0.24	<0.001	0.07	0.29	<0.001
40	0.14	0.08	0.23	<0.001	0.06	0.29	<0.001
50	0.12	0.07	0.21	<0.001	0.06	0.27	<0.001
60	0.12	0.07	0.22	<0.001	0.05	0.29	<0.001
70	0.13	0.07	0.24	<0.001	0.05	0.31	<0.001
80	0.13	0.07	0.25	<0.001	0.05	0.34	<0.001

90	0.12	0.05	0.27	<0.001	0.04	0.38	<0.001
100	0.11	0.04	0.32	<0.001	0.03	0.49	<0.001
Global Test: CS vs CF		DF = 10 Wald Statistic = 120.9 p < 0.001					
Threshold (rad/s ²)	Ratio of Mean Impacts per Practice	Lower 95% CL	Upper 95% CL	Uncorrected p-value	Bonferroni Lower 95% CL	Bonferroni Upper 95% CL	Bonferroni p-value
0	0.56	0.36	0.87	0.010	0.30	1.07	0.123
2000	0.38	0.23	0.62	<0.001	0.18	0.78	0.002
4000	0.22	0.13	0.36	<0.001	0.10	0.45	<0.001
6000	0.16	0.10	0.26	<0.001	0.08	0.32	<0.001
8000	0.14	0.08	0.23	<0.001	0.07	0.29	<0.001
10000	0.14	0.08	0.26	<0.001	0.06	0.34	<0.001
12000	0.13	0.07	0.23	<0.001	0.05	0.30	<0.001
14000	0.12	0.06	0.23	<0.001	0.04	0.31	<0.001
16000	0.11	0.05	0.24	<0.001	0.04	0.34	<0.001
18000	0.07	0.03	0.18	<0.001	0.02	0.27	<0.001
20000	0.05	0.02	0.16	<0.001	0.01	0.28	<0.001
22000	0.03	0.00	0.19	<0.001	0.00	0.47	0.003
Global Test: CS vs CF		DF = 12 Wald Statistic = 825.8 p < 0.001					

College Lacrosse vs. High School Football

Threshold (g)	Ratio of Mean Impacts per Practice	Lower 95% CL	Upper 95% CL	Uncorrected p-value	Bonferroni Lower 95% CL	Bonferroni Upper 95% CL	Bonferroni p-value
10	0.65	0.40	1.06	0.081	0.32	1.30	0.813
20	0.46	0.29	0.75	0.002	0.23	0.92	0.017
30	0.43	0.27	0.67	<0.001	0.22	0.82	0.003
40	0.42	0.27	0.65	<0.001	0.22	0.79	0.001
50	0.40	0.26	0.61	<0.001	0.21	0.74	<0.001
60	0.33	0.22	0.51	<0.001	0.18	0.61	<0.001
70	0.31	0.20	0.47	<0.001	0.17	0.57	<0.001
80	0.26	0.14	0.48	<0.001	0.10	0.63	<0.001
90	0.28	0.13	0.61	0.001	0.09	0.85	0.013
100	0.31	0.11	0.89	0.029	0.07	1.39	0.289
Global Test: CL vs HF		DF = 10 Wald Statistic = 54.9 p < 0.001					
Threshold (rad/s ²)	Ratio of Mean Impacts per Practice	Lower 95% CL	Upper 95% CL	Uncorrected p-value	Bonferroni Lower 95% CL	Bonferroni Upper 95% CL	Bonferroni p-value
0	0.65	0.40	1.06	0.081	0.32	1.32	0.976
2000	0.51	0.31	0.85	0.009	0.25	1.07	0.109
4000	0.45	0.27	0.75	0.002	0.22	0.95	0.027
6000	0.47	0.29	0.77	0.003	0.23	0.97	0.035

8000	0.43	0.27	0.69	0.001	0.21	0.86	0.006
10000	0.45	0.28	0.71	0.001	0.23	0.87	0.007
12000	0.40	0.26	0.62	<0.001	0.21	0.76	<0.001
14000	0.37	0.23	0.62	<0.001	0.18	0.78	0.001
16000	0.36	0.23	0.56	<0.001	0.19	0.69	<0.001
18000	0.31	0.17	0.56	<0.001	0.13	0.74	0.001
20000	0.2	0.09	0.41	<0.001	0.07	0.58	<0.001
22000	0.2	0.07	0.53	0.001	0.05	0.85	0.017
Global Test: CL vs HF		DF = 12	Wald Statistic = 48.1		p < 0.001		

College Soccer vs. High School Football

Threshold (g)	Ratio of Mean Impacts per Practice	Lower	Upper	Uncorrected	Bonferroni	Bonferroni	Bonferroni
		95% CL	95% CL	p-value	Lower 95% CL	Upper 95% CL	p-value
10	1.55	0.86	2.81	0.145	0.67	3.63	1.000
20	0.64	0.34	1.21	0.170	0.26	1.59	1.000
30	0.51	0.28	0.95	0.034	0.21	1.24	0.339
40	0.53	0.29	0.97	0.040	0.22	1.26	0.404
50	0.54	0.31	0.95	0.034	0.24	1.22	0.337
60	0.53	0.30	0.94	0.029	0.24	1.20	0.289
70	0.58	0.34	0.99	0.045	0.27	1.25	0.450
80	0.61	0.34	1.09	0.096	0.26	1.41	0.965
90	0.55	0.22	1.40	0.208	0.14	2.09	1.000
100	0.77	0.25	2.32	0.641	0.16	3.74	1.000
Global Test: CS vs HF		DF = 10	Wald Statistic = 84.1		p < 0.001		
Threshold (rad/s ²)	Ratio of Mean Impacts per Practice	Lower	Upper	Uncorrected	Bonferroni	Bonferroni	Bonferroni
		95% CL	95% CL	p-value	Lower 95% CL	Upper 95% CL	p-value
0	1.55	0.86	2.81	0.145	0.65	3.69	1.000
2000	1.06	0.54	2.08	0.863	0.40	2.84	1.000
4000	0.65	0.33	1.30	0.223	0.24	1.78	1.000
6000	0.54	0.28	1.07	0.078	0.20	1.46	0.931
8000	0.50	0.26	0.96	0.036	0.20	1.29	0.432
10000	0.56	0.30	1.03	0.063	0.23	1.37	0.752
12000	0.52	0.30	0.92	0.025	0.23	1.19	0.294
14000	0.47	0.24	0.92	0.027	0.17	1.26	0.33
16000	0.51	0.26	1.01	0.052	0.19	1.37	0.623
18000	0.29	0.12	0.68	0.004	0.08	1.01	0.053
20000	0.19	0.06	0.62	0.006	0.03	1.06	0.069
22000	0.1	0.01	0.67	0.018	0.01	1.64	0.215
Global Test: CS vs HF		DF = 12	Wald Statistic = 139.5		p < 0.001		

College Lacrosse vs. College Soccer

Threshold (g)	Ratio of Mean Impacts per Practice	Lower 95% CL	Upper 95% CL	Uncorrected p-value	Bonferroni Lower 95% CL	Bonferroni Upper 95% CL	Bonferroni p-value
10	0.42	0.27	0.65	<0.001	0.22	0.79	0.001
20	0.72	0.48	1.08	0.115	0.41	1.29	1.000
30	0.84	0.54	1.28	0.413	0.45	1.55	1.000
40	0.79	0.50	1.26	0.323	0.41	1.54	1.000
50	0.73	0.45	1.20	0.219	0.36	1.49	1.000
60	0.62	0.35	1.11	0.107	0.27	1.42	1.000
70	0.54	0.30	0.94	0.031	0.24	1.21	0.308
80	0.42	0.21	0.85	0.017	0.15	1.16	0.166
90	0.51	0.22	1.20	0.122	0.15	1.73	1.000
100	0.41	0.12	1.36	0.143	0.07	2.28	1.000
Global Test: CL vs CS		DF = 10	Wald Statistic = 40.9		p < 0.001		
Threshold (rad/s ²)	Ratio of Mean Impacts per Practice	Lower 95% CL	Upper 95% CL	Uncorrected p-value	Bonferroni Lower 95% CL	Bonferroni Upper 95% CL	Bonferroni p-value
0	0.42	0.27	0.65	0.000	0.22	0.80	0.002
2000	0.48	0.31	0.75	0.001	0.25	0.92	0.015
4000	0.69	0.44	1.10	0.118	0.36	1.35	1.000
6000	0.87	0.56	1.35	0.533	0.45	1.66	1.000
8000	0.85	0.55	1.34	0.491	0.44	1.64	1.000
10000	0.80	0.50	1.26	0.333	0.41	1.56	1.000
12000	0.77	0.46	1.27	0.300	0.37	1.60	1.000
14000	0.80	0.44	1.47	0.470	0.33	1.94	1.000
16000	0.70	0.36	1.36	0.290	0.27	1.84	1.000
18000	1.07	0.46	2.51	0.868	0.31	3.72	1.000
20000	1.02	0.33	3.12	0.975	0.20	5.24	1.000
22000	2.04	0.25	16.65	0.507	0.09	43.94	1.000
Global Test: CL vs CS		DF = 12	Wald Statistic = 84.2		p < 0.001		

Table 3. Ratio of Mean Impacts per Game at Multiple Thresholds. Ratio of mean impacts per game at multiple PRLA and PRRA thresholds. For each pairwise team comparison and each PRLA or PRRA threshold the following information is provided: ratio of mean impacts per game, uncorrected and Bonferroni corrected 95% confidence limits (95% CL), uncorrected and Bonferroni corrected p-values. For each PRLA and PRRA pairwise global test degrees of freedom (DF), Wald statistic, and p-values are also provided.

High School Football vs. College Football							
Threshold (g)	Ratio of Mean Impacts per Game	Lower 95% CL	Upper 95% CL	Uncorrected p-value	Bonferroni Lower 95% CL	Bonferroni Upper 95% CL	Bonferroni p-value
10	0.59	0.34	1.03	0.062	0.28	1.24	0.369
20	0.61	0.35	1.08	0.089	0.29	1.31	0.534
30	0.57	0.32	1.02	0.059	0.26	1.25	0.356
40	0.54	0.3	0.97	0.039	0.24	1.19	0.233
50	0.48	0.26	0.87	0.016	0.21	1.07	0.095
60	0.47	0.26	0.87	0.016	0.21	1.07	0.094
70	0.43	0.22	0.84	0.014	0.18	1.06	0.083
80	0.47	0.23	0.95	0.034	0.18	1.21	0.206
Global Test: HF vs CF		DF = 8		Wald Statistic = 18.6		p = 0.017	
Threshold (rad/s ²)	Ratio of Mean Impacts per Game	Lower 95% CL	Upper 95% CL	Uncorrected p-value	Bonferroni Lower 95% CL	Bonferroni Upper 95% CL	Bonferroni p-value
0	0.59	0.34	1.03	0.062	0.28	1.24	0.369
2000	0.59	0.34	1.04	0.067	0.28	1.26	0.401
4000	0.61	0.34	1.08	0.087	0.28	1.31	0.524
6000	0.59	0.33	1.06	0.075	0.27	1.29	0.451
8000	0.57	0.31	1.05	0.069	0.25	1.29	0.413
10000	0.51	0.27	0.97	0.041	0.22	1.22	0.248
12000	0.53	0.25	1.10	0.087	0.20	1.41	0.523
14000	0.47	0.20	1.10	0.082	0.15	1.47	0.493
Global Test: HF vs CF		DF = 8		Wald Statistic = 27.6		p < 0.001	

College Lacrosse vs. College Football							
Threshold (g)	Ratio of Mean Impacts per Game	Lower 95% CL	Upper 95% CL	Uncorrected p-value	Bonferroni Lower 95% CL	Bonferroni Upper 95% CL	Bonferroni p-value
10	0.47	0.30	0.76	0.002	0.25	0.89	0.010
20	0.32	0.19	0.53	<0.001	0.16	0.63	<0.001
30	0.20	0.10	0.41	<0.001	0.08	0.52	<0.001
40	0.13	0.07	0.25	<0.001	0.06	0.31	<0.001
50	0.09	0.05	0.18	<0.001	0.04	0.23	<0.001

60	0.08	0.03	0.24	<0.001	0.02	0.34	<0.001
70	0.09	0.03	0.25	<0.001	0.02	0.35	<0.001
80	0.10	0.02	0.43	0.002	0.01	0.71	0.012
Global Test: CL vs CF		DF = 8	Wald Statistic = 2025.4		p < 0.001		
Threshold (rad/s ²)	Ratio of Mean Impacts per Game	Lower 95% CL	Upper 95% CL	Uncorrected p-value	Bonferroni Lower 95% CL	Bonferroni Upper 95% CL	Bonferroni p-value
0	0.47	0.30	0.76	0.002	0.25	0.89	0.010
2000	0.36	0.24	0.54	<0.001	0.21	0.62	<0.001
4000	0.25	0.14	0.45	<0.001	0.12	0.55	<0.001
6000	0.20	0.10	0.39	<0.001	0.08	0.50	<0.001
8000	0.17	0.07	0.39	<0.001	0.06	0.51	<0.001
10000	0.16	0.06	0.39	<0.001	0.05	0.54	<0.001
12000	0.11	0.05	0.26	<0.001	0.03	0.34	<0.001
14000	0.03	0.00	0.15	<0.001	0.00	0.28	<0.001
Global Test: CL vs CF		DF = 8	Wald Statistic = 264.1		p < 0.001		

College Soccer vs. College Football

Threshold (g)	Ratio of Mean Impacts per Game	Lower 95% CL	Upper 95% CL	Uncorrected p-value	Bonferroni Lower 95% CL	Bonferroni Upper 95% CL	Bonferroni p-value
10	1.28	0.59	2.80	0.531	0.45	3.67	1.000
20	0.49	0.30	0.78	0.003	0.26	0.92	0.017
30	0.37	0.19	0.70	0.003	0.15	0.88	0.015
40	0.30	0.13	0.68	0.004	0.10	0.90	0.023
50	0.19	0.09	0.42	<0.001	0.06	0.55	<0.001
60	0.16	0.08	0.30	<0.001	0.07	0.37	<0.001
70	0.19	0.10	0.37	<0.001	0.08	0.46	<0.001
80	0.13	0.04	0.45	0.001	0.02	0.69	0.008
Global Test: CS vs CF		DF = 8	Wald Statistic = 408.0		p < 0.001		
Threshold (rad/s ²)	Ratio of Mean Impacts per Game	Lower 95% CL	Upper 95% CL	Uncorrected p-value	Bonferroni Lower 95% CL	Bonferroni Upper 95% CL	Bonferroni p-value
0	1.28	0.59	2.80	0.531	0.45	3.67	1.000
2000	0.86	0.39	1.87	0.698	0.30	2.45	1.000
4000	0.47	0.26	0.85	0.013	0.22	1.05	0.077
6000	0.35	0.18	0.68	0.002	0.15	0.85	0.010
8000	0.24	0.13	0.46	<0.001	0.10	0.57	<0.001
10000	0.20	0.09	0.43	<0.001	0.07	0.57	<0.001
12000	0.14	0.05	0.38	<0.001	0.04	0.54	0.001
14000	0.08	0.03	0.21	<0.001	0.02	0.29	<0.001

Global Test: CS vs CF	DF = 8	Wald Statistic = 233.1	p < 0.001
------------------------------	---------------	-------------------------------	---------------------

College Lacrosse vs. High School Football

Threshold (g)	Ratio of Mean Impacts per Game	Lower 95% CL	Upper 95% CL	Uncorrected p-value	Bonferroni Lower 95% CL	Bonferroni Upper 95% CL	Bonferroni p-value
10	0.80	0.46	1.39	0.433	0.38	1.68	1.000
20	0.52	0.30	0.88	0.015	0.25	1.06	0.090
30	0.36	0.18	0.73	0.004	0.14	0.93	0.026
40	0.25	0.14	0.45	<0.001	0.11	0.55	<0.001
50	0.19	0.10	0.37	<0.001	0.08	0.46	<0.001
60	0.18	0.06	0.49	0.001	0.04	0.70	0.006
70	0.21	0.08	0.56	0.002	0.06	0.79	0.011
80	0.21	0.05	0.90	0.035	0.03	1.48	0.212
Global Test: CL vs HF		DF = 8	Wald Statistic = 1333.9		p < 0.001		
Threshold (rad/s ²)	Ratio of Mean Impacts per Game	Lower 95% CL	Upper 95% CL	Uncorrected p-value	Bonferroni Lower 95% CL	Bonferroni Upper 95% CL	Bonferroni p-value
0	0.80	0.46	1.39	0.433	0.38	1.68	1.000
2000	0.60	0.38	0.96	0.033	0.32	1.13	0.196
4000	0.42	0.23	0.75	0.003	0.19	0.91	0.019
6000	0.34	0.18	0.64	0.001	0.14	0.80	0.005
8000	0.30	0.14	0.65	0.002	0.10	0.85	0.013
10000	0.31	0.13	0.71	0.006	0.10	0.95	0.034
12000	0.20	0.10	0.42	<0.001	0.08	0.53	<0.001
14000	0.05	0.01	0.29	0.001	0.01	0.51	0.004
Global Test: CL vs HF		DF = 8	Wald Statistic = 232.4		p < 0.001		

College Soccer vs. High School Football

Threshold (g)	Ratio of Mean Impacts per Game	Lower 95% CL	Upper 95% CL	Uncorrected p-value	Bonferroni Lower 95% CL	Bonferroni Upper 95% CL	Bonferroni p-value
10	2.17	0.94	5.00	0.068	0.71	6.67	0.407
20	0.80	0.48	1.31	0.371	0.41	1.56	1.000
30	0.64	0.33	1.25	0.192	0.26	1.57	1.000
40	0.56	0.26	1.23	0.151	0.19	1.62	0.903
50	0.40	0.18	0.86	0.019	0.14	1.12	0.112
60	0.33	0.18	0.61	<0.001	0.15	0.75	0.002
70	0.45	0.25	0.82	0.009	0.20	1.01	0.055
80	0.28	0.08	0.94	0.039	0.05	1.43	0.236
Global Test: CS vs HF		DF =	Wald Statistic = 148.3		p < 0.001		

		8					
Threshold (rad/s ²)	Ratio of Mean Impacts per Game	Lower 95% CL	Upper 95% CL	Uncorrected p-value	Bonferroni Lower 95% CL	Bonferroni Upper 95% CL	Bonferroni p-value
0	1.71	0.72	4.04	0.224	0.51	5.68	1.000
2000	1.15	0.50	2.64	0.749	0.36	3.67	1.000
4000	0.62	0.31	1.24	0.175	0.23	1.63	1.000
6000	0.46	0.21	0.97	0.042	0.16	1.31	0.335
8000	0.32	0.15	0.68	0.003	0.12	0.91	0.024
10000	0.31	0.14	0.66	0.003	0.10	0.90	0.021
12000	0.23	0.10	0.52	<0.001	0.08	0.71	0.003
14000	0.14	0.05	0.35	<0.001	0.04	0.50	<0.001
Global Test: CS vs HF		DF = 8		Wald Statistic = 247.5		p < 0.001	

College Lacrosse vs. College Soccer

Threshold (g)	Ratio of Mean Impacts per Game	Lower 95% CL	Upper 95% CL	Uncorrected p-value	Bonferroni Lower 95% CL	Bonferroni Upper 95% CL	Bonferroni p-value
10	0.37	0.17	0.80	0.012	0.13	1.05	0.073
20	0.65	0.42	1.00	0.048	0.36	1.16	0.291
30	0.56	0.26	1.20	0.133	0.20	1.56	0.799
40	0.44	0.19	0.99	0.048	0.15	1.32	0.288
50	0.49	0.21	1.13	0.093	0.16	1.50	0.560
60	0.53	0.19	1.51	0.234	0.13	2.17	1.000
70	0.47	0.18	1.22	0.123	0.13	1.70	0.735
80	0.76	0.13	4.45	0.758	0.07	8.22	1.000
Global Test: CL vs CS		DF = 8		Wald Statistic = 2437.1		p < 0.001	
Threshold (rad/s ²)	Ratio of Mean Impacts per Game	Lower 95% CL	Upper 95% CL	Uncorrected p-value	Bonferroni Lower 95% CL	Bonferroni Upper 95% CL	Bonferroni p-value
0	0.25	0.10	0.64	0.004	0.07	0.92	0.030
2000	0.34	0.13	0.88	0.026	0.09	1.28	0.209
4000	0.51	0.22	1.23	0.135	0.15	1.73	1.000
6000	0.57	0.23	1.44	0.237	0.16	2.07	1.000
8000	0.69	0.27	1.75	0.438	0.19	2.53	1.000
10000	0.78	0.28	2.19	0.638	0.19	3.29	1.000
12000	0.94	0.33	2.64	0.903	0.22	3.97	1.000
14000	1.22	0.47	3.22	0.680	0.32	4.71	1.000
Global Test: CL vs CS		DF = 8		Wald Statistic = 423.7		p < 0.001	

Table 4. Summary for each subject's captured athletic events – All Games Included.

Summary for each subject's captured athletic events for the all games included analysis.

For each athlete the following information is provided: player position, number of captured events for each event type, mean number of impacts for each event type, geometric mean peak resultant linear acceleration (PRLA) per impact per event and peak resultant rotational acceleration (PRRA) per impact per event.

Participant Number	Position	<u>Game Summary</u>			
		Number of Events	Mean Hits per Game	Geometric Mean PRLA per Hit per Practice (g)	Geometric Mean PRRA per Hit per Game (rad/s ²)
CF1	FB	12	13.6	35	7165.6
CF2	FB	11	9.5	29.4	4990.1
CF3	SS	9	32.2	32.5	7148.4
CF4	DT	7	7	25.3	5844.9
CF5	WR	10	19.6	27.2	5203
CF6	LB	8	21.4	27.3	5072.2
CF8	DE	11	15.3	32.4	5878.3
CF9	WR	8	33	17.1	3084.7
CF10	DT	6	24.3	29.7	6288.6
CF11	T	4	6.5	21.1	3720.4
CF12	TE	9	18.1	27.8	5560.1
CF13	DT	11	55.5	33.5	7519.2
CF14	LS	9	12.8	19.7	3860.8
CF16	LB	9	17.4	35.1	7087.9
Mean (SD) or GM†		8.9 (2.2)	21.2 (13.0)	28.7	5669
Median		9	17.8	28.6	5702.5
Range		[4, 12]	[6.5, 55.5]	[17.1, 35.1]	[3084.7, 7519.2]
CL1	Midfield	4	13.3	26.3	4377.4
CL2	Attack	7	1.6	33.3	5900.4
CL3	Midfield	10	10.8	23.3	4268.2
CL4	Attack	11	12.1	23.2	4591.8
CL6	Midfield	10	2	27.6	3711
CL7	Midfield	7	0.6	40.6	6409.1
CL8	Midfield	11	3.1	24.8	4573.1
CL9	Midfield	11	6.4	20.4	3627.4
CL10	Midfield	10	8.1	27.6	5531.4
CL11	Midfield	8	0.4	18.7	1849.8
CL12	Midfield	11	2.6	17.4	2714.9
CL13	Midfield	11	15.4	17.7	2438.5
CL14	Defense	6	0.8	37.9	7621.2

CL15	Defense	9	0.6	40	9632.5
Mean (SD) or GM†		9.0 (2.3)	5.8 (5.1)	24.2	4615.2
Median		10	2.9	25.6	4475.3
Range		[4, 11]	[0.4, 15.4]	[17.4, 40.6]	[1849.8, 9632.5]
CS6	Defense	7	20.9	18.1	2589.8
CS7	Midfield	6	4.7	14.7	3013.6
CS8	Forward	7	18	19.9	2726.6
CS9	Midfield	4	4.3	18.7	3706.6
CS10	Defense	5	17	19.7	2825.6
CS11	Defense	7	71	15.1	2817
CS12	Goalkeeper	2	2.5	32.9	4659.6
CS14	Goalkeeper	1	2	19.2	5133.1
CS15	Goalkeeper	3	6	15.9	2984
Mean (SD) or GM†		4.7 (2.3)	22.0 (22.9)	17.9	2815.6
Median		5	6	18.7	2984
Range		[1, 7]	[2.0, 71.0]	[14.7, 32.9]	[2589.8, 5133.1]

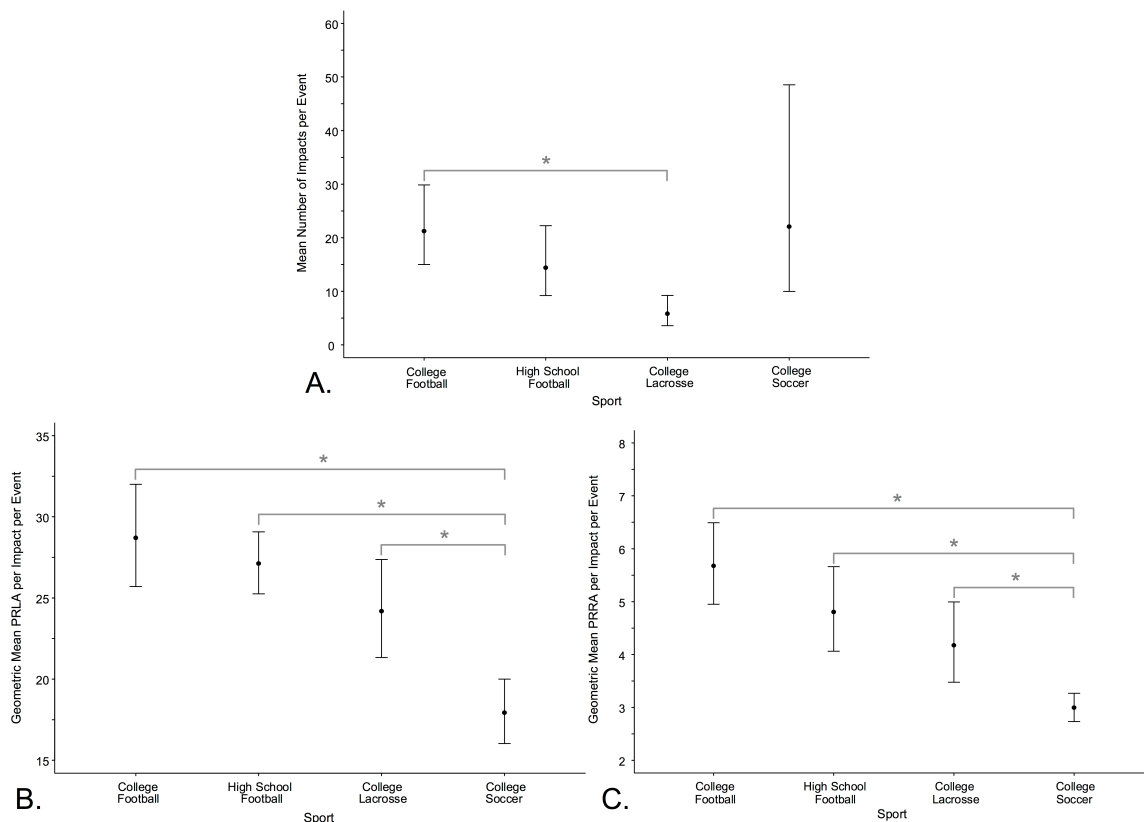


Figure 5. Average Quantity and Severity of Impacts per Game – All Games Included. For the all games included analysis, graph showing impact rates per game according to sport (A). Geometric mean PRLA (g) (B) and PRRA ($\text{rad/s}^2 / 1000$) (C) per individual impact. Black circles identify the mean impact rate or geometric mean peak acceleration per impact, and vertical lines identify the 95% confidence interval. Brackets with an asterisk indicate that the indicated sports' differed at the $p \leq 0.05$ Bonferroni corrected level of statistical significance for that measure.

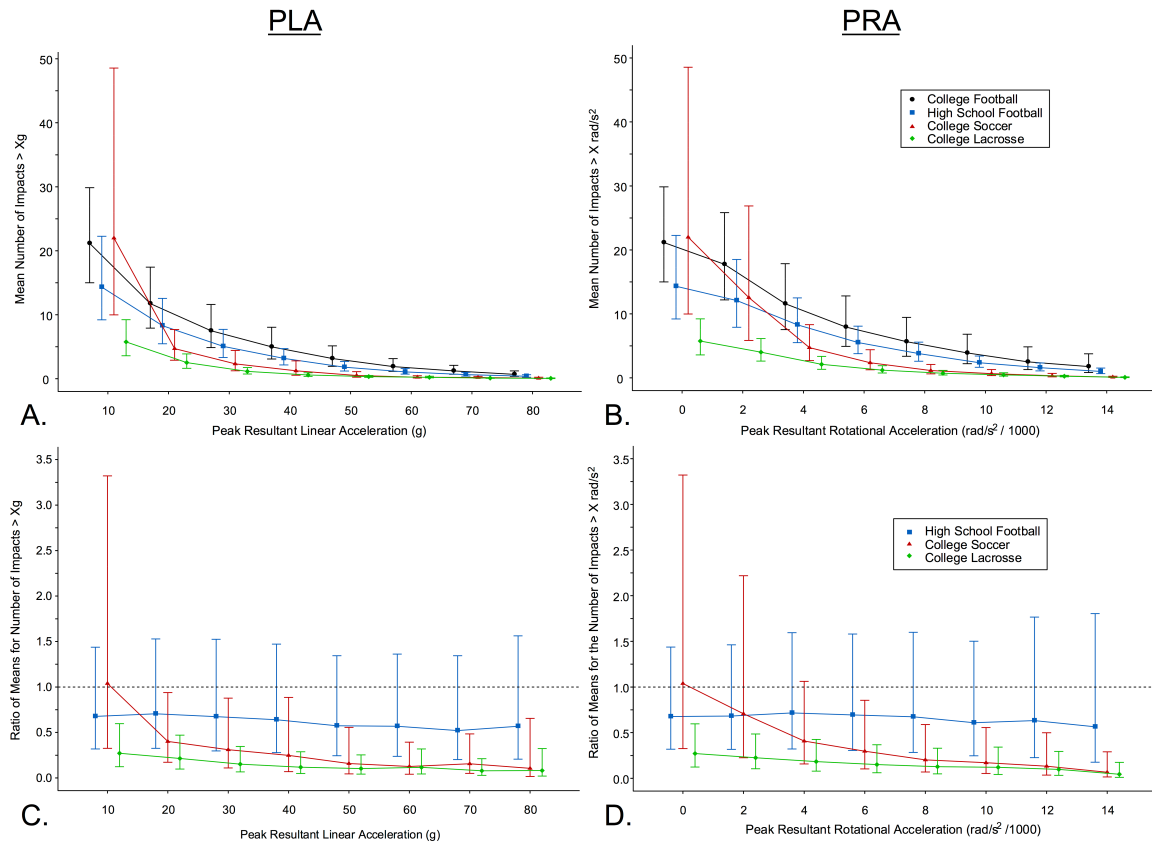


Figure 6. Impacts per Game with Respect to Multiple Thresholds – All Games Included. For the all games included analysis, graphs of the mean number of impacts greater than the PRLA (A) or PRRA (B) threshold for CF, HF, CL, and CS games. Vertical lines identify the 95% confidence interval for the mean number of impacts per game greater than threshold. Graphs showing the ratio of means for comparing the mean number of impacts greater than the PRLA (C) or PRRA (D) threshold between CF games and HF, CL, and CS games. Data points identify the mean impact rate ratio (e.g., HF:CF games) and vertical lines identify the Bonferroni corrected 95% confidence interval. Dotted line identifies the line of equality (i.e. ratio equals 1).

Games

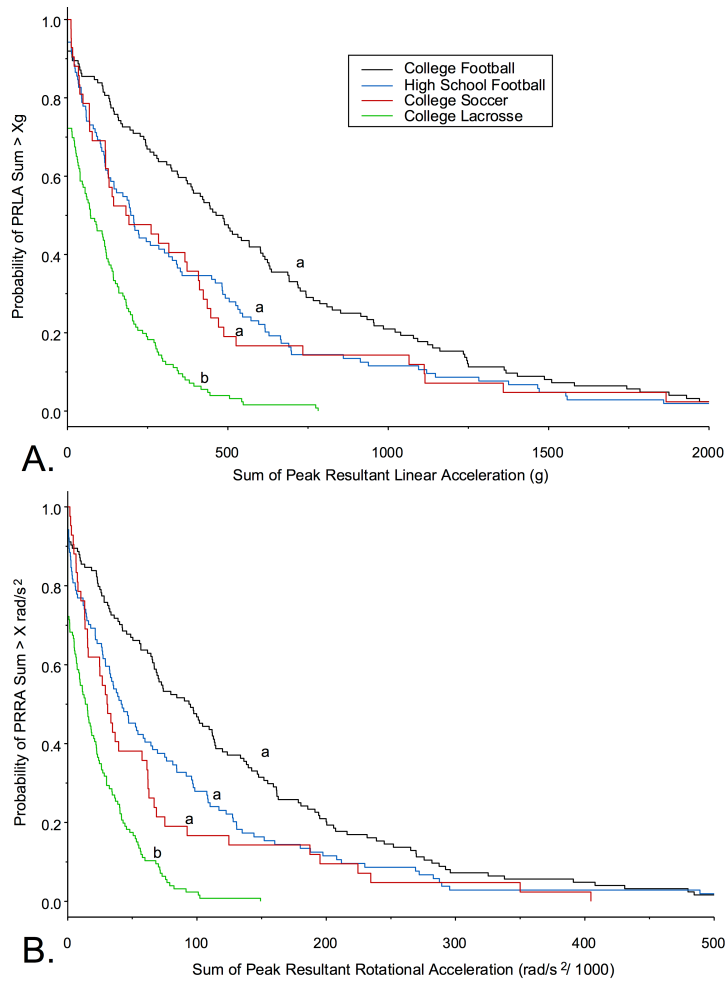


Figure 7. Impact Burden per Game – All Games Included. For the all games included analysis, graphs showing cumulative distributions per game for the PRLA sum (A) and PRRA sum (B). The cumulative distribution is expressed as cumulative probability for observing a single athletic exposure PRLA or PRRA sum greater than X. Curves with different lowercase letters (a–b) differed at the $p \leq 0.05$ Bonferroni corrected level of statistical significance.

Table 5. Ratio of Mean Impacts per Game at Multiple Thresholds – All Games Included. Ratio of mean impacts per game at multiple PRLA and PRRA thresholds for the all games included analysis. For each pairwise team comparison and each PRLA or PRRA threshold the following information is provided: ratio of mean impacts per game, uncorrected and Bonferroni corrected 95% confidence limits (95% CL), uncorrected and Bonferroni corrected p-values. For each PRLA and PRRA pairwise global test degrees of freedom (DF), Wald statistic, and p-values are also provided.

High School Football vs. College Football							
Threshold (g)	Ratio of Mean Impacts per Game	Lower 95% CL	Upper 95% CL	Uncorrected p-value	Bonferroni Lower 95% CL	Bonferroni Upper 95% CL	Bonferroni p-value
10	0.68	0.39	1.18	0.171	0.32	1.44	1.000
20	0.71	0.4	1.25	0.234	0.33	1.53	1.000
30	0.67	0.37	1.24	0.202	0.30	1.52	1.000
40	0.64	0.34	1.19	0.157	0.28	1.47	0.942
50	0.57	0.3	1.08	0.085	0.24	1.34	0.509
60	0.57	0.3	1.09	0.088	0.24	1.36	0.527
70	0.52	0.26	1.05	0.07	0.20	1.34	0.417
80	0.57	0.27	1.2	0.14	0.21	1.56	0.840
Global Test: HF vs CF		DF = 8		Wald Statistic = 9.2		p = 0.332	
Threshold (rad/s ²)	Ratio of Mean Impacts per Game	Lower 95% CL	Upper 95% CL	Uncorrected p-value	Bonferroni Lower 95% CL	Bonferroni Upper 95% CL	Bonferroni p-value
0	0.68	0.39	1.18	0.171	0.32	1.44	1.000
2000	0.68	0.39	1.20	0.185	0.32	1.46	1.000
4000	0.72	0.39	1.30	0.270	0.32	1.59	1.000
6000	0.69	0.38	1.28	0.242	0.31	1.58	1.000
8000	0.67	0.35	1.28	0.228	0.28	1.60	1.000
10000	0.61	0.31	1.19	0.147	0.25	1.50	0.880
12000	0.63	0.30	1.36	0.239	0.23	1.77	1.000
14000	0.56	0.24	1.34	0.193	0.18	1.80	1.000
Global Test: HF vs CF		DF = 8		Wald Statistic = 23.6		p = 0.003	

College Lacrosse vs. College Football							
Threshold (g)	Ratio of Mean Impacts per Game	Lower 95% CL	Upper 95% CL	Uncorrected p-value	Bonferroni Lower 95% CL	Bonferroni Upper 95% CL	Bonferroni p-value
10	0.27	0.15	0.49	<0.001	0.12	0.60	<0.001
20	0.21	0.12	0.38	<0.001	0.10	0.47	<0.001
30	0.15	0.08	0.28	<0.001	0.07	0.35	<0.001
40	0.12	0.06	0.23	<0.001	0.05	0.29	<0.001

50	0.10	0.05	0.20	<0.001	0.04	0.25	<0.001
60	0.12	0.06	0.25	<0.001	0.04	0.32	<0.001
70	0.08	0.04	0.16	<0.001	0.03	0.21	<0.001
80	0.08	0.03	0.23	<0.001	0.02	0.32	<0.001
Global Test: CL vs CF		DF = 8	Wald Statistic = 103.6		p < 0.001		
Threshold (rad/s ²)	Ratio of Mean Impacts per Game	Lower 95% CL	Upper 95% CL	Uncorrected p-value	Bonferroni Lower 95% CL	Bonferroni Upper 95% CL	Bonferroni p-value
0	0.27	0.15	0.49	<0.001	0.12	0.60	<0.001
2000	0.23	0.13	0.40	<0.001	0.11	0.49	<0.001
4000	0.18	0.10	0.34	<0.001	0.08	0.43	<0.001
6000	0.15	0.08	0.29	<0.001	0.06	0.37	<0.001
8000	0.13	0.06	0.26	<0.001	0.05	0.33	<0.001
10000	0.12	0.06	0.26	<0.001	0.04	0.34	<0.001
12000	0.10	0.04	0.22	<0.001	0.03	0.29	<0.001
14000	0.04	0.02	0.12	<0.001	0.01	0.18	<0.001
Global Test: CL vs CF		DF = 8	Wald Statistic = 73.1		p < 0.001		

College Soccer vs. College Football

Threshold (g)	Ratio of Mean Impacts per Game	Lower 95% CL	Upper 95% CL	Uncorrected p-value	Bonferroni Lower 95% CL	Bonferroni Upper 95% CL	Bonferroni p-value
10	1.04	0.44	2.46	0.930	0.33	3.32	1.000
20	0.40	0.21	0.75	0.005	0.17	0.94	0.027
30	0.31	0.14	0.67	0.003	0.11	0.88	0.018
40	0.25	0.10	0.64	0.004	0.07	0.89	0.023
50	0.16	0.06	0.40	<0.001	0.05	0.56	0.001
60	0.13	0.05	0.29	<0.001	0.04	0.39	<0.001
70	0.16	0.07	0.36	<0.001	0.05	0.48	<0.001
80	0.11	0.03	0.41	0.001	0.02	0.65	0.007
Global Test: CS vs CF		DF = 8	Wald Statistic = 178.4		p < 0.001		
Threshold (rad/s ²)	Ratio of Mean Impacts per Game	Lower 95% CL	Upper 95% CL	Uncorrected p-value	Bonferroni Lower 95% CL	Bonferroni Upper 95% CL	Bonferroni p-value
0	1.04	0.44	2.46	0.93	0.33	3.32	1.000
2000	0.71	0.30	1.65	0.424	0.23	2.22	1.000
4000	0.41	0.20	0.83	0.013	0.16	1.06	0.081
6000	0.30	0.14	0.65	0.002	0.10	0.85	0.015
8000	0.20	0.09	0.45	<0.001	0.07	0.59	<0.001
10000	0.17	0.07	0.41	<0.001	0.05	0.56	<0.001
12000	0.13	0.05	0.35	<0.001	0.04	0.50	<0.001

14000	0.07	0.02	0.20	<0.001	0.02	0.29	<0.001
Global Test: CS vs CF		DF = 8	Wald Statistic = 160.9		p < 0.001		

College Lacrosse vs. High School Football

Threshold (g)	Ratio of Mean Impacts per Game	Lower 95% CL	Upper 95% CL	Uncorrected p-value	Bonferroni Lower 95% CL	Bonferroni Upper 95% CL	Bonferroni p-value
10	0.40	0.21	0.77	0.006	0.17	0.96	0.034
20	0.30	0.17	0.55	<0.001	0.14	0.68	0.001
30	0.23	0.12	0.41	<0.001	0.10	0.51	<0.001
40	0.18	0.10	0.34	<0.001	0.08	0.42	<0.001
50	0.18	0.10	0.33	<0.001	0.08	0.41	<0.001
60	0.21	0.10	0.41	<0.001	0.08	0.52	<0.001
70	0.15	0.08	0.29	<0.001	0.06	0.37	<0.001
80	0.14	0.06	0.37	<0.001	0.04	0.52	<0.001
Global Test: CL vs HF		DF = 8	Wald Statistic = 74.1		p < 0.001		
Threshold (rad/s ²)	Ratio of Mean Impacts per Game	Lower 95% CL	Upper 95% CL	Uncorrected p-value	Bonferroni Lower 95% CL	Bonferroni Upper 95% CL	Bonferroni p-value
0	0.40	0.21	0.77	0.006	0.17	0.96	0.034
2000	0.33	0.18	0.61	<0.001	0.15	0.75	0.002
4000	0.26	0.14	0.47	<0.001	0.11	0.58	<0.001
6000	0.22	0.12	0.39	<0.001	0.10	0.48	<0.001
8000	0.19	0.10	0.35	<0.001	0.08	0.43	<0.001
10000	0.20	0.10	0.38	<0.001	0.08	0.47	<0.001
12000	0.16	0.08	0.29	<0.001	0.07	0.36	<0.001
14000	0.08	0.04	0.18	<0.001	0.03	0.24	<0.001
Global Test: CL vs HF		DF = 8	Wald Statistic = 92.4		p < 0.001		

College Soccer vs. High School Football

Threshold (g)	Ratio of Mean Impacts per Game	Lower 95% CL	Upper 95% CL	Uncorrected p-value	Bonferroni Lower 95% CL	Bonferroni Upper 95% CL	Bonferroni p-value
10	1.54	0.62	3.80	0.353	0.45	5.20	1.000
20	0.57	0.30	1.08	0.085	0.24	1.35	0.512
30	0.46	0.21	0.99	0.047	0.16	1.29	0.284
40	0.39	0.16	0.96	0.040	0.12	1.31	0.242
50	0.28	0.11	0.67	0.005	0.08	0.92	0.028
60	0.22	0.10	0.49	<0.001	0.08	0.64	0.001
70	0.30	0.14	0.66	0.003	0.10	0.86	0.015
80	0.19	0.05	0.69	0.012	0.03	1.08	0.070

Global Test: CS vs HF		DF = 8 Wald Statistic = 85.1 p < 0.001					
Threshold (rad/s ²)	Ratio of Mean Impacts per Game	Lower 95% CL	Upper 95% CL	Uncorrected p-value	Bonferroni Lower 95% CL	Bonferroni Upper 95% CL	Bonferroni p-value
0	1.54	0.62	3.80	0.353	0.45	5.20	1.000
2000	1.04	0.43	2.48	0.934	0.32	3.36	1.000
4000	0.57	0.28	1.15	0.115	0.22	1.46	0.690
6000	0.43	0.21	0.89	0.022	0.16	1.14	0.135
8000	0.30	0.15	0.61	0.001	0.11	0.79	0.006
10000	0.28	0.13	0.60	0.001	0.10	0.79	0.007
12000	0.21	0.09	0.48	<0.001	0.07	0.64	0.001
14000	0.12	0.05	0.29	<0.001	0.04	0.40	<0.001
Global Test: CS vs HF		DF = 8 Wald Statistic = 387.6 p < 0.001					

College Lacrosse vs. College Soccer

Threshold (g)	Ratio of Mean Impacts per Game	Lower 95% CL	Upper 95% CL	Uncorrected p-value	Bonferroni Lower 95% CL	Bonferroni Upper 95% CL	Bonferroni p-value
10	0.26	0.10	0.66	0.004	0.08	0.90	0.026
20	0.53	0.28	1.03	0.060	0.22	1.29	0.358
30	0.49	0.23	1.06	0.068	0.17	1.38	0.411
40	0.47	0.19	1.21	0.117	0.14	1.66	0.702
50	0.65	0.26	1.63	0.358	0.19	2.23	1.000
60	0.93	0.39	2.23	0.877	0.29	3.02	1.000
70	0.50	0.22	1.13	0.095	0.17	1.49	0.570
80	0.78	0.18	3.41	0.739	0.11	5.69	1.000
Global Test: CL vs CS		DF = 8 Wald Statistic = 57.6 p < 0.001					
Threshold (rad/s ²)	Ratio of Mean Impacts per Game	Lower 95% CL	Upper 95% CL	Uncorrected p-value	Bonferroni Lower 95% CL	Bonferroni Upper 95% CL	Bonferroni p-value
0	0.26	0.10	0.66	0.004	0.08	0.90	0.026
2000	0.32	0.13	0.77	0.010	0.10	1.04	0.063
4000	0.45	0.22	0.92	0.030	0.17	1.19	0.179
6000	0.51	0.23	1.10	0.087	0.18	1.44	0.522
8000	0.63	0.29	1.37	0.244	0.22	1.79	1.000
10000	0.70	0.30	1.65	0.417	0.22	2.22	1.000
12000	0.74	0.31	1.77	0.496	0.23	2.40	1.000
14000	0.67	0.23	1.89	0.446	0.16	2.71	1.000
Global Test: CL vs CS		DF = 8 Wald Statistic = 29.4 p < 0.001					

DISCUSSION

This study quantitatively describes differences in head impact frequency and severity during live play of college football (CF), high school football (HF), college men's soccer (CS), and college men's lacrosse (CL). While the majority of these impacts do not result in a clinical diagnosis of concussion, the hypothesized short-term and long-term effects of repetitive subconcussive head impacts on brain structure^{50,97,106,221} and function^{20,89,106,187}, coupled with their proposed role in increasing susceptibility to neurodegenerative disorders^{101,140}, suggest that quantification of subconcussion may be important for assessing each sport's overall safety. Previous studies have measured the frequency and severity of subconcussive head impacts in these sports, but methodological differences in impact measurement or estimation have generally made it difficult to compare their results. This is the first study to use the same biomechanical sensor to quantify subconcussion in disparate sports to provide data for a direct comparison between them.

CF has the most impacts per practice and second most per game, as well as the highest average linear and rotational impact severity. These high values for CF cause it to have the highest impact burden (PRLA and PRRA sum per event) of all of the quantified teams. HF has the third most impacts per event, but an average linear and rotational impact severity per game and average linear impact severity per practice that is on par with CF. CS has the second most impacts per practice and most impacts per game, but has the lowest average linear and rotational impact severity. Interestingly, HF's moderate impact rate with high average impact severity and CS's high impact rate with low average impact severity results in statistically equivalent impact burden curves. CL has

the fewest impacts per event and the third lowest average linear and rotational impact severity per practice and per game. Ultimately, the low impact rate and relatively low impact severity causes CL to have the lowest impact burden in both practices and games.

The ratio of means plots at multiple linear and rotational acceleration thresholds for practices and games shows that differences in the number of impacts per event are consistent across multiple thresholds. The exception is CS, which experiences a sharp drop in number of impacts as the linear acceleration threshold increased from 10g to 20g. At 10g, CS is second to, or higher than CF in number of impacts per event (CS:CF RoM = 0.56/practice, 1.28/game), but is much lower at 20g (CS:CF RoM = 0.21/practice, 0.49/game). McCuen et al. (2015) hypothesized that head accelerations of 10g-20g in soccer could be caused by “hard stops, cuts, and hard kicks¹²⁶.” Both football and lacrosse have hard stops and cuts, but hard kicks are unique to soccer and may be responsible for the higher proportion of low severity head accelerations in soccer. While these head accelerations may not be caused by a direct impact to the head, the lower limits of physiological relevance for head acceleration is not known, thus this study analyzed all impacts recorded by the sensor, which triggers at 10g.

The present study has several notable points of agreement and disagreement with published live play data using the helmet-based HITS in football. CF’s 13.2 impacts per practice and 24.2 impacts per game are a little higher than the reported range for college football from Crisco et al. (2010), 4.8 to 7.5 impacts per practice and 12.1 to 16.3 impacts per game⁴⁴. CF’s PRLA per impact of 26.8g and 29.3g for practices and games is similar to published values for PRLA per impact in college football, which range from 20.5g to 32.0g^{45,56,131,162}, but CF’s PRRA per impact of 5140.0rad/s² and 5805.8rad/s² for practices

and games is substantially higher than the published values for PRRA per impact, in college football which range from 1355rad/s^2 to 1400rad/s^2 ^{45,162}. Similarly, HF's 5.3 impacts per practice and 14.3 impacts per game are similar to published values for high school football, which range from 3.1 to 10.7 impacts per practice and 15.7 to 28.7 impacts per game^{25,26,120,185}. HF's PRLA per impact of 25.2g and 27.1g for practices and games were also similar to published values in high school football, which range from 21.9g to 28.6g^{24-26,120,185,191}, but HF's PRRA per impact values, 4327.1rad/s^2 for practices and 4796.6rad/s^2 for games, are more than double the highest published values in high school football, which range from 973rad/s^2 to 1777rad/s^2 ^{24-26,120,185,191}. While the difference between the presented data and the published data could reflect true head impact differences in our population, it is more likely due to differences between the xPatch and HITS. HITS is a helmet-mounted sensor system that was used to collect most of the published football data, but its helmet-mounted nature does not allow for use in non-helmeted sports like lacrosse and soccer.

CS' impact data values of 7.4 impacts per practice with an average PRLA and PRRA per impact of 18.5g and 2960.4rad/s^2 , and 31.1 impacts per game with an average PRLA and PRRA per impact of 17.6g and 2713.8rad/s^2 differ with some of the published data for soccer. One study used a modified accelerometer suite from HITS and measured head impacts during a small number of scrimmages; they reported an average PRLA and PRRA per impact of 19.4g and 1666.8rad/s^2 for non-header impacts⁷⁵. McCuen et al. (2015) also used the xPatch sensor to measure head impacts during high school (girls') and college (women's) soccer, and they reported an average PRLA and PRRA per impact of 37.6g-39.3g and 7523rad/s^2 - 7713rad/s^2 ¹²⁶. However, these differences are likely

driven by their decision to use a minimum threshold of 20g in their analysis; since the distribution of head impact severities is highly weighted toward lower values, differences in the minimum threshold can have large effects on the calculated average severity values. This reality makes it difficult to compare published results from biomechanical studies of head impact, as the minimum threshold is arbitrarily set for each study (although 10g, 15g, or 20g thresholds seem to be most common). In the present study, we chose to use the default 10g setting of the device, as the minimum threshold for physiologically significant impacts is unknown. Furthermore, a plurality of biomechanical head impact studies in sport use a 10g threshold⁹⁵, which enables wider comparison to the existing literature across sports.

The most current analysis on the epidemiology of sports-related concussion in college sports reports that college football, soccer, and lacrosse have a concussion incidence rate of 30.07, 9.69, and 9.31 concussions per 10,000 games, and 4.20, 1.75, and 1.95 concussions per 10,000 practices, respectively²²⁸. If the incidence of concussion is tied to head impact exposure, it would follow that one of the head impact metrics would mirror concussion incidence, with football much higher than soccer and lacrosse but with similar values for soccer and lacrosse. CF indeed has indeed the highest number of impacts per event, but for impacts per game CS is close to CF and much higher than CL. CF also has the highest average PRLA and PRRA per impact, and is significantly higher than CS and CL for both practices and games. CS and CL are differentiable in average PRLA and PRRA per impact in practices but not games. Median PRLA and PRRA sum per game is 567g and 111,800rad/s² for CF, 410g and 61,700rad/s² for CS, and 219g and 40,200rad/s² for CL. Median PRLA and PRRA sum per practice is 277.3g and

53,800rad/s² for CF, 84.9g and 13,900rad/s² for CS, and 41.6g and 7,600rad/s² for CL.

While none of these metrics exactly mirror the relative concussion rates, average impact severity comes closest to matching the pattern of concussive risk in these sports.

Limitations. Several factors could affect the generalizability of the comparisons between these teams. This study reports findings from only one college football team, one high school football team, one college men's lacrosse team, and one college men's soccer team. The college teams were Division I, with a national championship men's soccer team, a top 20 men's lacrosse team, and an unranked football team. The high school football team was from a small private school in the Virginia Independent Schools Athletic Association Division II. In football, head impact can be affected by the style of offensive play¹²⁰, and given that in this study only one team represents each sport, the results could be affected by team selection (i.e. less elite lacrosse or soccer teams could result in lower head impact values, and/or more competitive football teams could result in higher head impact values). Considering that CF had the highest impact burden, HF and CS tied in the middle, and CL had the lowest, it would stand to reason that choosing more competitive football teams or less competitive soccer and lacrosse teams would only further differentiate the teams' head impact values.

The xPatch accelerometer used in the present study appears in six published studies^{47,94,126,185,186,208}, three of which test biomechanical validity in different settings^{47,126,208}. Wu et al. (2015) compared in vivo performance of the xPatch against video capture in a simulated low-impact soccer setting; that study examined 25 impacts, one impact location, one mastoid placement location, and one xPatch device. In one subject, they found the xPatch overestimated individual linear and rotational

accelerations (normalized root-mean-squared error (RMSE) of 120% for PRLA and 290% for PRRA) in ways likely related to the viscoelastic properties of that individual's soft tissues²⁰⁸. As prelude to a live play soccer study, McCuen et al. (2015) evaluated xPatch performance on a Hybrid 3 headform; this study examined 250 impacts, spread over five impact locations, in two mastoid placement locations, and included data from five different xPatch devices. McCuen et al. (2015) also found significant xPatch measurement error related to individual impacts (RMSE of ~50% for individual PRLA and PRRA values). McCuen et al. (2015) also looked at aggregate performance over larger numbers of impacts and concluded, "average values over a large number of acceleration events can be determined with good accuracy¹²⁶."

Cummiskey et al. (2016) performed the most thorough comparison to date of the reliability and accuracy of helmet-mounted and head-mounted accelerometer systems. The study included both the current gold-standard HIT system and the xPatch, among other accelerometer systems⁴⁷. Cummiskey et al. (2016) used two devices for each system, used right and left sensor locations for the xPatch, and delivered 140 impacts across 7 impact locations to evaluate each device and sensor location. Root mean squared error (RMSE) was calculated for each device, sensor location, and impact location using the values generated from accelerometers inside a Hybrid III headform to which the devices were attached. The xPatch did produce considerable RMSE across impact locations (8%-58% for PRLA and 11%-350% for PRRA), but across devices, sensor locations, and impact locations the xPatch produced RMSE that were considerably lower than, or at least comparable to, the RMSE produced by the HIT system. Cummiskey et al. (2016) does rightly point out that the RMSE for the xPatch could have been

underestimated in their study as the Hybrid III headform does not realistically mimic the skin surface, which could shift slightly in response to a head impact. Cummiskey et al. (2016) also demonstrates that RMSE was consistently lower when the xPatch was applied behind the right ear⁴⁷. This study includes data from collected from left and right sensor locations, but the majority of the data was collected when the sensor was behind the right ear as that was used as the default location.

A separate publication studying college football with the xPatch sensor¹⁵⁶ reported head impact quantities and linear acceleration severities comparable to similar studies using helmet-based systems^{26,45,131,162,163}. But in the same study, discrepancies existed between rotational severity of head impact measured by the mastoid accelerometer and similar published data from helmeted systems, which could be a result of the high RMSE found in Wu et al. (2015), McCuen et al. (2015), and Cummiskey et al (2016). We believe the transformed values reported by all head impact sensors in live play settings should be viewed skeptically, as they probably do not reflect the “ground truth” biomechanical forces experienced by the brain. The xPatch data for individual hits is almost certainly noisy, but if the errors are systematic or random, comparison of across situations and groups with large numbers of impacts should still be valid. The present study addresses this limitation by testing relative impact comparisons (college vs. high school and football vs. soccer vs. lacrosse) rather than focusing on the absolute values reported.

Conclusions. This study demonstrates how a mastoid patch accelerometer can be deployed in a variety of helmeted and non-helmeted sports to collect head impact data that can be used to compare the relative subconcussive head impact burden in each sport.

Although the concept of subconcussion is drawing increased attention from the scientific, medical, and athletic communities, it is still unclear how subconcussion relates to concussion incidence and what levels of subconcussive head impact are physiologically relevant. However, the variety and gravity of the research-supported consequences of subconcussion make the head impact profile of each sport (impacts/event, PRLA/impact, PRLA sum/event, etc.) an important aspect in the evaluation of a sport's risk, just as the incidence of concussion or knee injuries has been for decades. In response to concerns about subconcussion, governing bodies for multiple sports are actively investigating ways to reduce their athletes' unnecessary head contact. College football players may experience the highest values for nearly every head impact metric, but there is also a wide range of head impact that can occur among different contact or collision sports. Level of play (high school vs. college) and type of sport (football vs. soccer vs. lacrosse) each have sizable effects on head impact values, indicating that larger and more comprehensive studies are still needed for each sport at every level of play to understand the amount of head impact experienced by the athletes. Open topics that could be addressed by large-scale quantification of head impact in sport include determining the effects of: competition level (youth to professional), gender in similar sports, player position, rule changes, and changes to protective equipment. This information could be useful in reducing the head impact across all contact and collision sports.

CHAPTER III: EFFECTS OF SUBCONCUSSION ON THE FUNCTIONAL ACTIVITY AND CONNECTIVITY IN THE BRAIN

INTRODUCTION

Multiple concussions over the course of a long career in American football can affect a player's brain long after participation in the sport has ended, possibly increasing the player's susceptibility for multiple neurodegenerative disorders^{101,128,140,180}. A patient with a concussion can present with any number or combination of concussion's symptoms (dizziness, blurred vision, nausea, headache, etc.) and signs (balance abnormalities, reaction time deficits, etc.)¹⁶. Heterogeneity in clinical presentation likely indicates spatial heterogeneity in the underlying injury location in the brain¹⁵⁸. Multiple biomechanical and biological factors play a role in where and how each unique head impact affects the brain^{149,219}. The effects of repetitive subconcussive head impacts that athletes receive during routine competition are even less understood. The majority of sports-related head impacts do not cause concussion, but there is mounting evidence that even subconcussive head impacts can affect brain structure^{50,97,106,221}, function^{1,20-21,89,132,157,169,185,187}, and performance^{82,92,190}. Aggregately, these studies suggest that subconcussive head impacts might produce spatially heterogeneous effects on the brain, that are similar to, but less severe than, the effects from concussion⁷.

Functional magnetic resonance imaging (fMRI) is a noninvasive method for measuring functional activity in the brain that had proven capable of detecting functional changes in the brain related to subconcussion. The first studies to indicate that subconcussive head impacts can cause functional changes in the brain used fMRI with a working memory task^{20,21,157,169,187}. These studies identified a group of athletes who were

not diagnosed with a concussion but exhibited functional impairment in multiple regions and experienced a higher subconcussive head impact load compared to athletes without functional impairment. Using task-independent resting state fMRI (rs-fMRI), Johnson et al. (2014) found changes in functional connections between multiple regions in the default mode network (DMN)⁸⁹, and Abbas et al. (2015) found changes in the number of regions connected to the DMN¹ after exposure to repetitive subconcussive head impacts. Task-based fMRI has found changes in working memory and rs-fMRI has found changes in the functional connectivity of the DMN, but there is no reason to assume that these tasks and networks are the only, or even the primary, areas affected by subconcussion. If the physiological effects of subconcussion have heterogeneity similar to concussion¹⁵⁸, then it may be more appropriate to use whole-brain fMRI analyses that are independent of specific brain functions and networks.

Resting-state fMRI data can be used to calculate many aspects of functional activity and connectivity for each grey matter voxel, including metrics reflecting spontaneous neural activity, and short- and long range functional connectivity. Amplitude of low-frequency fluctuations (ALFF) is a commonly used measure spontaneous brain activity that calculates the strength of activity in the brain within a specific frequency range (0.01-0.10Hz) associated with neural activity²¹⁶. Fractional ALFF (fALFF) is also a commonly used measure of spontaneous brain activity that calculates the power of the ALFF signal divided by the power of the entire frequency spectrum²²⁷. Regional homogeneity (ReHo) is a commonly used measure of local connectivity that calculates connectivity between a grey matter voxel and its immediate contiguous neighboring voxels. Degree centrality (DC) is a commonly used measure of global connectivity that

calculates connectivity between one grey matter voxel and all other grey matter voxels in the brain. Zhan (2016) recently investigated whether ALFF and fALFF changed after patients sustained a mild traumatic brain injury (mTBI). Their analyses revealed multiple brain regions that contained areas with statistically significant increases or decreases in ALFF or fALFF in the days following injury. Meier, Bellgowan, and Mayer (2016) recently investigated whether ReHo and DC changed after athletes sustain a concussion and made several compelling findings. Their analyses revealed several brain regions that contained areas with statistically significant increases or decreases in ReHo one-month after a concussion, but no areas experienced a significant change in DC¹²⁹. If repetitive subconcussive head impacts affect changes similar to mTBI and concussion, then ALFF, fALFF, ReHo and DC may be useful metrics to detect those changes.

In fMRI data analysis, mass-univariate application of the general linear model (GLM) accounts for the vast majority of publications over the last 20 years and all of the fMRI studies of mTBI publications to date. Mass-univariate analysis of fMRI data is most useful for identifying situations where the same region of interest shows the same type of change across the entire population under investigation. However, if the underlying change of interest exhibits spatial heterogeneity across participants, mass-univariate application of the GLM becomes poorly matched to the problem under investigation. Studies of mTBI from different domains – clinical, biomechanical, and fMRI – support the idea that spatial heterogeneity of injury is likely a dominant feature of mTBI¹⁵⁸. It is well-described that concussion presents with a variable set of signs and symptoms¹⁶, to the point that physicians who see concussion patients are fond of the statement, “If you have seen one concussion, you have seen one concussion”. Data from

both biomechanical simulations and live action sports competition suggest the clinical variability may exist because each unique head impact likely imparts different forces on different brain regions^{14,25,44,149,160,203}. The existing fMRI studies of concussion support this idea, with many reporting different areas of change in brain activity²¹³, suggesting spatial differences between populations with similar mechanisms of injury. If we hypothesize that subconcussion affects similar brain regions as concussion, in a less severe manner, mass-univariate application of the GLM may be insufficient to detect changes related to subconcussion.

To address some of the weaknesses of mass-univariate analysis, some fMRI researchers have started using multivariate analyses as a complement to standard mass univariate analyses¹¹⁶. For example, multivoxel pattern analyses (MVPA) can probe the information in distributed neural patterns without assuming a specific spatial model. MVPA is often performed within the framework of supervised learning classification, using a training set of data to create classification algorithms that discriminate between two known groups, before testing classifier performance on novel data¹¹⁶. The resulting algorithms differentially weight voxels across the brain that might collectively discriminate between two (or more) groups of interest. This general approach has the benefit of being more robust in detecting changes that are spatially heterogeneous or spatially distributed across a group. Linear support vector machine (SVM) classification is an increasingly common technique in fMRI that tries to create a hyperplane decision boundary that separates the two groups' feature sets with the maximum possible margin^{41,192}. For fMRI data, the strength of linear SVM lies in its ability to deal with high dimensionality data and resistance to overtraining^{61,130}; but a significant weakness is the

open question of whether resulting classifier weight maps contain useful information about spatial distribution of effects in the brain⁷⁷.

We hypothesize that the hundreds of subconcussive head impacts sustained in college football produce spatially heterogeneous changes in brain functional connectivity that should be measurable with resting state fMRI (rs-fMRI). To test this hypothesis, the present study collected preseason and postseason rs-fMRI data from college football, soccer, and lacrosse players and a matched control group. At each time point, ALFF, fALFF, ReHo, and DC were respectively used as voxel-based measures of spontaneous brain activity, local functional connectivity, and global functional connectivity throughout the brain. Changes in ALFF, fALFF, ReHo, and DC between the two time points were tested with both: 1) mass-univariate application of the GLM and 2) paired implementation a linear SVM classification. In addition, a ranking distance measure was used to test if the spatial information resulting from the mass-univariate analysis shared any information with the weight maps resulting from the SVM classification, despite the disparate ways these maps are generated.

METHODS

Participants. From 2013 to 2015, preseason and postseason resting-state fMRI data was collected from 31 college football players (CF), 18 college men's lacrosse players (CL), 14 college men's soccer players (CS), and 30 male controls (MC) (mean (SD) age: 20.3 (1.5) years, 20.2 (1.2) years, 20.4 (1.2) years, 21.7 (3.3) years, respectively). For the college athletes, preseason data was collected less than one week into the sports season; postseason data was collected less than two weeks after the final game or practice of the

season or postseason (mean (SD) days between scans: CF=133.5(9.2), CL=63.6(13.2), CS=86.6(4.5)). Football player data was collected during their fall competitive season, while lacrosse and soccer player data was collected during their respective fall and spring practice seasons. For male controls, the two scanning sessions were separated by 3-4 months to approximate the length of an athletic season (mean (SD) days between scans: 108.7 (6.4)). College athletes were volunteers from NCAA Division I teams without a history of developmental or neurological disorder, or moderate to severe traumatic brain injury. Nineteen CF, seven ML, and six MS players had a history of concussion prior to the start of the season. Male controls were excluded if they had a history of concussion. Four football players sustained an injury or illness that resulted in substantial lost playing time, and three additional players were diagnosed with a concussion during the season; these athletes were excluded from further analyses. For the rs-fMRI analyses, the participants were divided into three groups: college football players (CF), other sports (OS) including both college lacrosse and soccer players, and male controls (MC). The three groups represented high, medium, and low subconcussive exposure, respectively. Six football players had a position and playing status that resulted in little to no expected head impact exposure (ex. redshirt quarterback or back-up kicker), and were therefore excluded from further analysis. The OS athletes also serve as a college athlete control group to account for possible aerobic training confounds, or other factors that may differentiate college athletes from their non-athlete peers.

Standard protocol approvals, registrations, and patient consents. The University of Virginia Institutional Review Board for Health Science Research approved the research protocol. All participants gave written informed consent.

Data acquisition. Data for this study was collected at the University of Virginia Health System on a Siemens MAGNETOM Trio MRI. A whole brain multiband BOLD sequence (University of Minnesota, CMMR sequence, <https://github.com/CMRR-C2P/MB>)^{59,133,210} (TR/TE=1000ms/32ms, slice thickness=3mm, slice spacing 0.75mm, in-plane dimensions 3x3 mm, flip angle=90°, matrix=64x64, multiband factor=4, volumes=480) was acquired during an eyes-open resting state: the participants were instructed to lie still and remain awake. A three-dimensional high resolution T1 magnetization-prepared rapid gradient-echo (MPRAGE) sequence (TR/TE=1200/2.27, slice thickness=1mm, in-plane dimensions=0.977x0.977 mm, flip angle=9°, matrix=256x256) was acquired as an anatomical reference.

Data preprocessing. Each participant's anatomical image was brain extracted using Advanced Normalization Tools (ANTs)⁵ antsBrainExtraction.sh script. A college athlete and control (CAC) template was created from a random selection of 30 participants' anatomical scans using antsMultivariateTemplateConstruction2.sh. The Desikan-Killiany-Tourville (DKT) atlas⁹⁶ was applied to the CAC template using antsJointLabelFusion.sh and twenty hand-labeled brains from the OASIS-TRT dataset⁹⁶. The following preprocessing steps were performed in ANTs with R (ANTsR)⁴ unless otherwise specified. The first 10 time points of the rs-fMRI were removed to allow the MRI to reach signal equilibrium. White matter signal, CSF signal, grey matter noise¹⁵, six-degrees of motion parameters and their squares, and derivatives of original and squared motion parameters were regressed from the rs-fMRI images. Time points that exceeded a framewise displacement of 0.5mm were removed from subsequent analyses, along with the following time point, and were replaced with β -spline interpolation. If

either a participant's preseason or postseason scan had a mean translation across all time points greater than 0.25mm compared to the participant's average BOLD image, that participant was removed from further analyses; this excluded three football players, two lacrosse players, two soccer players, and one control. rs-fMRI images were then transformed to the CAC template using `antsRegistration` and `antsApplyTransforms` commands.

Calculating measures of spontaneous brain activity and functional brain

connectivity (Figure 1). Preprocessed BOLD images were used to calculate measures of functional connectivity using the Data Processing Assistant for Resting State fMRI (DPARSF) version 4.0³². A cortical grey matter mask, segmented from the CAC template, was used to mask the data before metric calculation. Amplitude of low-frequency fluctuations (ALFF) and fractional amplitude of low-frequency fluctuations (fALFF) for each set of BOLD images. ALFF is a measure of the strength of spontaneous activity in the brain within a specific frequency range (0.01-0.10Hz) associated with neural activity²¹⁶. Fractional ALFF (fALFF) is a measure of the power of the ALFF signal divided by the power of the entire frequency spectrum²²⁷. BOLD images were then bandpass filtered (0.01-0.10 Hz) before calculation of the two metrics. Regional homogeneity (ReHo) and degree centrality (DC) were calculated for each set of BOLD images. ReHo is the Kendall's coefficient of concordance (KCC) for a 27 voxel cube, and is a measure of local functional connectivity within that small neighborhood²²⁰. Weighted degree centrality (DC) is the sum of Pearson correlations between a voxel's time series and that of all other voxels, and is a measure of global functional connectivity. The resulting ALFF, fALFF, ReHo and DC brain maps were then Fisher z-transformed by

subtracting the mean of the brain map from each voxel, and then dividing each voxel's resulting value by the standard deviation of the brain map. Metric difference maps (ex. $\Delta ReHo$) were created, by subtracting a participant's preseason metric map from their postseason metric map (ex. $postReHo - preReHo = \Delta ReHo$).

Mass-univariate analyses. Individual metric post-pre difference maps for subjects within a group were merged into 4D images using the Oxford Centre for Functional MRI of the Brain (FMRIB) Software Library's (FSL) `fslmerge` command⁸⁶. In order to identify voxel clusters of statistically significant metric change over the course of the season, a permutation-based one-sample two-tailed t-test was performed with FSL's `randomise` (v5.0, 5000 permutations)²⁰⁴ using threshold-free cluster enhancement¹⁷⁶ with a ten voxel cluster threshold.

Multivariate analyses. Linear support vector machine (SVM) classification was chosen as the multivariate analysis method^{134,143}. Classifier training and testing was implemented using Pattern Recognition for Neuroimaging Toolbox (PRoNTv2.0)¹⁶⁵. A linear kernel was used to avoid overtraining due to the high dimensionality of the data set (1000s of voxels) with relatively few examples (participants)^{19,135,193}. A paired version of the SVM was implemented to distinguish between a participant's metric difference map (ex. $\Delta ReHo$) and its opposite (ex. $-\Delta ReHo$)¹⁷⁹. Pioneered by Sripada et al. (2013)¹⁷⁹, the paired SVM is analogous to a paired t-test, in which the mean of a subject's two observations is subtracted from their values. For the paired SVM, the metric difference map (ex. $\Delta ReHo$) and the negative metric difference map (ex. $-\Delta ReHo$) are used as classes for the algorithm to differentiate between, rather than the preseason and postseason metric maps; accounting for the within-subjects design of the study. The

paired SVM ensures that the algorithm output for each subject's difference metric maps (ex. ΔReHo and $-\Delta\text{ReHo}$) are centered around the classification decision line, resulting in equivalent class accuracy and total accuracy for each particular group and metric. The SVM classifier is trained through leave-one-out cross-validation (LOOCV) on all but one subject's difference maps and then the classifier is tested on the left-out subject. LOOCV is a method to train with the maximum number of examples without testing the classifier on a subject on which the classifier was trained. Each LOOCV iteration results in a weight map, this weight map is multiplied by the difference map being classified and then summed to get a single classifier value that indicates the predicted class. Further weight map analysis uses the average weight map among all LOOCV iterations. For permutation testing, the classification labels were permuted 5000 times to determine the statistical strength of the classifier's accuracy, with a significance level of $p < 0.05$.

68,150,165

Ranking distance comparisons. Ranking distance is a measure of correspondence between any two rankings that consist of the same items¹⁰², in this case brain regions. Schrouff et al. (2013a) used a very similar measure to compare the correspondence between SVM weight maps¹⁶⁴. Unthresholded t-statistic and SVM weight maps were divided into 66 regions using the DKT atlas. The regions were ranked according to each region's average t-statistic or SVM weight values, resulting in a t-statistic region (T_{ROI}) ranking and SVM weight region (W_{ROI}) ranking for each group and metric. The correspondence between the T_{ROI} and W_{ROI} rankings for a particular group and functional connectivity metric was calculated using a measure of distance:

$$RD(T_{ROI}, W_{ROI}) = \frac{2}{n * (n - 1)} \sum_{i=1}^n \sum_{j=1}^n I_{(T_{ROI}, W_{ROI})}(i, j)$$

where

if $T_{ROI}(i) < T_{ROI}(j)$ and $W_{ROI}(i) > W_{ROI}(j)$, then

$$I_{(T_{ROI}, W_{ROI})}(i, j) = 1$$

else

$$I_{(T_{ROI}, W_{ROI})}(i, j) = 0$$

with $RD(T_{ROI}, W_{ROI})$ as the distance between the T_{ROI} and W_{ROI} rankings, and n as the number of ROI (66). The ranking distance values range from 0 (identical rankings) to 1 (exactly opposite rankings)¹⁶⁴. If the rankings have low ranking distance values, it indicates the mass-univariate and multivariate analyses are converging on similar underlying trends in the data. Statistical significance of the ranking was determined by randomly shuffling the rankings for 5000 permutations and identifying how many random permutations had a lower ranking distance than the actual rankings. Statistical tests were two-tailed, with significantly high ranking distances signifying anti-correspondence, such as regional increases in one group but decreases in another group. The ranking distance was calculated for W_{ROI} rankings between all measures in CF to determine if the spontaneous activity and functional connectivity metrics are experiencing similar spatial trends in college football. The ranking distance was calculated for W_{ROI} rankings between CF and MC for ALFF and fALFF to determine if those groups are experiencing similar spatial effects in these metrics.

College football metric difference maps. To visualize and compare college football's longitudinal trends related to subconcussion with previous findings in concussion^{129,222-}

²²⁴, we created a region average brain map where group mean Δ ALFF, Δ fALFF, Δ ReHo and Δ DC values were averaged over each region in the DKT atlas.

RESULTS

Mass-univariate analyses. For the voxel-wise analyses, testing for spatially homogeneous preseason to postseason differences in ALFF, fALFF, ReHo and DC, no statistically significant clusters with more than ten voxels were found in any group.

Multivariate analyses (Table 6). For the paired SVM classifier trained with a linear kernel with LOOCV, a few metrics and groups produced statistically significant accuracy. CF had a significant class accuracy for ALFF (80%, $p=0.012$), fALFF (87%, $p=0.006$), and ReHo (87%, $p=0.009$) (Figures 9A, 9B, 10A, and 10C), but was not significantly accurate for DC (73%, $p=0.084$) (Figures 10B and 10D). OS did not have significant class accuracy for ALFF (57%, $p=0.323$), fALFF (64%, $p=0.116$), ReHo (50%, $p=0.617$), or DC (57%, $p=0.317$). MC had significant class accuracy for ALFF (76%, $p=0.003$) and fALFF (72%, $p=0.017$), but not for ReHo (62%, $p=0.102$) or DC (55%, $p=0.311$).

Mass-univariate and multivariate ranking distance comparisons. While SVM weight maps are not considered to be spatially interpretable, spatial information is a key component of t-statistic maps output from mass-univariate analyses. Ranking distance is a way to test if the spatial information of an SVM weight map is similar to the spatial information of the corresponding t-statistic map. A low ranking distance would indicate that these mass-univariate and multivariate approaches are converging upon similar underlying effects in the data. All groups and metrics had statistically significant low

ranking distances between SVM weight map and t-statistic map region rankings:

ALFF(CF: RD=0.131, $p<0.001$; OS: RD=0.100, $p<0.001$; MC: RD=0.146, $p<0.001$),

fALFF(CF: RD=0.067, $p<0.001$; OS: RD=0.082, $p<0.001$; MC: RD=0.082, $p<0.001$),

ReHo(CF: RD=0.120, $p<0.001$; OS: RD=0.145, $p<0.001$; MC: RD=0.122, $p<0.001$), and

DC (CF: RD=0.073, $p<0.001$; OS: RD=0.142, $p<0.001$; MC: RD=0.089, $p<0.001$) (Table

7). These ranking distance values were substantially lower than all values calculated

during permutation testing, indicating a very high level of correspondence between the t-statistic and SVM weight maps (Figure 3).

Ranking distance between metrics for college football (Table 8). While the SVM did not produce a significantly high classification accuracy for DC in college football, there appeared to be a trend toward significance. To determine if the findings in CF in ALFF, fALFF, ReHo, and trends in DC exhibited a similar spatial pattern, W_{ROI} rankings were compared using ranking distance with 5000 iterations of permutation testing to determine significance. All comparisons of fALFF, ReHo, and DC in college football's W_{ROI} rankings resulted in a significantly low ranking distances (fALFF vs. ReHo: RD=0.283, $p<0.001$; fALFF vs. DC: RD=0.336, $p<0.001$; ReHo vs. DC: RD=0.398, $p<0.014$). ALFF only yielded a significantly low ranking distance when compared to fALFF (RD=0.341, $p<0.001$), but not when compared to ReHo (RD=0.449, $p=0.223$) or DC (RD=0.462, $p=0.369$).

Ranking difference comparisons for ALFF and fALFF (Table 9). To determine if the findings for ALFF and fALFF in CF, OS, and MC are demonstrating similar spatial changes, W_{ROI} rankings between the groups were compared for these metrics.

Comparisons of CF vs. MC and OS vs. MC did not exhibit significantly low ranking

distances for either metric (CF vs. MC ALFF: $RD=0.506$, $p=0.862$; CF vs. MC fALFF: $RD=0.450$, $p=0.260$; OS vs. MC ALFF: $RD=0.4876$, $p=0.431$; OS vs. MC fALFF: $RD=0.5179$, $p=0.339$), indicating that the region trends for these groups and metrics are not experiencing similar effects. Conversely, comparisons of CF vs. OS did result in significantly low ranking distances for (ALFF: $RD=0.3483$, $p<0.001$; fALFF: $RD=0.3706$, $p=0.001$).

College football metric difference maps (Figure 12). In college football among the 66 regions in the DKT atlas, the five most increased regions for ALFF are (in order) the left paracentral lobule, right paracentral lobule, right cuneus, left cuneus, and the left medial orbitofrontal cortex. The five most decreased regions for ALFF are the right temporal pole, right parahippocampal gyrus, left pars triangularis, right pars triangularis, and left parahippocampal gyrus (Table 10). The five most increased regions for fALFF are the right cuneus, left pericalcarine cortex, right lateral occipital cortex, right lingual gyrus, and left lingual gyrus. The five most decreased regions for fALFF are the right temporal pole, left rostral anterior cingulate, left caudal anterior cingulate, right rostral anterior cingulate, and right caudal anterior cingulate (Table 11). The five most increased regions for ReHo are the left pericalcarine cortex, right lingual gyrus, left lingual gyrus, right pericalcarine cortex, and left postcentral gyrus. The five most decreased regions for ReHo are the right rostral anterior cingulate, left caudal anterior cingulate, right pars triangularis, left rostral anterior cingulate, and left pars orbitalis (Table 12). The five most increased regions for DC are the right parahippocampal gyrus, right entorhinal cortex, left temporal pole, right fusiform gyrus, and left parahippocampal gyrus. The five most decreased regions for DC are the right pars triangularis, right rostral middle frontal gyrus,

right supramarginal gyrus, right inferior parietal gyrus, and left caudal anterior cingulate (Table 13). Results for ALFF and fALFF in the male control group are presented in figure 13 and tables 14 and 15, respectively.

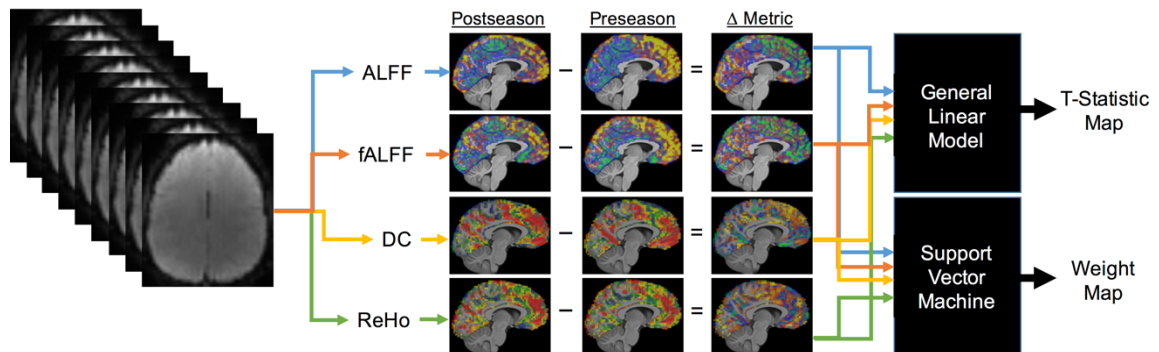


Figure 8. Analysis framework. At each time point (preseason and postseason), amplitude of low-frequency fluctuations (ALFF), fractional ALFF (fALFF), regional homogeneity (ReHo) and degree centrality (DC) metrics are calculated for each participant's preprocessed rs-fMRI data, resulting in ALFF, fALFF, ReHo, and DC values for each grey matter voxel. To control for variability between subjects, metric difference maps (Δ Metric) are created by subtracting the participants' preseason metric map from their postseason metric map. Then metric difference maps are analyzed using mass-univariate (general linear model) and multivariate (support vector machine) analyses, resulting in group t-statistic and SVM weight maps.

METRIC	GROUP	CLASS ACCURACY	TOTAL ACCURACY	P-VALUE
ALFF	CF	80.00%	80.00%	0.001
	OS	57.14%	57.14%	0.323
	MC	75.86%	75.86%	0.003
fALFF	CF	86.67%	86.67%	0.006
	OS	64.29%	64.29%	0.116
	MC	72.41%	72.41%	0.017
ReHo	CF	86.67%	86.67%	0.009
	OS	50.00%	50.00%	0.617
	MC	62.07%	62.07%	0.102
DC	CF	73.33%	73.33%	0.084
	OS	57.14%	57.14%	0.317
	MC	55.17%	55.17%	0.311

Table 6. Support vector machine classification results. CF=college football, OS=other sports (soccer and lacrosse), MC=male controls, ALFF=amplitude of low-frequency fluctuations, fALFF=fractional ALFF, ReHo=regional homogeneity, DC=degree centrality.

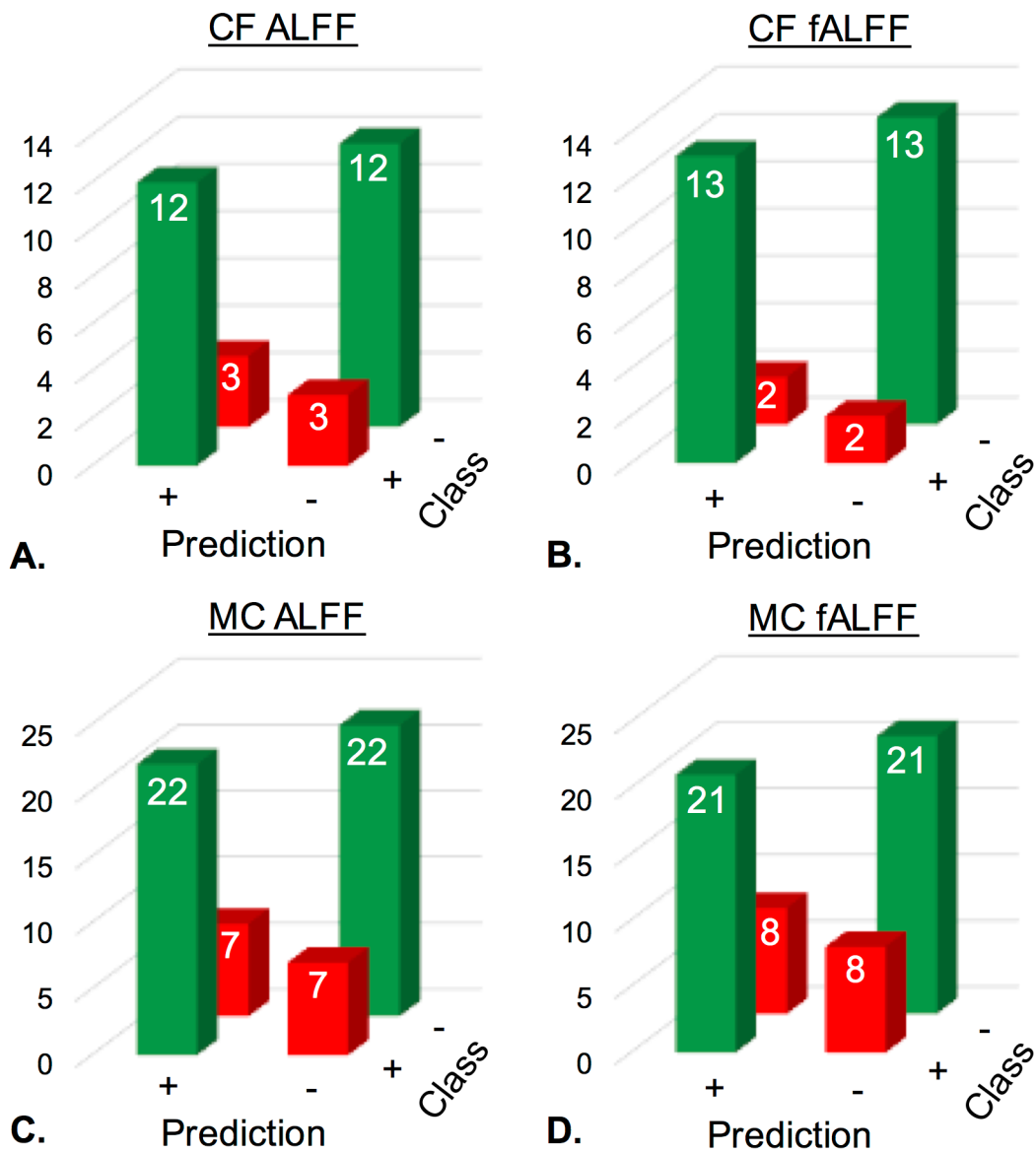


Figure 9. SVM classification ALFF and fALFF. College football's (CF) SVM classification confusion matrix for ALFF (A) and fALFF (B) and the control group's (MC) SVM classification confusion matrix for ALFF (C) and fALFF (D) depict the number of correct and incorrect predictions for each class (ex. Δ ALFF vs $-\Delta$ ALFF).

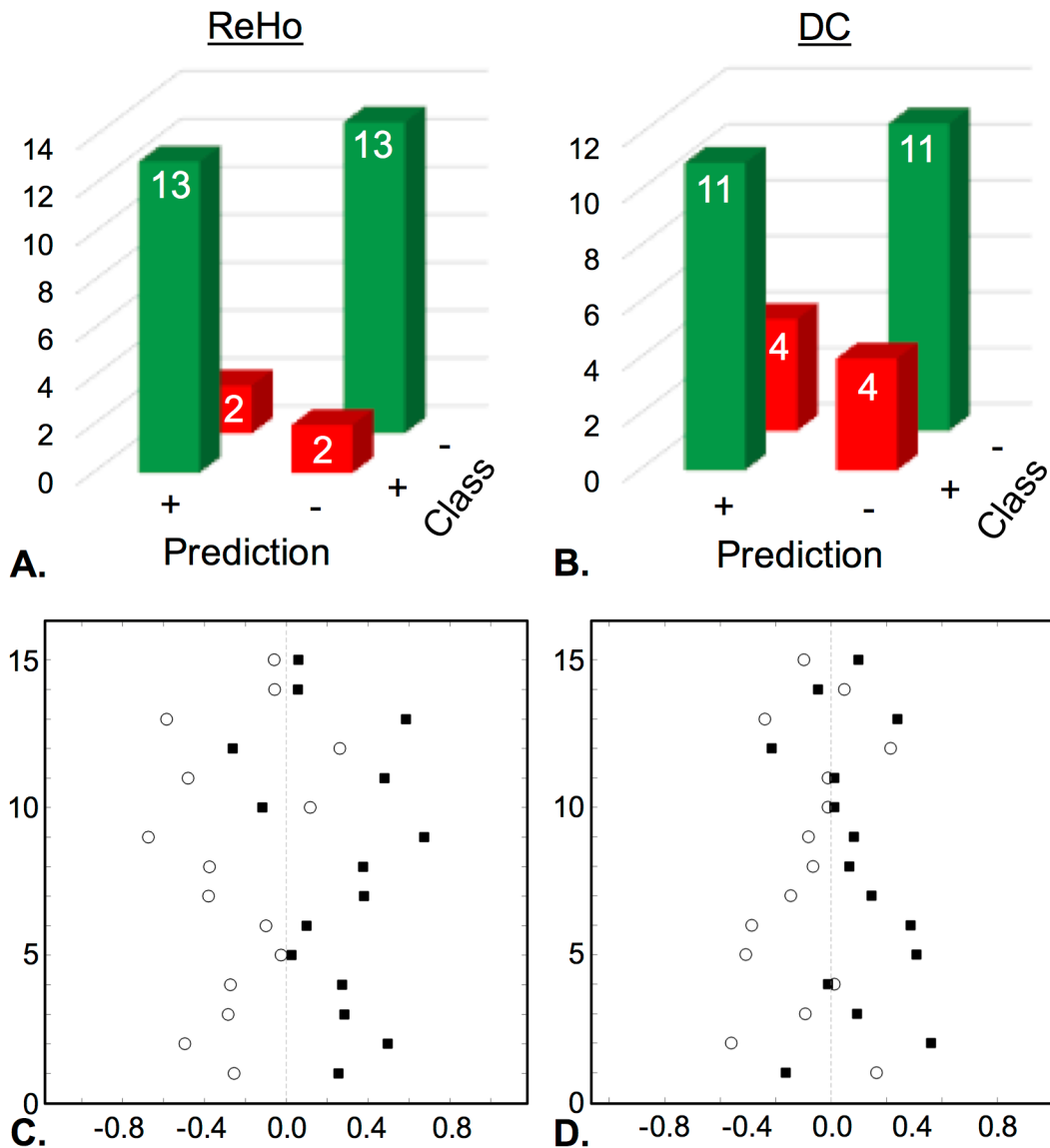


Figure 10. SVM classification for college football. College football's SVM classification confusion matrix for ReHo (A) and DC (B) depict the number of correct and incorrect predictions for each class (ex. ΔReHo vs $-\Delta\text{ReHo}$). The SVM prediction plot for ReHo (C) and DC (D) shows result of the SVM decision function for each participant. Dotted line at zero represents the decision threshold which is zero-centered by the paired nature of the SVM. Closed black squares represent metric difference maps (ex. ΔReHo) and open circles represent their opposite (ex. $-\Delta\text{ReHo}$). ReHo=regional homogeneity, DC=degree centrality

METRIC	GROUP	RANKING DISTANCE	P-VALUE
ALFF	CF	0.131	<0.001
	OS	0.100	<0.001
	MC	0.146	<0.001
fALFF	CF	0.067	<0.001
	OS	0.082	<0.001
	MC	0.082	<0.001
ReHo	CF	0.120	<0.001
	OS	0.145	<0.001
	MC	0.122	<0.001
DC	CF	0.073	<0.001
	OS	0.142	<0.001
	MC	0.089	<0.001

Table 7. Ranking distance for each group's comparison of T_{ROI} and W_{ROI} rankings.

Ranking distance of 0 indicates identical rankings and 1 indicates opposite rankings.

CF=college football, OS=other sports (soccer and lacrosse), MC=male controls,

ALFF=amplitude of low-frequency fluctuations, fALFF=fractional ALFF,

ReHo=regional homogeneity, DC=degree centrality.

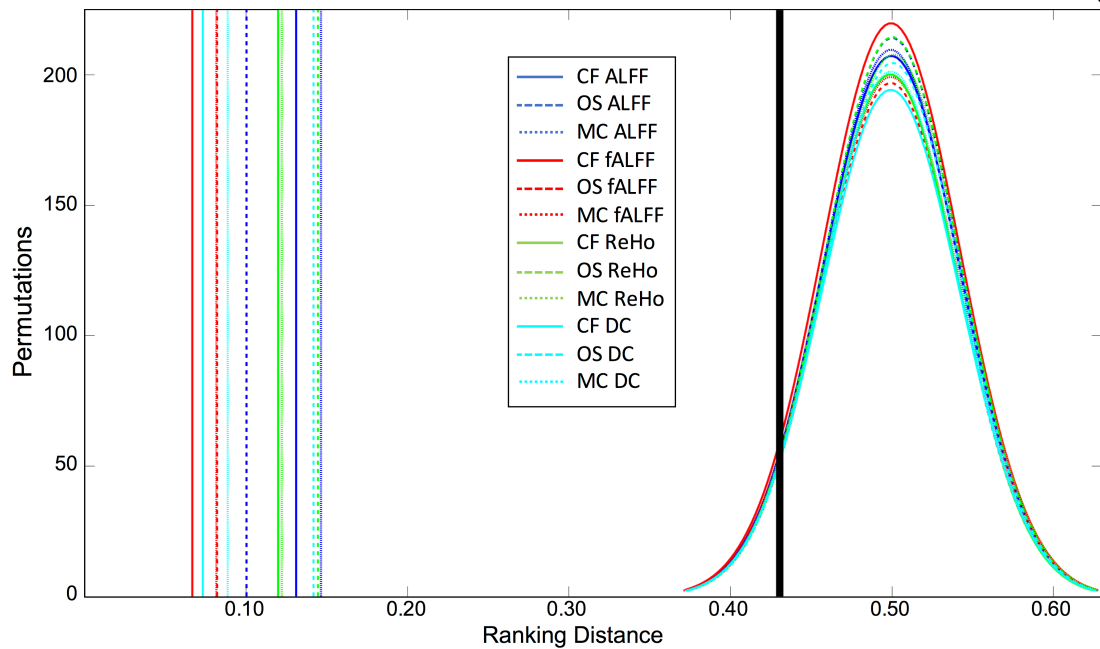


Figure 11. Ranking distance results and permutation testing. Twelve tests are shown for four metrics (ALFF, fALFF, ReHo and DC) in three groups (CF, OS, MC). Vertical lines on the left of the figure depict the calculated ranking distance for each group's comparison of T_{ROI} and W_{ROI} rankings. Curves on the right depict the distribution for each of the twelve permutation tests (5000 iterations) of ranking distance. Thick black vertical line (actually six superimposed vertical lines) represents the $p < 0.05$ decision line for the twelve permutation tests. CF=college football, OS=other sports(soccer and lacrosse), MC=male controls, ALFF=amplitude of low-frequency fluctuations, fALFF=fractional amplitude of low-frequency fluctuations, ReHo=regional homogeneity, DC=degree centrality.

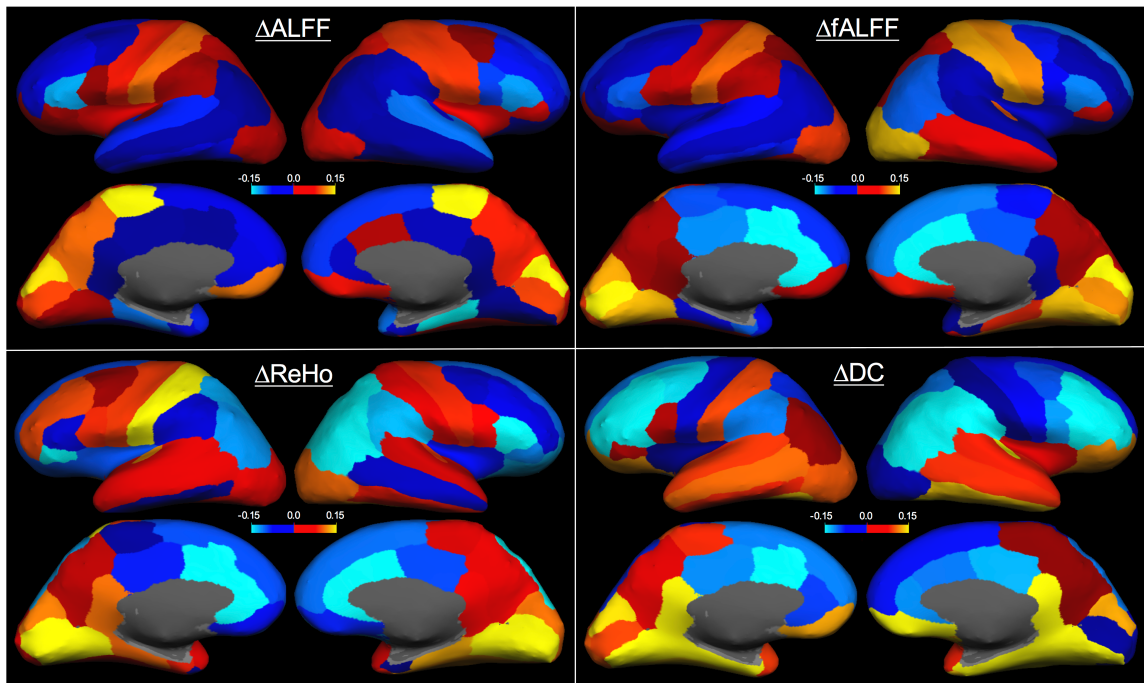


Figure 12. College football ALFF, fALFF, ReHo and DC trends for each region.

Longitudinal changes for college football's metrics were averaged over each region in the DKT atlas. Trends are depicted with warm colors depicting increases and cool colors depicting decreases. In preprocessing functional connectivity metric were Fisher-z transformed, therefore values indicate preseason-to-postseason changes in the Fisher-z value. ALFF=amplitude of low-frequency fluctuations, fALFF=fractional ALFF, ReHo=regional homogeneity, DC=degree centrality.

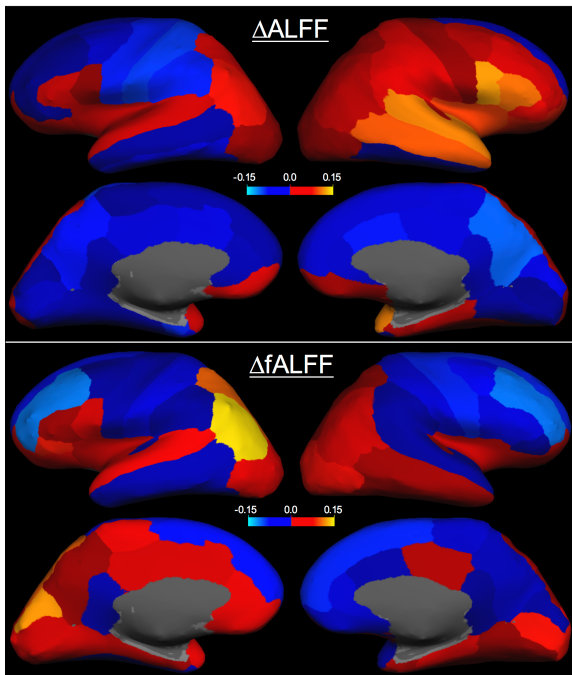


Figure 13. Control group's ALFF and fALFF trends for each region. Longitudinal changes for the control group's metrics were averaged over each region in the DKT atlas. Trends are depicted with warm colors depicting increases and cool colors depicting decreases. In preprocessing functional connectivity metric were Fisher-z transformed, therefore values indicate preseason-to-postseason changes in the Fisher-z value. ALFF=amplitude of low-frequency fluctuations, fALFF=fractional amplitude of low-frequency fluctuations.

METRIC	METRIC COMPARISON	RANKING DISTANCE	P-VALUE
College Football	ALFF vs fALFF	0.341	<0.001
	ALFF vs ReHo	0.448	0.111
	ALFF vs DC	0.462	0.185
	fALFF vs ReHo	0.283	<0.001
	fALFF vs DC	0.336	<0.001
	ReHo vs DC	0.398	0.007

Table 8. Ranking distance for comparisons between college football's metrics. Ranking distance of 0 indicates identical rankings and 1 indicates opposite rankings. ALFF=amplitude of low-frequency fluctuations, fALFF=fractional ALFF, ReHo=regional homogeneity, DC=degree centrality.

METRIC	GROUP COMPARISON	RANKING DISTANCE	P-VALUE
ALFF	CF vs. OS	0.3483	<0.001
	CF vs. MC	0.5063	0.431
	OS vs. MC	0.4876	0.393
fALFF	CF vs. OS	0.3706	0.001
	CF vs. MC	0.4503	0.130
	OS vs. MC	0.5179	0.339

Table 9. Ranking distance for comparisons between groups for ALFF and fALFF. Ranking distance of 0 indicates identical rankings and 1 indicates opposite rankings. CF=college football, OS=other sports, MC=male controls, ALFF=amplitude of low-frequency fluctuations, fALFF=fractional ALFF.

Table 10. Region rankings for college football players' amplitude of low-frequency fluctuations.

SVM Weight Ranking		T Statistic Ranking		ΔFC Metric	
Left Paracentral	0.0044	Left Paracentral	0.8244	Left Paracentral	0.2049
Right Cuneus	0.0043	Right Paracentral	0.7411	Right Paracentral	0.1750
Left Cuneus	0.0038	Left Cuneus	0.5898	Right Cuneus	0.1604
Right Paracentral	0.0033	Right Cuneus	0.5544	Left Cuneus	0.1413
Left Medial Orbitofrontal	0.0026	Left Precuneus	0.5135	Left Medial Orbitofrontal	0.0976
Right Pars Orbitalis	0.0023	Right Pericalcarine	0.4956	Left Postcentral	0.0936
Right Lateral Occipital	0.0022	Left Medial Orbitofrontal	0.4693	Left Precuneus	0.0914
Right Pericalcarine	0.0018	Right Precuneus	0.3716	Left Pericalcarine	0.0754
Right Medial Orbitofrontal	0.0017	Left Pericalcarine	0.3622	Right Pericalcarine	0.0753
Left Postcentral	0.0017	Left Postcentral	0.3597	Right Postcentral	0.0721
Left Precuneus	0.0017	Right Postcentral	0.2732	Right Precentral	0.0700
Left Pericalcarine	0.0016	Right Precentral	0.2365	Right Precuneus	0.0604
Left Pars Orbitalis	0.0015	Right Medial Orbitofrontal	0.2344	Left Precentral	0.0584
Right Precentral	0.0014	Right Fusiform	0.2317	Right Superior Parietal	0.0545
Left Lateral Orbitofrontal	0.0014	Right Superior Parietal	0.2236	Right Medial Orbitofrontal	0.0544
Right Postcentral	0.0014	Left Insula	0.2051	Right Lateral Occipital	0.0530
Right Fusiform	0.0012	Left Precentral	0.1972	Right Insula	0.0458
Left Lateral Occipital	0.0008	Right Pars Orbitalis	0.1720	Right Pars Orbitalis	0.0425
Left Precentral	0.0008	Right Insula	0.1457	Right Fusiform	0.0399
Left Caudal Anterior Cingulate	0.0008	Left Superior Parietal	0.1315	Left Insula	0.0384
Right Precuneus	0.0007	Right Lateral Occipital	0.1095	Left Superior Parietal	0.0262
Right Superior Parietal	0.0007	Left Pars Orbitalis	0.0946	Left Lateral Orbitofrontal	0.0245
Right Insula	0.0004	Left Lingual	0.0866	Left Lateral Occipital	0.0214
Left Lingual	0.0004	Left Lateral Orbitofrontal	0.0656	Left Pars Orbitalis	0.0178
Right Lateral Orbitofrontal	0.0003	Right Isthmus Cingulate	0.0598	Right Caudal Anterior Cingulate	0.0158
Left Transverse Temporal	0.0003	Right Caudal Anterior Cingulate	0.0543	Left Lingual	0.0143
Right Middle Temporal	0.0003	Left Transverse Temporal	0.0475	Left Supramarginal	0.0107
Left Posterior Cingulate	0.0002	Left Pars Opercularis	0.0352	Left Pars Opercularis	0.0066
Right Inferior Temporal	0.0002	Left Supramarginal	0.0308	Right Caudal Middle Frontal	0.0024
Right Caudal Anterior Cingulate	0.0002	Right Lingual	0.0040	Left Transverse Temporal	0.0022
Left Superior Parietal	0.0001	Left Temporal Pole	0.0031	Right Isthmus Cingulate	-0.0005
Left Supramarginal	0.0001	Left Caudal Anterior Cingulate	0.0024	Left Isthmus Cingulate	-0.0026
Right Lingual	0.0000	Right Caudal Middle Frontal	-0.0047	Right Lingual	-0.0027
Left Insula	0.0000	Left Isthmus Cingulate	-0.0121	Left Caudal Anterior Cingulate	-0.0033

Right Isthmus Cingulate	-0.0001	Left Lateral Occipital	-0.0290	Right Inferior Temporal	-0.0054
Right Supramarginal	-0.0003	Left Inferior Parietal	-0.0389	Left Inferior Parietal	-0.0065
Right Posterior Cingulate	-0.0003	Right Inferior Temporal	-0.0402	Left Posterior Cingulate	-0.0067
Left Superior Frontal	-0.0003	Right Middle Temporal	-0.0450	Left Temporal Pole	-0.0101
Left Isthmus Cingulate	-0.0005	Left Middle Temporal	-0.0755	Right Middle Temporal	-0.0104
Right Caudal Middle Frontal	-0.0005	Right Inferior Parietal	-0.0812	Left Middle Temporal	-0.0113
Left Rostral Middle Frontal	-0.0005	Left Posterior Cingulate	-0.0934	Right Inferior Parietal	-0.0161
Left Inferior Parietal	-0.0005	Left Caudal Middle Frontal	-0.0963	Right Posterior Cingulate	-0.0192
Left Rostral Anterior Cingulate	-0.0006	Right Supramarginal	-0.0983	Left Caudal Middle Frontal	-0.0224
Left Middle Temporal	-0.0007	Right Lateral Orbitofrontal	-0.1293	Right Supramarginal	-0.0237
Right Rostral Anterior Cingulate	-0.0007	Right Rostral Middle Frontal	-0.1398	Right Lateral Orbitofrontal	-0.0242
Left Fusiform	-0.0008	Left Rostral Anterior Cingulate	-0.1514	Right Rostral Anterior Cingulate	-0.0258
Right Frontal Pole	-0.0008	Left Superior Frontal	-0.1634	Left Rostral Anterior Cingulate	-0.0368
Right Inferior Parietal	-0.0009	Right Rostral Anterior Cingulate	-0.1677	Left Inferior Temporal	-0.0372
Right Entorhinal	-0.0010	Left Rostral Middle Frontal	-0.1728	Right Entorhinal	-0.0382
Left Caudal Middle Frontal	-0.0011	Right Posterior Cingulate	-0.1763	Left Fusiform	-0.0385
Left Pars Opercularis	-0.0011	Right Superior Frontal	-0.1862	Left Entorhinal	-0.0406
Left Entorhinal	-0.0012	Right Entorhinal	-0.1909	Left Superior Frontal	-0.0406
Left Temporal Pole	-0.0012	Left Entorhinal	-0.2010	Left Rostral Middle Frontal	-0.0477
Left Inferior Temporal	-0.0013	Right Transverse Temporal	-0.2399	Right Transverse Temporal	-0.0494
Right Rostral Middle Frontal	-0.0013	Left Superior Temporal	-0.2446	Right Rostral Middle Frontal	-0.0563
Right Superior Frontal	-0.0014	Left Inferior Temporal	-0.2967	Left Superior Temporal	-0.0613
Right Transverse Temporal	-0.0014	Right Superior Temporal	-0.2986	Right Frontal Pole	-0.0661
Left Parahippocampal	-0.0016	Right Pars Opercularis	-0.3043	Right Superior Frontal	-0.0689
Right Pars Opercularis	-0.0018	Left Fusiform	-0.3413	Right Pars Opercularis	-0.0743
Left Superior Temporal	-0.0019	Right Frontal Pole	-0.3713	Left Frontal Pole	-0.0911
Right Superior Temporal	-0.0019	Right Pars Triangularis	-0.3999	Right Superior Temporal	-0.0963
Right Pars Triangularis	-0.0025	Left Pars Triangularis	-0.4226	Left Parahippocampal	-0.0973
Left Frontal Pole	-0.0025	Left Frontal Pole	-0.4829	Right Pars Triangularis	-0.1127
Right Parahippocampal	-0.0032	Left Parahippocampal	-0.5944	Left Pars Triangularis	-0.1193
Left Pars Triangularis	-0.0038	Right Parahippocampal	-0.7868	Right Parahippocampal	-0.1528
Right Temporal Pole	-0.0149	Right Temporal Pole	-1.5747	Right Temporal Pole	-0.6138

Table 11. Region rankings for college football players' fractional amplitude of low-frequency fluctuations.

SVM Weight Ranking		T Statistic Ranking		ΔFC Metric	
Right Cuneus	0.0038	Right Lingual	0.5791	Right Cuneus	0.1514
Left Pericalcarine	0.0035	Left Lingual	0.5468	Left Pericalcarine	0.1484
Left Cuneus	0.0033	Left Pericalcarine	0.5205	Right Lateral Occipital	0.1305
Right Lingual	0.0032	Right Cuneus	0.4739	Right Lingual	0.1284
Left Frontal Pole	0.0032	Right Fusiform	0.4699	Left Lingual	0.1251
Left Lingual	0.0029	Right Pericalcarine	0.4466	Left Frontal Pole	0.1241
Right Lateral Occipital	0.0027	Right Lateral Occipital	0.4238	Left Cuneus	0.1179
Right Pericalcarine	0.0025	Left Frontal Pole	0.4221	Right Postcentral	0.1175
Right Precentral	0.0025	Left Cuneus	0.4099	Right Pericalcarine	0.1072
Right Transverse Temporal	0.0024	Right Postcentral	0.4037	Right Precentral	0.1072
Left Postcentral	0.0020	Right Transverse Temporal	0.3950	Right Fusiform	0.1012
Right Postcentral	0.0020	Right Precentral	0.3378	Left Postcentral	0.0926
Right Fusiform	0.0019	Right Parahippocampal	0.3172	Right Transverse Temporal	0.0870
Left Lateral Occipital	0.0014	Left Postcentral	0.3071	Left Lateral Occipital	0.0720
Right Parahippocampal	0.0013	Right Medial Orbitofrontal	0.2490	Right Parahippocampal	0.0638
Right Medial Orbitofrontal	0.0012	Right Frontal Pole	0.2241	Right Medial Orbitofrontal	0.0574
Right Superior Parietal	0.0011	Left Lateral Occipital	0.2191	Right Frontal Pole	0.0472
Right Pars Orbitalis	0.0010	Right Pars Orbitalis	0.1584	Right Middle Temporal	0.0415
Left Temporal Pole	0.0009	Left Medial Orbitofrontal	0.1491	Right Inferior Temporal	0.0385
Left Precentral	0.0008	Right Middle Temporal	0.1419	Right Pars Orbitalis	0.0360
Right Middle Temporal	0.0008	Right Inferior Temporal	0.1309	Left Precentral	0.0337
Right Frontal Pole	0.0007	Left Pars Opercularis	0.1244	Left Medial Orbitofrontal	0.0320
Left Superior Parietal	0.0006	Right Superior Parietal	0.1095	Right Superior Parietal	0.0293
Left Supramarginal	0.0006	Left Lateral Orbitofrontal	0.0965	Left Pars Opercularis	0.0285
Left Lateral Orbitofrontal	0.0005	Left Precentral	0.0824	Left Supramarginal	0.0192
Left Medial Orbitofrontal	0.0005	Left Supramarginal	0.0668	Left Lateral Orbitofrontal	0.0186
Left Pars Opercularis	0.0004	Left Precuneus	0.0502	Left Precuneus	0.0155
Right Inferior Temporal	0.0003	Left Isthmus Cingulate	0.0438	Left Fusiform	0.0143
Right Entorhinal	0.0001	Left Fusiform	0.0368	Right Precuneus	0.0110
Left Precuneus	0.0001	Right Precuneus	0.0290	Left Isthmus Cingulate	0.0066
Left Fusiform	-0.0001	Left Superior Parietal	0.0218	Left Superior Parietal	0.0026
Right Superior Temporal	-0.0001	Left Temporal Pole	-0.0116	Right Entorhinal	-0.0013
Right Precuneus	-0.0001	Right Entorhinal	-0.0155	Left Temporal Pole	-0.0058
Right Supramarginal	-0.0001	Right Rostral Middle Frontal	-0.0530	Right Superior Temporal	-0.0100

Left Transverse Temporal	-0.0001	Right Supramarginal	-0.0587	Right Lateral Orbitofrontal	-0.0116
Left Caudal Middle Frontal	-0.0003	Right Lateral Orbitofrontal	-0.0608	Right Isthmus Cingulate	-0.0152
Left Insula	-0.0003	Right Superior Temporal	-0.0650	Right Rostral Middle Frontal	-0.0164
Right Lateral Orbitofrontal	-0.0004	Left Transverse Temporal	-0.0762	Left Transverse Temporal	-0.0187
Left Rostral Middle Frontal	-0.0004	Right Isthmus Cingulate	-0.0769	Right Supramarginal	-0.0189
Right Rostral Middle Frontal	-0.0004	Left Inferior Parietal	-0.0812	Left Insula	-0.0200
Right Isthmus Cingulate	-0.0006	Left Insula	-0.0841	Left Middle Temporal	-0.0238
Left Inferior Parietal	-0.0006	Left Rostral Middle Frontal	-0.0995	Left Inferior Parietal	-0.0250
Left Pars Orbitalis	-0.0006	Left Caudal Middle Frontal	-0.1091	Right Insula	-0.0294
Left Isthmus Cingulate	-0.0007	Left Middle Temporal	-0.1248	Left Rostral Middle Frontal	-0.0302
Left Parahippocampal	-0.0008	Right Insula	-0.1269	Left Caudal Middle Frontal	-0.0303
Left Superior Temporal	-0.0008	Right Paracentral	-0.1997	Left Parahippocampal	-0.0440
Right Insula	-0.0009	Right Pars Opercularis	-0.2036	Right Pars Opercularis	-0.0474
Right Paracentral	-0.0009	Left Pars Orbitalis	-0.2042	Left Pars Orbitalis	-0.0514
Left Middle Temporal	-0.0009	Right Caudal Middle Frontal	-0.2141	Left Superior Temporal	-0.0516
Right Caudal Middle Frontal	-0.0009	Left Superior Temporal	-0.2289	Right Paracentral	-0.0535
Right Pars Opercularis	-0.0012	Left Parahippocampal	-0.2481	Right Caudal Middle Frontal	-0.0558
Left Superior Frontal	-0.0012	Left Superior Frontal	-0.2519	Left Inferior Temporal	-0.0571
Left Paracentral	-0.0012	Left Paracentral	-0.2931	Left Superior Frontal	-0.0666
Left Entorhinal	-0.0016	Right Inferior Parietal	-0.3001	Left Paracentral	-0.0808
Right Posterior Cingulate	-0.0017	Left Pars Triangularis	-0.3395	Right Posterior Cingulate	-0.0816
Right Inferior Parietal	-0.0017	Right Posterior Cingulate	-0.3478	Left Pars Triangularis	-0.0869
Left Inferior Temporal	-0.0020	Left Inferior Temporal	-0.3552	Right Inferior Parietal	-0.0878
Left Pars Triangularis	-0.0020	Right Superior Frontal	-0.3742	Left Entorhinal	-0.0886
Right Superior Frontal	-0.0021	Right Pars Triangularis	-0.4039	Right Superior Frontal	-0.1013
Left Posterior Cingulate	-0.0022	Left Posterior Cingulate	-0.4691	Right Pars Triangularis	-0.1015
Right Pars Triangularis	-0.0024	Left Entorhinal	-0.5189	Left Posterior Cingulate	-0.1064
Left Caudal Anterior Cingulate	-0.0025	Right Caudal Anterior Cingulate	-0.6262	Right Caudal Anterior Cingulate	-0.1502
Right Caudal Anterior Cingulate	-0.0029	Left Caudal Anterior Cingulate	-0.6307	Right Rostral Anterior Cingulate	-0.1565
Right Rostral Anterior Cingulate	-0.0031	Right Rostral Anterior Cingulate	-0.6744	Left Caudal Anterior Cingulate	-0.1608
Left Rostral Anterior Cingulate	-0.0034	Left Rostral Anterior Cingulate	-0.7849	Left Rostral Anterior Cingulate	-0.1966
Right Temporal Pole	-0.0036	Right Temporal Pole	-0.9232	Right Temporal Pole	-0.2035

Table 12. Region rankings for college football players' regional homogeneity.

SVM Weight Ranking		T Statistic Ranking		ΔFC Metric	
Left Pericalcarine	0.0061	Right Lingual	1.3128	Left Pericalcarine	0.2868
Right Lingual	0.0046	Left Pericalcarine	1.1220	Right Lingual	0.2642
Left Lingual	0.0045	Left Lingual	1.1046	Left Lingual	0.2324
Left Postcentral	0.0043	Left Temporal Pole	0.9067	Right Pericalcarine	0.2236
Left Cuneus	0.0034	Right Pericalcarine	0.8287	Left Postcentral	0.1734
Right Cuneus	0.0030	Left Postcentral	0.6967	Left Temporal Pole	0.1582
Right Frontal Pole	0.0029	Right Frontal Pole	0.6718	Right Frontal Pole	0.1359
Right Pericalcarine	0.0026	Right Parahippocampal	0.6243	Right Parahippocampal	0.1196
Right Precentral	0.0025	Left Transverse Temporal	0.6221	Right Fusiform	0.1104
Left Temporal Pole	0.0021	Right Fusiform	0.5884	Left Transverse Temporal	0.1091
Left Precentral	0.0019	Left Parahippocampal	0.5511	Left Cuneus	0.1004
Left Rostral Middle Frontal	0.0018	Left Isthmus Cingulate	0.4948	Right Cuneus	0.0952
Left Pars Opercularis	0.0015	Left Cuneus	0.4509	Left Isthmus Cingulate	0.0940
Right Pars Opercularis	0.0015	Right Transverse Temporal	0.4104	Right Lateral Occipital	0.0912
Right Caudal Middle Frontal	0.0015	Left Entorhinal	0.3556	Left Parahippocampal	0.0908
Left Entorhinal	0.0013	Right Inferior Temporal	0.3507	Left Rostral Middle Frontal	0.0783
Right Lateral Occipital	0.0012	Right Cuneus	0.3471	Right Transverse Temporal	0.0728
Right Parahippocampal	0.0011	Right Lateral Occipital	0.3361	Left Precentral	0.0721
Right Fusiform	0.0011	Left Rostral Middle Frontal	0.3128	Left Pars Opercularis	0.0647
Left Transverse Temporal	0.0010	Left Precentral	0.2722	Right Precentral	0.0643
Right Inferior Temporal	0.0009	Right Precentral	0.2341	Left Entorhinal	0.0599
Right Paracentral	0.0009	Left Pars Opercularis	0.2287	Right Inferior Temporal	0.0565
Left Caudal Middle Frontal	0.0008	Left Superior Temporal	0.2231	Right Pars Opercularis	0.0502
Right Precuneus	0.0007	Left Middle Temporal	0.2216	Right Isthmus Cingulate	0.0459
Left Middle Temporal	0.0007	Right Isthmus Cingulate	0.2206	Left Lateral Occipital	0.0452
Left Isthmus Cingulate	0.0005	Right Pars Opercularis	0.2019	Right Postcentral	0.0451
Right Postcentral	0.0005	Right Precuneus	0.1846	Left Middle Temporal	0.0416
Left Parahippocampal	0.0004	Right Postcentral	0.1831	Right Precuneus	0.0414
Right Transverse Temporal	0.0003	Right Superior Temporal	0.1629	Left Superior Temporal	0.0413
Right Superior Temporal	0.0002	Left Lateral Occipital	0.1587	Right Paracentral	0.0350
Left Superior Temporal	0.0002	Right Paracentral	0.1255	Right Superior Temporal	0.0307
Left Precuneus	0.0000	Left Precuneus	0.1141	Left Fusiform	0.0301
Left Supramarginal	-0.0001	Left Fusiform	0.1047	Left Precuneus	0.0227
Right Isthmus Cingulate	-0.0002	Left Caudal Middle Frontal	0.0058	Left Caudal Middle Frontal	0.0111
Right Rostral Middle Frontal	-0.0002	Left Inferior Temporal	-0.0205	Right Entorhinal	-0.0025

Left Superior Parietal	-0.0003	Left Paracentral	-0.0353	Left Inferior Temporal	-0.0038
Right Entorhinal	-0.0005	Right Entorhinal	-0.0636	Left Paracentral	-0.0094
Left Inferior Temporal	-0.0005	Right Middle Temporal	-0.1139	Right Middle Temporal	-0.0249
Left Lateral Occipital	-0.0006	Right Caudal Middle Frontal	-0.1305	Right Caudal Middle Frontal	-0.0293
Left Paracentral	-0.0008	Left Supramarginal	-0.1367	Left Supramarginal	-0.0336
Right Middle Temporal	-0.0008	Left Pars Triangularis	-0.1410	Left Pars Triangularis	-0.0344
Left Fusiform	-0.0011	Right Rostral Middle Frontal	-0.1726	Right Rostral Middle Frontal	-0.0448
Left Superior Frontal	-0.0013	Left Posterior Cingulate	-0.2676	Right Insula	-0.0534
Left Pars Triangularis	-0.0014	Left Medial Orbitofrontal	-0.2986	Left Medial Orbitofrontal	-0.0534
Right Medial Orbitofrontal	-0.0015	Left Superior Frontal	-0.3182	Left Posterior Cingulate	-0.0586
Right Superior Parietal	-0.0016	Right Insula	-0.3302	Right Medial Orbitofrontal	-0.0610
Right Insula	-0.0016	Right Posterior Cingulate	-0.3683	Left Frontal Pole	-0.0752
Left Inferior Parietal	-0.0016	Left Superior Parietal	-0.3703	Right Posterior Cingulate	-0.0779
Left Posterior Cingulate	-0.0017	Right Medial Orbitofrontal	-0.3718	Left Superior Frontal	-0.0800
Left Frontal Pole	-0.0017	Right Superior Frontal	-0.4097	Left Insula	-0.0820
Left Insula	-0.0018	Left Frontal Pole	-0.4347	Left Lateral Orbitofrontal	-0.0822
Right Pars Orbitalis	-0.0018	Left Lateral Orbitofrontal	-0.4372	Right Superior Frontal	-0.0940
Right Superior Frontal	-0.0019	Left Inferior Parietal	-0.4866	Right Temporal Pole	-0.1020
Right Supramarginal	-0.0020	Left Insula	-0.4996	Right Pars Orbitalis	-0.1037
Left Lateral Orbitofrontal	-0.0021	Right Supramarginal	-0.5188	Left Inferior Parietal	-0.1110
Left Medial Orbitofrontal	-0.0021	Right Pars Orbitalis	-0.5469	Left Superior Parietal	-0.1180
Right Posterior Cingulate	-0.0024	Right Temporal Pole	-0.5738	Right Lateral Orbitofrontal	-0.1224
Right Inferior Parietal	-0.0025	Right Lateral Orbitofrontal	-0.6534	Right Supramarginal	-0.1249
Right Lateral Orbitofrontal	-0.0029	Right Superior Parietal	-0.6686	Right Caudal Anterior Cingulate	-0.1569
Right Caudal Anterior Cingulate	-0.0034	Right Inferior Parietal	-0.7150	Right Inferior Parietal	-0.1799
Left Rostral Anterior Cingulate	-0.0043	Right Caudal Anterior Cingulate	-0.7866	Right Superior Parietal	-0.1909
Right Rostral Anterior Cingulate	-0.0046	Left Pars Orbitalis	-0.9185	Left Pars Orbitalis	-0.2018
Left Caudal Anterior Cingulate	-0.0050	Right Pars Triangularis	-1.0133	Left Rostral Anterior Cingulate	-0.2119
Right Pars Triangularis	-0.0053	Left Caudal Anterior Cingulate	-1.0455	Right Pars Triangularis	-0.2230
Right Temporal Pole	-0.0054	Left Rostral Anterior Cingulate	-1.0721	Left Caudal Anterior Cingulate	-0.2257
Left Pars Orbitalis	-0.0054	Right Rostral Anterior Cingulate	-1.2675	Right Rostral Anterior Cingulate	-0.2525

Table 13. Region rankings for college football players' degree centrality.

SVM Weight Ranking		T Statistic Ranking		ΔFC Metric	
Right Parahippocampal	0.0047	Right Parahippocampal	0.9829	Right Parahippocampal	0.2786
Left Frontal Pole	0.0044	Right Entorhinal	0.8406	Right Entorhinal	0.2091
Left Temporal Pole	0.0038	Left Parahippocampal	0.7401	Left Temporal Pole	0.2031
Right Isthmus Cingulate	0.0037	Left Temporal Pole	0.7240	Right Fusiform	0.2029
Right Entorhinal	0.0036	Right Fusiform	0.6972	Left Parahippocampal	0.2017
Right Fusiform	0.0035	Right Medial Orbitofrontal	0.6737	Right Transverse Temporal	0.1917
Left Parahippocampal	0.0034	Right Isthmus Cingulate	0.6512	Right Isthmus Cingulate	0.1905
Right Lingual	0.0030	Left Entorhinal	0.6189	Left Frontal Pole	0.1815
Right Transverse Temporal	0.0030	Right Transverse Temporal	0.5701	Right Medial Orbitofrontal	0.1800
Left Isthmus Cingulate	0.0029	Right Lingual	0.5593	Right Lingual	0.1760
Left Entorhinal	0.0027	Left Lingual	0.5468	Left Lingual	0.1741
Right Medial Orbitofrontal	0.0026	Left Frontal Pole	0.5292	Left Entorhinal	0.1548
Left Lingual	0.0025	Right Inferior Temporal	0.5190	Left Isthmus Cingulate	0.1481
Left Cuneus	0.0024	Left Isthmus Cingulate	0.5173	Left Cuneus	0.1406
Right Pars Orbitalis	0.0022	Left Fusiform	0.4484	Left Fusiform	0.1328
Right Cuneus	0.0021	Left Lateral Orbitofrontal	0.4447	Right Inferior Temporal	0.1313
Right Inferior Temporal	0.0020	Right Lateral Orbitofrontal	0.4445	Right Cuneus	0.1171
Left Fusiform	0.0019	Left Medial Orbitofrontal	0.4436	Left Medial Orbitofrontal	0.1165
Left Middle Temporal	0.0017	Left Cuneus	0.4295	Left Lateral Orbitofrontal	0.1115
Right Middle Temporal	0.0016	Right Pars Orbitalis	0.3917	Right Lateral Orbitofrontal	0.1087
Right Lateral Orbitofrontal	0.0014	Right Cuneus	0.3506	Right Pars Orbitalis	0.1069
Left Lateral Orbitofrontal	0.0014	Left Middle Temporal	0.3025	Left Middle Temporal	0.0911
Left Lateral Occipital	0.0014	Left Inferior Temporal	0.2448	Left Lateral Occipital	0.0850
Left Medial Orbitofrontal	0.0014	Left Lateral Occipital	0.2385	Left Postcentral	0.0776
Left Paracentral	0.0013	Left Pericalcarine	0.2382	Left Pericalcarine	0.0768
Left Postcentral	0.0013	Left Superior Temporal	0.2332	Left Superior Temporal	0.0713
Left Transverse Temporal	0.0011	Left Postcentral	0.2259	Right Middle Temporal	0.0671
Right Superior Temporal	0.0011	Right Middle Temporal	0.2250	Left Paracentral	0.0645
Left Superior Temporal	0.0009	Right Superior Temporal	0.2152	Left Transverse Temporal	0.0636
Left Precuneus	0.0009	Left Transverse Temporal	0.1966	Left Inferior Temporal	0.0628
Right Insula	0.0008	Left Paracentral	0.1883	Right Superior Temporal	0.0611
Left Inferior Temporal	0.0004	Left Precuneus	0.1484	Left Precuneus	0.0399
Left Pars Opercularis	0.0004	Right Insula	0.1109	Right Insula	0.0374
Left Inferior Parietal	0.0003	Left Pars Orbitalis	0.0910	Left Pars Orbitalis	0.0248
Left Insula	0.0001	Left Pars Opercularis	0.0872	Left Pars Opercularis	0.0187
Left Pericalcarine	0.0001	Left Inferior Parietal	0.0280	Left Inferior Parietal	0.0065

Right Precuneus	-0.0002	Right Precuneus	0.0096	Right Paracentral	0.0014
Left Pars Orbitalis	-0.0002	Right Paracentral	0.0014	Right Precuneus	0.0008
Right Paracentral	-0.0004	Right Postcentral	-0.0035	Left Insula	-0.0020
Left Superior Parietal	-0.0006	Right Pericalcarine	-0.0051	Right Postcentral	-0.0069
Right Caudal Middle Frontal	-0.0006	Left Insula	-0.0080	Right Pericalcarine	-0.0081
Left Precentral	-0.0006	Right Lateral Occipital	-0.0951	Right Lateral Occipital	-0.0282
Right Postcentral	-0.0007	Left Precentral	-0.0973	Left Precentral	-0.0356
Right Caudal Anterior Cingulate	-0.0007	Right Precentral	-0.1503	Right Precentral	-0.0509
Right Lateral Occipital	-0.0008	Left Superior Parietal	-0.1688	Right Superior Frontal	-0.0548
Right Precentral	-0.0008	Right Superior Frontal	-0.1907	Left Superior Parietal	-0.0641
Right Superior Frontal	-0.0008	Left Rostral Anterior Cingulate	-0.2724	Left Rostral Anterior Cingulate	-0.0728
Left Rostral Anterior Cingulate	-0.0008	Right Caudal Middle Frontal	-0.2755	Right Frontal Pole	-0.0784
Right Pars Opercularis	-0.0012	Left Supramarginal	-0.2874	Right Caudal Middle Frontal	-0.0833
Left Supramarginal	-0.0014	Right Superior Parietal	-0.2887	Right Caudal Anterior Cingulate	-0.0981
Right Pericalcarine	-0.0014	Right Frontal Pole	-0.2980	Right Temporal Pole	-0.0987
Right Superior Parietal	-0.0014	Left Posterior Cingulate	-0.3141	Right Superior Parietal	-0.0992
Right Rostral Anterior Cingulate	-0.0015	Right Caudal Anterior Cingulate	-0.3157	Left Supramarginal	-0.1010
Left Superior Frontal	-0.0016	Right Pars Opercularis	-0.3185	Left Superior Frontal	-0.1011
Left Caudal Middle Frontal	-0.0021	Right Temporal Pole	-0.3303	Left Posterior Cingulate	-0.1060
Left Posterior Cingulate	-0.0022	Left Superior Frontal	-0.3442	Right Rostral Anterior Cingulate	-0.1070
Left Rostral Middle Frontal	-0.0024	Right Posterior Cingulate	-0.3676	Right Pars Opercularis	-0.1127
Right Posterior Cingulate	-0.0025	Right Rostral Anterior Cingulate	-0.4030	Right Posterior Cingulate	-0.1224
Right Inferior Parietal	-0.0028	Left Caudal Middle Frontal	-0.4511	Left Caudal Middle Frontal	-0.1421
Right Supramarginal	-0.0029	Left Rostral Middle Frontal	-0.5034	Left Rostral Middle Frontal	-0.1504
Left Caudal Anterior Cingulate	-0.0030	Right Supramarginal	-0.5294	Left Pars Triangularis	-0.1868
Left Pars Triangularis	-0.0033	Right Inferior Parietal	-0.5940	Left Caudal Anterior Cingulate	-0.1886
Right Rostral Middle Frontal	-0.0033	Left Pars Triangularis	-0.6052	Right Inferior Parietal	-0.1925
Right Pars Triangularis	-0.0036	Right Rostral Middle Frontal	-0.6542	Right Supramarginal	-0.1940
Right Frontal Pole	-0.0043	Right Pars Triangularis	-0.6572	Right Rostral Middle Frontal	-0.1970
Right Temporal Pole	-0.0054	Left Caudal Anterior Cingulate	-0.6597	Right Pars Triangularis	-0.2029

Table 14. Region rankings for controls' amplitude of low-frequency fluctuations.

SVM Weight Ranking		T Statistic Ranking		ΔFC Metric	
Right Frontal Pole	0.0062	Right Frontal Pole	2.4602	Right Frontal Pole	0.2722
Right Pars Opercularis	0.0037	Right Pars Opercularis	0.7343	Right Pars Opercularis	0.1111
Left Frontal Pole	0.0036	Right Middle Temporal	0.6627	Right Superior Temporal	0.1015
Right Superior Temporal	0.0026	Right Insula	0.6099	Right Pars Triangularis	0.0936
Right Pars Triangularis	0.0025	Right Pars Triangularis	0.5453	Right Middle Temporal	0.0838
Left Superior Parietal	0.0025	Right Superior Temporal	0.4795	Right Insula	0.0739
Right Lateral Orbitofrontal	0.0025	Left Frontal Pole	0.4154	Right Lateral Orbitofrontal	0.0607
Right Middle Temporal	0.0023	Right Lateral Orbitofrontal	0.3544	Left Frontal Pole	0.0580
Left Inferior Parietal	0.0021	Right Pars Orbitalis	0.3457	Left Inferior Parietal	0.0549
Right Supramarginal	0.0021	Right Parahippocampal	0.2842	Right Pars Orbitalis	0.0519
Right Postcentral	0.0019	Right Supramarginal	0.2434	Right Supramarginal	0.0390
Left Medial Orbitofrontal	0.0019	Left Medial Orbitofrontal	0.2261	Right Parahippocampal	0.0378
Right Insula	0.0016	Right Postcentral	0.2115	Right Postcentral	0.0377
Left Lateral Orbitofrontal	0.0015	Right Transverse Temporal	0.1901	Left Medial Orbitofrontal	0.0376
Right Pars Orbitalis	0.0013	Left Lateral Orbitofrontal	0.1850	Left Lateral Orbitofrontal	0.0362
Right Superior Parietal	0.0012	Left Insula	0.1787	Left Superior Parietal	0.0357
Right Medial Orbitofrontal	0.0012	Left Inferior Parietal	0.1773	Right Rostral Middle Frontal	0.0353
Right Inferior Parietal	0.0011	Left Superior Temporal	0.1463	Left Superior Temporal	0.0319
Left Insula	0.0008	Right Fusiform	0.1423	Right Transverse Temporal	0.0267
Right Parahippocampal	0.0008	Right Entorhinal	0.1372	Right Entorhinal	0.0244
Right Caudal Middle Frontal	0.0007	Right Caudal Middle Frontal	0.1351	Left Pars Triangularis	0.0242
Right Rostral Middle Frontal	0.0007	Right Inferior Parietal	0.1330	Right Inferior Parietal	0.0227
Left Lateral Occipital	0.0006	Left Pars Triangularis	0.1269	Right Caudal Middle Frontal	0.0219
Right Precentral	0.0005	Right Rostral Middle Frontal	0.1091	Left Insula	0.0213
Left Superior Temporal	0.0005	Left Transverse Temporal	0.1087	Left Transverse Temporal	0.0195
Left Paracentral	0.0004	Right Medial Orbitofrontal	0.0760	Right Medial Orbitofrontal	0.0107
Left Pars Triangularis	0.0004	Right Pericalcarine	0.0692	Right Superior Parietal	0.0099
Right Lateral Occipital	0.0002	Left Superior Parietal	0.0556	Left Lateral Occipital	0.0089
Right Pericalcarine	0.0002	Right Lateral Occipital	0.0468	Right Precentral	0.0068
Left Temporal Pole	0.0001	Left Lateral Occipital	0.0437	Right Fusiform	0.0065
Right Entorhinal	0.0001	Right Precentral	0.0373	Right Lateral Occipital	0.0044
Left Transverse Temporal	-0.0001	Right Inferior Temporal	0.0200	Left Pars Opercularis	-0.0003
Right Paracentral	-0.0002	Left Pars Opercularis	0.0106	Right Pericalcarine	-0.0020
Left Pars Orbitalis	-0.0002	Left Cuneus	-0.0071	Left Rostral Middle Frontal	-0.0023
Right Fusiform	-0.0003	Right Superior Parietal	-0.0465	Left Paracentral	-0.0026
Left Isthmus Cingulate	-0.0003	Left Rostral Middle Frontal	-0.0522	Left Cuneus	-0.0033

Left Pars Opercularis	-0.0004	Left Pericalcarine	-0.0561	Right Inferior Temporal	-0.0034
Left Cuneus	-0.0004	Left Parahippocampal	-0.0691	Left Pars Orbitalis	-0.0087
Right Rostral Anterior Cingulate	-0.0005	Left Superior Frontal	-0.0761	Right Lingual	-0.0102
Right Inferior Temporal	-0.0005	Left Pars Orbitalis	-0.0780	Left Middle Temporal	-0.0103
Left Rostral Middle Frontal	-0.0005	Left Rostral Anterior Cingulate	-0.1069	Left Superior Frontal	-0.0108
Left Lingual	-0.0005	Left Middle Temporal	-0.1090	Left Parahippocampal	-0.0114
Left Pericalcarine	-0.0005	Left Paracentral	-0.1135	Left Lingual	-0.0115
Left Posterior Cingulate	-0.0006	Right Lingual	-0.1618	Left Isthmus Cingulate	-0.0128
Left Middle Temporal	-0.0006	Left Caudal Middle Frontal	-0.1742	Left Rostral Anterior Cingulate	-0.0165
Left Rostral Anterior Cingulate	-0.0007	Left Lingual	-0.1917	Left Pericalcarine	-0.0195
Left Parahippocampal	-0.0008	Left Temporal Pole	-0.1996	Right Isthmus Cingulate	-0.0210
Right Isthmus Cingulate	-0.0008	Right Rostral Anterior Cingulate	-0.2084	Left Fusiform	-0.0226
Right Lingual	-0.0009	Right Superior Frontal	-0.2119	Left Caudal Middle Frontal	-0.0270
Right Posterior Cingulate	-0.0009	Left Isthmus Cingulate	-0.2139	Right Rostral Anterior Cingulate	-0.0286
Right Transverse Temporal	-0.0009	Right Cuneus	-0.2263	Right Superior Frontal	-0.0312
Left Caudal Middle Frontal	-0.0010	Left Caudal Anterior Cingulate	-0.3121	Left Posterior Cingulate	-0.0327
Left Caudal Anterior Cingulate	-0.0011	Right Isthmus Cingulate	-0.3311	Right Paracentral	-0.0339
Left Fusiform	-0.0011	Left Fusiform	-0.3372	Right Posterior Cingulate	-0.0348
Left Precuneus	-0.0013	Left Precuneus	-0.3827	Left Caudal Anterior Cingulate	-0.0375
Left Supramarginal	-0.0013	Left Inferior Temporal	-0.3871	Left Inferior Temporal	-0.0384
Left Superior Frontal	-0.0014	Left Supramarginal	-0.3988	Right Cuneus	-0.0416
Left Postcentral	-0.0015	Right Posterior Cingulate	-0.4103	Left Temporal Pole	-0.0428
Left Inferior Temporal	-0.0015	Right Paracentral	-0.4142	Left Precuneus	-0.0545
Right Cuneus	-0.0016	Left Posterior Cingulate	-0.4171	Right Caudal Anterior Cingulate	-0.0567
Right Superior Frontal	-0.0019	Left Precentral	-0.4173	Left Precentral	-0.0592
Left Precentral	-0.0020	Left Entorhinal	-0.4279	Left Supramarginal	-0.0602
Right Precuneus	-0.0022	Left Postcentral	-0.4740	Left Entorhinal	-0.0634
Right Caudal Anterior Cingulate	-0.0023	Right Caudal Anterior Cingulate	-0.4896	Left Postcentral	-0.0714
Left Entorhinal	-0.0032	Right Precuneus	-0.5353	Right Precuneus	-0.0878
Right Temporal Pole	-0.0090	Right Temporal Pole	-0.9173	Right Temporal Pole	-0.2291

Table 15. Region rankings for controls' fractional amplitude of low-frequency fluctuations.

SVM Weight Ranking		T Statistic Ranking		ΔFC Metric	
Right Temporal Pole	0.0048	Right Frontal Pole	1.0021	Left Inferior Parietal	0.1386
Left Inferior Parietal	0.0042	Right Temporal Pole	0.8994	Right Frontal Pole	0.1316
Left Temporal Pole	0.0038	Left Temporal Pole	0.7934	Right Temporal Pole	0.1270
Left Cuneus	0.0036	Left Inferior Parietal	0.6407	Left Cuneus	0.1090
Left Superior Parietal	0.0028	Left Cuneus	0.5464	Left Temporal Pole	0.0980
Right Frontal Pole	0.0028	Left Superior Parietal	0.3986	Left Superior Parietal	0.0893
Left Pars Orbitalis	0.0022	Right Parahippocampal	0.3659	Left Pars Orbitalis	0.0583
Left Paracentral	0.0020	Left Pars Orbitalis	0.3646	Right Pericalcarine	0.0548
Right Lateral Occipital	0.0020	Left Lateral Orbitofrontal	0.3626	Right Lateral Occipital	0.0532
Left Lateral Orbitofrontal	0.0019	Right Pericalcarine	0.3103	Left Lateral Orbitofrontal	0.0484
Left Medial Orbitofrontal	0.0018	Left Superior Temporal	0.3100	Left Superior Temporal	0.0477
Left Superior Temporal	0.0017	Left Medial Orbitofrontal	0.3043	Left Lateral Occipital	0.0451
Left Lateral Occipital	0.0017	Left Rostral Anterior Cingulate	0.2798	Left Paracentral	0.0450
Right Pericalcarine	0.0017	Left Paracentral	0.2672	Right Parahippocampal	0.0444
Left Frontal Pole	0.0016	Left Parahippocampal	0.2642	Left Medial Orbitofrontal	0.0431
Right Parahippocampal	0.0016	Right Lateral Orbitofrontal	0.2610	Left Rostral Anterior Cingulate	0.0415
Left Caudal Anterior Cingulate	0.0016	Right Lateral Occipital	0.2560	Left Caudal Anterior Cingulate	0.0337
Left Pars Opercularis	0.0015	Left Posterior Cingulate	0.2529	Left Posterior Cingulate	0.0336
Left Rostral Anterior Cingulate	0.0013	Right Fusiform	0.2454	Left Pars Opercularis	0.0336
Left Parahippocampal	0.0013	Left Pars Opercularis	0.2313	Right Lateral Orbitofrontal	0.0335
Right Lateral Orbitofrontal	0.0012	Left Caudal Anterior Cingulate	0.2279	Right Inferior Parietal	0.0330
Left Posterior Cingulate	0.0012	Left Lateral Occipital	0.2115	Left Lingual	0.0292
Left Insula	0.0010	Left Lingual	0.2076	Left Pericalcarine	0.0272
Right Inferior Parietal	0.0009	Right Insula	0.2037	Right Insula	0.0270
Right Fusiform	0.0007	Left Pericalcarine	0.1782	Right Fusiform	0.0256
Left Lingual	0.0007	Right Entorhinal	0.1650	Left Parahippocampal	0.0237
Left Pars Triangularis	0.0007	Right Inferior Parietal	0.1541	Left Frontal Pole	0.0208
Right Entorhinal	0.0006	Left Insula	0.1517	Right Entorhinal	0.0203
Right Insula	0.0006	Left Entorhinal	0.1481	Left Insula	0.0202
Right Transverse Temporal	0.0005	Left Frontal Pole	0.1390	Right Posterior Cingulate	0.0153
Left Entorhinal	0.0004	Right Posterior Cingulate	0.1280	Left Entorhinal	0.0137
Left Pericalcarine	0.0004	Right Middle Temporal	0.0803	Right Middle Temporal	0.0096
Right Supramarginal	0.0002	Right Inferior Temporal	0.0634	Left Pars Triangularis	0.0079
Left Caudal Middle Frontal	0.0002	Left Pars Triangularis	0.0611	Left Precuneus	0.0069

Right Posterior Cingulate	0.0002	Right Transverse Temporal	0.0342	Right Superior Parietal	0.0063
Left Precuneus	0.0001	Right Lingual	0.0315	Right Lingual	0.0056
Right Middle Temporal	0.0001	Left Precuneus	0.0274	Right Transverse Temporal	0.0048
Right Inferior Temporal	0.0001	Right Superior Parietal	0.0272	Right Inferior Temporal	0.0017
Right Caudal Anterior Cingulate	0.0000	Right Isthmus Cingulate	-0.0006	Right Isthmus Cingulate	-0.0007
Right Superior Parietal	-0.0002	Right Supramarginal	-0.0209	Right Superior Temporal	-0.0077
Right Lingual	-0.0002	Left Caudal Middle Frontal	-0.0370	Right Supramarginal	-0.0082
Left Transverse Temporal	-0.0004	Right Superior Temporal	-0.0430	Left Supramarginal	-0.0088
Left Fusiform	-0.0004	Left Fusiform	-0.0455	Right Cuneus	-0.0089
Right Superior Temporal	-0.0004	Right Cuneus	-0.0462	Right Pars Orbitalis	-0.0093
Right Postcentral	-0.0005	Left Supramarginal	-0.0575	Left Fusiform	-0.0101
Left Precentral	-0.0005	Right Pars Orbitalis	-0.0648	Left Caudal Middle Frontal	-0.0106
Right Isthmus Cingulate	-0.0005	Left Precentral	-0.0672	Left Isthmus Cingulate	-0.0130
Right Pars Orbitalis	-0.0006	Right Precuneus	-0.0688	Right Caudal Anterior Cingulate	-0.0133
Left Supramarginal	-0.0006	Left Isthmus Cingulate	-0.0793	Left Precentral	-0.0158
Left Postcentral	-0.0006	Right Caudal Anterior Cingulate	-0.0860	Right Precuneus	-0.0170
Left Isthmus Cingulate	-0.0006	Left Middle Temporal	-0.1204	Left Middle Temporal	-0.0191
Right Medial Orbitofrontal	-0.0007	Right Paracentral	-0.1247	Left Transverse Temporal	-0.0212
Right Precuneus	-0.0009	Right Postcentral	-0.1456	Left Inferior Temporal	-0.0222
Left Inferior Temporal	-0.0009	Right Pars Opercularis	-0.1506	Right Medial Orbitofrontal	-0.0248
Left Middle Temporal	-0.0010	Left Transverse Temporal	-0.1594	Right Paracentral	-0.0259
Right Paracentral	-0.0011	Left Inferior Temporal	-0.1595	Right Pars Opercularis	-0.0332
Right Cuneus	-0.0012	Right Medial Orbitofrontal	-0.1618	Right Rostral Anterior Cingulate	-0.0332
Right Pars Opercularis	-0.0013	Left Postcentral	-0.1850	Right Postcentral	-0.0343
Right Pars Triangularis	-0.0013	Right Rostral Anterior Cingulate	-0.1929	Left Postcentral	-0.0356
Right Rostral Anterior Cingulate	-0.0013	Right Pars Triangularis	-0.1986	Right Pars Triangularis	-0.0365
Right Caudal Middle Frontal	-0.0014	Right Caudal Middle Frontal	-0.2202	Right Caudal Middle Frontal	-0.0506
Right Precentral	-0.0018	Left Superior Frontal	-0.2780	Left Superior Frontal	-0.0538
Left Superior Frontal	-0.0020	Right Precentral	-0.2871	Right Precentral	-0.0623
Right Superior Frontal	-0.0022	Right Superior Frontal	-0.3230	Right Superior Frontal	-0.0627
Left Rostral Middle Frontal	-0.0029	Right Rostral Middle Frontal	-0.4651	Right Rostral Middle Frontal	-0.0956
Right Rostral Middle Frontal	-0.0029	Left Rostral Middle Frontal	-0.4906	Left Rostral Middle Frontal	-0.0992

DISCUSSION

This study used a combination of mass-univariate and multivariate analyses applied to rs-fMRI data to investigate effects of subconcussion effects on metrics thought to represent proxies for spontaneous brain activity (ALFF/fALFF), and local (ReHo) and long-range (DC) functional connectivity. The college-age male control (MC) group served as a low-to-no subconcussive exposure control group. Mass-univariate analyses found no significant changes in any of the twelve statistical tests (i.e. 4 metrics in 3 groups), but the paired SVM found significantly high class accuracy for preseason-to-postseason changes in ALFF in CF (80%, $p=0.012$) and MC (76%, $p=0.003$), fALFF in CF (87%, $p=0.006$) and MC (72%, $p=0.017$), and ReHo in CF (87%, $p=0.009$). At a superficial level this finding agrees with prior studies in concussion^{129,222-224}, although direct comparison is limited by the nature of the spatial information resulting from SVM analyses. However, our ranking distance finding of significant correspondence between the t-statistic maps and SVM weight maps for all six statistical tests supports the ideas that: 1) these disparate analyses are converging upon similar underlying effects and 2) meaningful spatial information may exist in the SVM weight maps. Further ranking distance analyses indicated that fALFF, ReHo, and DC may be experiencing similar trends for the college football athletes, and that college football and control groups are not experiencing similar trends in ALFF and fALFF.

Comparing mass-univariate and multivariate analyses. While mass-univariate analyses were unable to detect changes in any group or metric, paired SVM classification demonstrated significantly high classification accuracy for CF's ALFF, fALFF, and ReHo difference maps. The high accuracy of SVM classification for CF's ALFF, fALFF,

and ReHo indicates that over the course of a single season college football players' spontaneous brain activity and local functional connectivity are changing. The fact that the multivariate analysis, which can use information from across the brain, was able to detect a change that was undetectable for mass-univariate analyses agrees with the hypothesis that changes affected by subconcussion are spatially heterogeneous across subjects and/or spatially distributed within subjects. The inability of mass-univariate analyses to identify effects, when they were identifiable in response to concussion, suggests that subconcussion may produce similarly distributed (but more subtle) effects than concussion.

Mass-univariate and multivariate ranking distance comparisons. The results from the ranking distance analyses showed that the mass-univariate analyses and paired SVM classification have a remarkable level of spatial correspondence. Every comparison between t-statistic and SVM weight region rankings resulted in a ranking distance that was substantially lower than the lowest value calculated in permutation testing (Figure 11). It is surprising that these maps have such a high level of agreement, as they use vastly dissimilar processes to produce their results. While voxel-wise analyses ostensibly treat the effects in each voxel independently, the SVM classifier is trained to weight a number of spatially distributed voxels to discriminate between the two groups. The resulting SVM weight maps are not generally considered to be spatially interpretable⁷⁷, but the high spatial correspondence with the t-statistic maps suggests that valuable spatial information may be contained in the weight maps.

Similarity to findings in concussion. Zhou et al. (2014) measured fALFF in mTBI patients 3-58 days after injury and compared those measures to those found in healthy

controls (HC). Zhou et al. (2014) found multiple clusters showing fALFF decreases in the frontal, occipital, and temporal cortices²²⁴. Zhan et al. (2016) measured ALFF and fALFF in mTBI patients 0.5-12 days after injury and compared those measures to those found in healthy controls (HC). Zhan et al (2016) found mTBI patients had increased ALFF in the right middle frontal gyrus, and decreased ALFF in the right lingual gyrus (LgG) and fusiform gyrus (FuG), left occipital gyrus, and left cuneus and LgG, compared to controls. For fALFF, there was an increase in the left precuneus, and decreases in the right LgG and FuG, and left middle occipital gyrus²²². Similar to Zhan et al. (2016), CF's ALFF and fALFF region average brain maps (Figure 13) indicated ALFF decreases in the right LgG, and fALFF increases in the left precuneus. However, all other Zhan et al (2016) findings disagreed with the trends found in the region average brain maps. Zhou et al. (2014) did not provide enough regional information for direct comparison with our data.

Zhan et al. (2015) measured ReHo in patients diagnosed with a mild traumatic brain injury (mTBI) a few days after injury and compared them to matched controls. Patients with mTBI, compared to the control group, had lower ReHo values in the left insula, left precentral (PrG) and postcentral gyri (PoG), and the supramarginal gyrus (SMG)²²³. Meier, Bellgowan, and Mayer (2016) measured DC and ReHo at multiple time points after athletes had sustained a sports-related concussion (SRC) (mean days after injury: T1=1.7, T2=8.4, T3=32.4) and compared those measures to those found in a healthy athlete (HA) control group. Similar to our data, they found no changes in DC at any time point relative to the athlete control group. At one-month post injury (T3) concussed athletes, compared to the HA control group, had increased ReHo at the

bilateral postcentral gyri (PoG), left paracentral lobule (PCL), right LgG, right FuG, right superior temporal gyrus (STG), right middle temporal gyrus (MTG), and the right supplementary motor area (SMA), and decreased ReHo in the right middle frontal gyrus (MFG), right superior frontal gyrus (SFG), and superior medial frontal gyrus (SMFG)¹²⁹.

Similar to the published results from Zhan et al. (2015) and Meier, Bellgowan, and Mayer (2016) the region average brain map (Figure 12) indicated increased ReHo in bilateral PoG, right LgG, right FuG, right STG, and ReHo decreased in left insula and SMG, and right superior and medial frontal gyri (Table 10). In the DKT atlas, the SMA and SMFG are included in the superior frontal gyrus, disallowing direct comparison to those regions in which Meier et al. showed increases and decreases, respectively. The only direct contradictions are with Meier et al.'s increases in the right MTG and left PCL, and Zhan et al.'s decreases in the left PrG and PoG.

Across the regional findings for ALFF and fALFF, our trends matched 2 of 9 previously published region findings. For ReHo, our trends matched 9 of 13 previously published region findings, with agreement in two additional regions unable to be determined. If the effects of concussion are spatially heterogeneous as indicated by heterogeneity in concussion's clinical presentation¹⁵⁸, then then the previously published voxel-wise analyses for ALFF, fALFF, and ReHo may only be detecting a subset of the changes occurring in their participants. The areas of change found in their studies may, or may not, be more susceptible to head impacts than other regions, and different populations may result in different findings. In this study of subconcussion, the spatial heterogeneity combined with subtler overall effects result in no significant clusters from voxel-wise analysis. While the underlying spatial trends in ReHo seem to agree

remarkably well with the published findings in concussion, the spatial trends for ALFF and fALFF appear to diverge from previous findings.

Ranking difference comparisons for ALFF and fALFF. Both of the college football and control groups had significantly high accuracies in SVM classification for ALFF and fALFF. The presence of a change in the control group casts doubt on whether the changes seen in CF's ALFF and fALFF values are abnormal. The findings in both groups underscore the importance of collecting control group data, even with longitudinal measures. It cannot be assumed that change itself is exceptional. To determine if the two groups were experiencing a similar change, the ranking distance was calculated between the college football and control groups' and MC's W_{ROI} rankings for ALFF and fALFF. The insignificant ranking distance between the two groups (RD=0.506, $p=0.862$; RD=0.450, $p=0.260$, respectively) suggests that the groups are not experiencing similar changes in ALFF and fALFF. While some longitudinal changes in controls may be normal, the changes experienced by college football players seem to be abnormal.

Ranking distance between metrics for college football. The low ranking distance for CF's fALFF, ReHo, and DC rankings suggest that the effects for these metrics may be similar. Although the SVM classifier does not reach a significantly high accuracy for CF's DC difference maps there seems to be a trend ($p=0.084$). ALFF and fALFF are very similar measures, which alone could account for their short ranking distance. ALFF is known to contain more physiological noise than fALFF²¹⁶, and that noise could account for why it does not have significantly short ranking distance with ReHo or DC. Increased spontaneous brain activity could result in increased local or global functional connectivity, or some other physiological changes in these regions could independently

cause changes in these metrics. Resting-state measures of spontaneous activity and functional connectivity are sensitive to a large number of underlying physiological changes in the brain. Previous research in mTBI, concussion, and subconcussion suggest several possible injury mechanisms that may be the cause of these disruptions in spontaneous activity and functional connectivity in the brain, including glial activation and chronic inflammation¹⁷², cytoskeletal disruption in neural axons and somas^{91,112}.

In athletes with a concussion, a disruption in the functional connectivity of the default mode network has been associated with increased cerebrovascular reactivity (CVR): a measure of how cerebral blood flow increases in response to a stimulus¹³². Svaldi et al. (2016) found that CVR was decreased in high school girls' soccer, and those players who experienced greater subconcussive impact load were more affected¹⁸⁵. While any of the proposed mechanisms could play a role in subconcussion's effect on ALFF, fALFF, or ReHo, CVR has the most direct pathway to affect fMRI-measured functional connectivity, and has already been found to be affected by subconcussive head impacts. Furthermore, the lack of a strong effect in global functional connectivity indicates that damage to long-range white matter tracts is not the primary method of subconcussive injury, as global functional connectivity should theoretically be more sensitive to white matter damage than spontaneous activity or local connectivity.

Limitations. There are a few factors about our participant groups that may affect the generalizability of our findings. First, the athlete populations in this study are relatively small and are all from the same Division I university. Second, previous research in football has shown that head impact can be affected by player position¹⁰, offensive style¹²⁰, or practice types¹⁵⁶, all of which could be different at other universities or teams.

It is possible that different results could be obtained at another university, and there are likely differences at lower levels of collegiate competition or for other levels of play (youth, adult amateur, and professional). Youth athletes tend to experience less severe subconcussive head impacts but may be more susceptible to their effects⁴⁹. Third, while our subset of athletes represents a wide variety of player positions, it may not offer an accurate cross-section of the entire team.

To control for differences between a collegiate athlete population and a non-athlete population, such as higher cardiorespiratory fitness²⁰⁰, we also collected data from athletes in lower impact sports like soccer and lacrosse. However, it is possible that other differences exist between CF and OS/MC groups that may be responsible for the differential longitudinal changes in the groups. Some factors that could be different between our two group samples and could affect functional connectivity include: caffeine use^{154,207}, alcohol use³¹, cannabis use³⁵, wakefulness during the rs-fMRI scan¹⁸³, prescription medications¹⁷⁹, and possibly others. Given the longitudinal nature of the study, these uncontrolled confounds would need to change between time points to produce the demonstrated effects. While these alternative explanations cannot be entirely ruled out, the authors believe that the correspondence with ReHo changes in concussion make a strong argument that subconcussive head impacts are the most likely cause of these effects.

Conclusions. This study demonstrates how mass-univariate analyses and paired SVM classification of rs-fMRI data can be combined to provide insight on the effect of subconcussion on spontaneous brain activity and brain functional connectivity. While American football was the high-impact sport under study, it is unlikely to be the only

sport in which these subconcussive effects occur; other high-impact sports like ice hockey, rugby, and combat sports may also result in similar effects. One of the main concerns regarding head impact in sports is its possible role in increasing the risk for developing chronic traumatic encephalopathy and other neurodegenerative disorders^{101,140}. It is not known whether concussion and/or subconcussion is responsible for the increased susceptibility to neurodegenerative disorders later in life, but this study suggests that the effects of subconcussion may be on the same spectrum as sports-related concussion, but with a smaller magnitude of change. Concussion and subconcussion's acute effects on functional connectivity could insidiously lay the foundation for these neurodegenerative diseases. Further research will be needed to determine the quantity and severity of subconcussive exposure needed to produce these disruptions in spontaneous brain activity and functional connectivity by biomechanically measuring head impact and acquiring longitudinal rs-fMRI in the same cohort. Furthermore, the neurophysiological underpinnings of these changes should be studied by acquiring multiple MRI modalities in the same cohort, and comparing their effects across modalities.

CHAPTER IV: CONCLUSIONS AND FUTURE DIRECTIONS

The first goal of this research was to quantify subconcussive head impact in college football, high school football, college soccer, and college lacrosse. Researchers have measured the quantity and severity of head impacts in football for over a decade using helmet-based accelerometer systems^{14,20,26,40,44-45,49,56-57,65,70,73,76,120,125,131,162-163,191,207}, but until recently it was not feasible to quantify head impact in non-helmeted sports. Chapter II presents an analysis of biomechanical impact data from the xPatch sensor in college football, soccer, and lacrosse players collected during their live-action practices and games. As concerns about the amount of subconcussive head impacts in football have risen, those concerns have spread to other contact and collision sports like soccer and lacrosse. The analyses show that college football players receive more head impacts and higher average impact severity than their counterparts in soccer and lacrosse. The only exception is that college soccer players receive more impacts in games than football players, but analysis at multiple thresholds shows that this effect is only true for the lowest impact thresholds (10g and 0rad/s²). At all other impacts thresholds, college football players again receive more impacts than college soccer or lacrosse players. When quantity and severity are both accounted for in measures of impact burden, college football is the clear outlier compared to high school football, college soccer, and college lacrosse. The data shows that while high school football and college soccer and lacrosse players do not receive a trivial amount of head impact, the burden of head impact in college football is much higher.

The xPatch sensors used in this study^{47,126,208}, and other head impact sensor systems^{47,84,208}, have substantial error on individual impacts, which reduces potential uses

for these sensors. For example, much of the biomechanical research in sports has been to find the acceleration threshold at which a concussion is likely to occur^{70,138,159,160}, but unpredictable discrepancies between the measured accelerations and the actual acceleration experienced by the head make this all but impossible. However, researchers can still use this data to find relative differences between two conditions (practice vs. game, high school vs. college, etc.)^{23,26,45,131,163}; as long as the error in the two conditions is constant, any significant comparative findings are reliable.

There are still important open questions regarding subconcussion in sports. First, this data was collected from a limited number of participants from one university and one small private high school, which may limit the generalizability of the results. Multi-site replication of these results with more participants and teams will help to further our understanding about subconcussive impact in these sports. Second, there is still little to no biomechanical head impact data for many other sports that have a high incidence of concussion, including: rugby, ice hockey, wrestling, cheerleading, and martial arts. Third, most of the biomechanical research focuses on the collegiate level, though many more children and teens participate in these sports, and it is possible that younger ages may be more affected by these head impacts. To address these questions research can and should at quantify head impact in different sports, at more competitive levels (youth, high school, college, etc.)^{126,163}, in different gendered versions of the same sport (ex. men's vs. women's soccer), to test the effects of particular head impact reduction programs¹⁸⁶, etc. While biomechanical engineers work to improve the accuracy of these head impact sensors, researchers can utilize the current generation of sensors to further our understanding about the relative amount of head impact in sport.

This is the first study to present live action biomechanical data in college men's soccer or lacrosse, and is also the first set of data that allows for direct comparison of the head impact values between these contact and collision sports. This type of research is vital to identify the relative head impact risk that different sports may pose to the athletes. Research using biomechanical sensors in unhelmeted sports could lead to an understanding of head impact that helps the relevant regulating agencies make informed decisions regarding how to limit unnecessary subconcussive impacts.

Functional MRI (fMRI) has shown particular sensitivity to the effects caused by concussion and subconcussion. First, researchers used task-based approaches to determine if changes in these task-based networks had occurred in response to subconcussion^{20,21,157,169,187}. Next, resting-state fMRI (rs-fMRI) was used to probe changes in the connectivity of the default mode network in response to subconcussion, but produced heterogeneous results^{1,90}. This research used ALFF, fALFF, ReHo, and DC, as metrics of functional activity, local connectivity, and global connectivity, to characterize changes in the brains of the athletes experiencing these subconcussive impacts. These metrics had previously been used to help characterize the effects of concussion, with differences found in spontaneous brain activity^{222,224} and local functional connectivity¹²⁹, but not global functional connectivity¹²⁹.

Chapter III presents data and analyses to determine if any changes in functional activity or connectivity were occurring in these athletes in response to the subconcussive head impacts. Although a voxel-wise analyses did not show any significant changes, the paired SVM revealed that ALFF, fALFF, and ReHo were changing over the course of the season for the football players, but not for the soccer and lacrosse players. The control

group did demonstrate changes as well, but subsequent analysis suggested that the changes in college football were different than those in the control group. Further analyses using the relationship between SVM weight region rankings, indicated that the spatial patterning of effects in fALFF, ReHo, and DC was very similar. These results suggest that long-range white matter tracts are not the primary location for subconcussive damage. If it were, we would have expected DC to be more affected than ReHo. One mechanism that does not directly involve changes in neural activity, but agrees well with these results is the perturbation of cerebral blood flow, particularly cerebrovascular reactivity (CVR). Recent research has shown that CVR can change in response to subconcussive impacts¹⁸⁵, and that in concussion changes in CVR may underlie changes in functional connectivity¹³². The goal of this research is to determine whether subconcussive head impacts affects brain function, and if they do, what is the underlying physiology of these changes. These results show that changes functional changes can occur in college football players, but only provide preliminary data on the underlying physiological mechanisms.

This research presents changes in functional activity and local connectivity in a group of football players over the course of a single season, but there are limitations to the research. First, while no differences were found for soccer and lacrosse players, it is possible that soccer and lacrosse athletes are experiencing changes similar to those in football players, but are beneath the detection threshold for these methods. Second, the increases in ALFF, fALFF and ReHo could be short lived and inconsequential, and it is unknown if these changes indicate microstructural damage of some kind or if they play any role in increased susceptibility to neurodegeneration or any other clinical effects

associated with repetitive brain injury. Third, while we believe the burden of subconcussive impact is the primary difference between these two groups and responsible for the functional changes, we are unable to definitively show that the changes are a direct result of the subconcussive head impacts. While the OS group is intended to control for inherent differences between college athletes and their non-athlete peers, the changes seen in CF could possibly be the result of another difference between the CF and OS groups, such as caffeine use^{154,207}, alcohol use³¹, cannabis use³⁵, wakefulness during the rs-fMRI scan¹⁸³, prescription medications¹⁷⁹, or other possibilities. However, the longitudinal nature of the study partially accounts for confounds of this nature as these factors would need to be change between time points to produce the demonstrated effects.

To address the limited participant sample, future research should attempt to replicate these findings in a larger sample. Using other neuroimaging techniques, such as diffusion tensor imaging, CVR, positron emission tomography, magnetic resonance spectroscopy, could help to further characterize the physiology of the changes occurring in response to subconcussion. Without understanding the underlying physiological effects, it is difficult to develop solutions to protect or restore the brain from these functional changes. Future studies should also attempt to measure head impact and rs-fMRI in the same cohort to determine whether these effects are linked to the burden of subconcussive head impact. Future research should also expand into different sports and levels of competition, because it seems unlikely that college football players are the only group that would experience these changes. Children participating in these sports could possibly be much more susceptible to effects from subconcussive impacts.

In total this thesis presents data showing that college football players receive more impacts with greater average impacts severity than college soccer and lacrosse players, and that college football players were the only group to experience changes in spontaneous brain activity and local functional connectivity over the course of the season. The implication of this research is that the burden of subconcussive head impact experienced in college football is affecting brain function in a way that may predispose these athletes to develop cognitive issues later on life. The hypothesis that subconcussion can affect brain function may be far from proven, but the research contained within this dissertation supports a connection between the two.

ACKNOWLEDGEMENTS

We thank the athletes, trainers, and coaches of the University of Virginia and football, men's lacrosse, and men's soccer teams and the athletes, trainers, and coaches of St. Anne's Belfield football team for their invaluable assistance in collecting this data. Access to the xPatch impact sensors was obtained through a research agreement with X2 Biosystems. Access to the multiband EPI sequence was provided through a research agreement with the University of Minnesota Center for Magnetic Resonance Research and Siemens Healthcare. Financial support that was provided by a University of Virginia Health System Research Award, NIH 2 T32 GM 8328-21, and the University of Virginia Department of Radiology and Medical Imaging.

REFERENCES

1. Abbas K, Shenk TE, Poole VN, Robinson ME, Leverenz LJ, Nauman EA, and Talavage TM. Effects of Repetitive Sub-Concussive Brain Injury on the Functional Connectivity of Default Mode Network in High School Football Athletes. *Developmental Neuropsychology*. 2015;40(1):51-6. doi:10.1080/87565641.2014.990455.
2. Agosta F, Sala S, Valsasina P, Meani A, Canu E, Magnani G, Cappa SF, Scola E, Quatto P, Horsfield MA, Falini A, Comi G, and Filippi M. Brain network connectivity assessed using graph theory in frontotemporal dementia. *Neurology*. 2013;81(2):134-43. doi:10.1212/WNL.0b013e31829a33f8.
3. An L, Cao QJ, Sui MQ, Sun L, Zou QH, Zang YF, and Wang YF. Local synchronization and amplitude of the fluctuation of spontaneous brain activity in attention-deficit/hyperactivity disorder: a resting-state fMRI study. *Neurosci Bull*. 2013;29(5):603-13. doi:10.1007/s12264-013-1353-8.
4. Avants BB, Duda JT, Kilroy E, Krasileva K, Jann K, Kandel BT, Tustison NJ, Yan L, Jog M, Smith R, Wang Y, Dapretto M, and Wang DJ. The pediatric template of brain perfusion. *Sci Data*. 2015;2:150003. doi:10.1038/sdata.2015.3.
5. Avants BB, Tustison NJ, Song G, Cook PA, Klein A, and Gee JC. A reproducible evaluation of ANTs similarity metric performance in brain image registration. *NeuroImage*. 2011;54(3):2033-2044. doi:10.1016/j.neuroimage.2010.09.025.
6. Baggio HC, Sala-Llonch R, Segura B, Marti MJ, Valldeoriola F, Compta Y, Tolosa E, and Junqué C. Functional brain networks and cognitive deficits in Parkinson's disease. *Hum Brain Mapp*. 2014;35(9):4620-34. doi:10.1002/hbm.22499.

7. Bailes JE, Petraglia AL, Omalu BI, Nauman E, and Talavage T. Role of subconcussion in repetitive mild traumatic brain injury. *J Neurosurg.* 2013;119(5):1235-1245.
doi:10.3171/2013.7.JNS121822.
8. Barth JT, Freeman JR, Broshek DK, and Varney RN. Acceleration-Deceleration Sport-Related Concussion: The Gravity of It All. *J Athl Train.* 2001;36(3):253-256.
9. Bauer JA, Thomas TS, Cauraugh JH, Kaminski TW, and Hass CJ. Impact forces and neck muscle activity in heading by collegiate female soccer players. *J Sports Sci.* 2001;19(3):171-9. doi:10.1080/026404101750095312.
10. Baugh CM, Kiernan PT, Kroshus E, Daneshvar DH, Montenigro PH, McKee AC, and Stern R. Frequency of head impact related outcomes by position in NCAA Division I collegiate football players. *Journal of Neurotrauma.* August 2014:140826004426002.
doi:10.1089/neu.2014.3582.
11. Beckmann CF, DeLuca M, Devlin JT, and Smith SM. Investigations into resting-state connectivity using independent component analysis. *Philos Trans R Soc Lond B Biol Sci.* 2005;360(1457):1001-13. doi:10.1098/rstb.2005.1634.
12. Beckwith JG, Greenwald RM, and Chu JJ. Measuring head kinematics in football: correlation between the head impact telemetry system and Hybrid III headform. *Ann Biomed Eng.* 2012;40(1):237-48. doi:10.1007/s10439-011-0422-2.
13. Beckwith JG, Greenwald RM, Chu JJ, Crisco JJ, Rowson S, Duma SM, Broglio SP, McAllister TW, Guskiewicz KM, Mihalik JP, Anderson S, Schnebel B, Brolinson PG, and Collins MW. Head Impact Exposure Sustained by Football Players on Days of Diagnosed Concussion. *Med Sci Sports Exerc.* 2013;45(4):737-746.
doi:10.1249/MSS.0b013e3182792ed7.

14. Beckwith JG, Greenwald RM, Chu JJ, Crisco JJ, Rowson S, Duma SM, Broglio SP, McAllister TW, Guskiewicz KM, Mihalik JP, Anderson S, Schnebel B, Brolinson PG, and Collins MW. Timing of Concussion Diagnosis is Related to Head Impact Exposure prior to Injury. *Med Sci Sports Exerc.* 2013;45(4):747-54.
doi:10.1249/MSS.0b013e3182793067.
15. Behzadi Y, Restom K, Liao J, and Liu TT. A component based noise correction method (CompCor) for BOLD and perfusion based fMRI. *NeuroImage.* 2007;37(1):90-101. doi:10.1016/j.neuroimage.2007.04.042.
16. Belanger HG, and Vanderploeg RD. The neuropsychological impact of sports-related concussion: a meta-analysis. *J Int Neuropsychol Soc.* 2005;11(4):345-57.
17. Biswal B, Yetkin FZ, Haughton VM, and Hyde JS. Functional connectivity in the motor cortex of resting human brain using echo-planar MRI. *Magn Reson Med.* 1995;34(4):537-41.
18. Biswal BB, Mennes M, Zuo XN, Gohel S, Kelly C, Smith SM, Beckmann CF, Adelstein JS, Buckner RL, Colcombe S, Dogonowski AM, Ernst M, Fair D, Hampson M, Hoptman MJ, Hyde JS, Kiviniemi VJ, Kötter R, Li SJ, Lin CP, Lowe MJ, Mackay C, Madden DJ, Madsen KH, Margulies DS, Mayberg HS, McMahon K, Monk CS, Mostofsky SH, Nagel BJ, Pekar JJ, Peltier SJ, Petersen SE, Riedl V, Rombouts SA, Rypma B, Schlaggar BL, Schmidt S, Seidler RD, Siegle GJ, Sorg C, Teng GJ, Veijola J, Villringer A, Walter M, Wang L, Weng XC, Whitfield-Gabrieli S, Williamson P, Windischberger C, Zang YF, Zhang HY, Castellanos FX, and Milham MP. Toward discovery science of human brain function. *Proc Natl Acad Sci U S A.* 2010;107(10):4734-9. doi:10.1073/pnas.0911855107.

19. Braun ML, Buhmann JM, and Müller K-R. On Relevant Dimensions in Kernel Feature Spaces. *J. Mach. Learn. Res.* 2008;9:1875-1908.
<http://dl.acm.org/citation.cfm?id=1390681.1442795>.
20. Breedlove EL, Robinson M, Talavage TM, Morigaki KE, Yoruk U, O'Keefe K, King J, Leverenz LJ, Gilger JW, and Nauman EA. Biomechanical correlates of symptomatic and asymptomatic neurophysiological impairment in high school football. *J Biomech.* 2012;45(7):1265-1272. doi:10.1016/j.jbiomech.2012.01.034.
21. Breedlove KM, Breedlove EL, Robinson M, Poole VN, King JR, Rosenberger P, Rasmussen M, Talavage TM, Leverenz LJ, and Nauman EA. Detecting Neurocognitive and Neurophysiological Changes as a Result of Subconcussive Blows Among High School Football Athletes. *Athletic Training & Sports Health Care.* 2014;6(3):119-127. doi:10.3928/19425864-20140507-02.
22. Broglio SP, Eckner JT, Martini D, Sosnoff JJ, Kutcher JS, and Randolph C. Cumulative head impact burden in high school football. *J Neurotrauma.* 2011;28(10):2069-78. doi:10.1089/neu.2011.1825.
23. Broglio SP, Eckner JT, Surma T, and Kutcher JS. Post-concussion cognitive declines and symptomatology are not related to concussion biomechanics in high school football players. *J Neurotrauma.* 2011;28(10):2061-8. doi:10.1089/neu.2011.1905.
24. Broglio SP, Martini D, Kasper L, Eckner JT, and Kutcher JS. Estimation of Head Impact Exposure in High School Football. *The American Journal of Sports Medicine.* September 2013:0363546513502458. doi:10.1177/0363546513502458.

25. Broglio SP, Schnebel B, Sosnoff JJ, Shin S, Fend X, He X, and Zimmerman J. Biomechanical properties of concussions in high school football. *Med Sci Sports Exerc.* 2010;42(11):2064-71. doi:10.1249/MSS.0b013e3181dd9156.
26. Broglio SP, Sosnoff JJ, Shin S, He X, Alcaraz C, and Zimmerman J. Head impacts during high school football: a biomechanical assessment. *J Athl Train.* 2009;44(4):342-9. doi:10.4085/1062-6050-44.4.342.
27. Broglio SP, Surma T, and Ashton-Miller JA. High school and collegiate football athlete concussions: a biomechanical review. *Ann Biomed Eng.* 2012;40(1):37-46. doi:10.1007/s10439-011-0396-0.
28. Bryer EJ, Medaglia JD, Rostami S, and Hillary FG. Neural Recruitment after Mild Traumatic Brain Injury Is Task Dependent: A Meta-analysis. *J Int Neuropsychol Soc.* May 2013;1-12. doi:10.1017/S1355617713000490.
29. Buckner RL, Sepulcre J, Talukdar T, Krienen FM, Liu H, Hedden T, Andrews-Hanna JR, Sperling RA, and Johnson KA. Cortical Hubs Revealed by Intrinsic Functional Connectivity: Mapping, Assessment of Stability, and Relation to Alzheimer's Disease. *The Journal of Neuroscience.* 2009;29(6):1860-1873. doi:10.1523/JNEUROSCI.5062-08.2009.
30. Caswell SV, Lincoln AE, Almquist JL, Dunn RE, and Hinton RY. Video Incident Analysis of Head Injuries in High School Girls' Lacrosse. *The American Journal of Sports Medicine.* 2012;40(4):756-762. doi:10.1177/0363546512436647.
31. Chanraud S, Pitel AL, Pfefferbaum A, and Sullivan EV. Disruption of functional connectivity of the default-mode network in alcoholism. *Cereb Cortex.* 2011;21(10):2272-81. doi:10.1093/cercor/bhq297.

32. Chao-Gan Y, and Yu-Feng Z. DPARSF: A MATLAB Toolbox for "Pipeline" Data Analysis of Resting-State fMRI. *Front Syst Neurosci.* 2010;4:13.
doi:10.3389/fnsys.2010.00013.
33. Chen C, Johnston J, S F, M P, K W, and A P. Functional abnormalities in symptomatic concussed athletes: an fMRI study. *NeuroImage.* 2004;22(1):68 - 82.
doi:10.1016/j.neuroimage.2003.12.032<http://www.sciencedirect.com/science/article/pii/S1053811904000060>.
34. Chen CJ, Wu CH, Liao YP, Hsu HL, Tseng YC, Liu HL, and Chiu WT. Working memory in patients with mild traumatic brain injury: functional MR imaging analysis. *Radiology.* 2012;264(3):844-51. doi:10.1148/radiol.12112154.
35. Cheng H, Skosnik PD, Pruce BJ, Brumbaugh MS, Vollmer JM, Fridberg DJ, O'Donnell BF, Hetrick WP, and Newman SD. Resting state functional magnetic resonance imaging reveals distinct brain activity in heavy cannabis users - a multi-voxel pattern analysis. *J Psychopharmacol.* 2014;28(11):1030-40.
doi:10.1177/0269881114550354.
36. Chen JK, Johnston KM, Collie A, McCrory P, and Ptito A. A validation of the post concussion symptom scale in the assessment of complex concussion using cognitive testing and functional MRI. *J Neurol Neurosurg Psychiatry.* 2007;78(11):1231-8.
doi:10.1136/jnnp.2006.110395.
37. Chen JK, Johnston KM, Petrides M, and Ptito A. Neural substrates of symptoms of depression following concussion in male athletes with persisting postconcussion symptoms. *Arch Gen Psychiatry.* 2008;65(1):81-9.
doi:10.1001/archgenpsychiatry.2007.8.

38. Chou YH, Panych LP, Dickey CC, Petrella JR, and Chen NK. Investigation of long-term reproducibility of intrinsic connectivity network mapping: a resting-state fMRI study. *AJNR Am J Neuroradiol*. 2012;33(5):833-8. doi:10.3174/ajnr.A2894.
39. Clarke KS. Epidemiology of athletic head injury. *Clin Sports Med*. 1998;17(1):1-12.
40. Cobb BR, Urban JE, Davenport EM, Rowson S, Duma SM, Maldjian JA, Whitlow CT, Powers AK, and Stitzel JD. Head Impact Exposure in Youth Football: Elementary School Ages 9-12 Years and the Effect of Practice Structure. *Ann Biomed Eng*. 2013;41(12):2463-73. doi:10.1007/s10439-013-0867-6.
41. Cortes C, and Vapnik V. Support-vector networks. *Machine learning*. 1995;20(3):273-297.
42. Covassin T, Swanik CB, and Sachs ML. Epidemiological considerations of concussions among intercollegiate athletes. *Appl Neuropsychol*. 2003;10(1):12-22. doi:10.1207/S15324826AN1001_3.
43. Crisco JJ, Costa L, Rich R, Schwartz J, and Wilcox B. Surrogate Headform Accelerations Associated with Stick Checks in Girls' Lacrosse. *J Appl Biomech*. 2014;31(2):122-127. doi:10.1123/jab.2014-0102.
44. Crisco JJ, Fiore R, Beckwith JG, Chu JJ, Brolinson PG, Duma S, McAllister TW, Duhaime AC, and Greenwald RM. Frequency and location of head impact exposures in individual collegiate football players. *J Athl Train*. 2010;45(6):549-59. doi:10.4085/1062-6050-45.6.549.
45. Crisco JJ, Wilcox BJ, Beckwith JG, Chu JJ, Duhaime AC, Rowson S, Duma SM, Maerlender AC, McAllister TW, and Greenwald RM. Head impact exposure in collegiate football players. *J Biomech*. 2011;44(15):2673-8. doi:10.1016/j.jbiomech.2011.08.003.

46. Cui Y, Jin Z, Chen X, He Y, Liang X, and Zheng Y. Abnormal baseline brain activity in drug-naïve patients with Tourette syndrome: a resting-state fMRI study. *Front Hum Neurosci.* 2014;7:913. doi:10.3389/fnhum.2013.00913.
47. Cummiskey B, Schmittmiller D, Talavage TM, Leverenz L, Meyer JJ, Adams D, and Nauman EA. Reliability and accuracy of helmet-mounted and head-mounted devices used to measure head accelerations. *Journal of Sports Engineering and Technology.* 2016.
48. Dajani DR, and Uddin LQ. Local brain connectivity across development in autism spectrum disorder: A cross-sectional investigation. *Autism Res.* June 2015. doi:10.1002/aur.1494.
49. Daniel RW, Rowson S, and Duma SM. Head impact exposure in youth football. *Ann Biomed Eng.* 2012;40(4):976-81. doi:10.1007/s10439-012-0530-7.
50. Davenport EM, Whitlow CT, Urban JE, Espeland MA, Jung Y, Rosenbaum DA, Gioia GA, Powers AK, Stitzel JD, and Maldjian JA. Abnormal White Matter Integrity Related to Head Impact Exposure in a Season of High School Varsity Football. *Journal of Neurotrauma.* 2014;31(19):1617-1624. doi:10.1089/neu.2013.3233.
51. Davenport ND, Lim KO, Armstrong MT, and Sponheim SR. Diffuse and spatially variable white matter disruptions are associated with blast-related mild traumatic brain injury. *Neuroimage.* 2012;59(3):2017-24. doi:10.1016/j.neuroimage.2011.10.050.
52. Davis GA, Iverson GL, Guskiewicz KM, Ptito A, and Johnston KM. Contributions of neuroimaging, balance testing, electrophysiology and blood markers to the assessment of sport-related concussion. *Br J Sports Med.* 2009;43 Suppl 1:i36-45. doi:10.1136/bjism.2009.058123.

53. Di Martino A, Zuo XN, Kelly C, Grzadzinski R, Mennes M, Schvarcz A, Rodman J, Lord C, Castellanos FX, and Milham MP. Shared and distinct intrinsic functional network centrality in autism and attention-deficit/hyperactivity disorder. *Biol Psychiatry*. 2013;74(8):623-32. doi:10.1016/j.biopsych.2013.02.011.
54. Dompier TP, Kerr ZY, Marshall SW, Hainline B, Snook EM, Hayden R, and Simon JE. Incidence of Concussion During Practice and Games in Youth, High School, and Collegiate American Football Players. *JAMA Pediatr*. 2015;169(7):659-65. doi:10.1001/jamapediatrics.2015.0210.
55. Dosenbach NU, Visscher KM, Palmer ED, Miezin FM, Wenger KK, Kang HC, Burgund ED, Grimes AL, Schlaggar BL, and Petersen SE. A core system for the implementation of task sets. *Neuron*. 2006;50(5):799-812. doi:10.1016/j.neuron.2006.04.031.
56. Duma SM, Manoogian SJ, Bussone WR, Brolinson PG, Goforth MW, Donnenwerth JJ, Greenwald RM, Chu JJ, and Crisco JJ. Analysis of real-time head accelerations in collegiate football players. *Clin J Sport Med*. 2005;15(1):3-8.
57. Eckner JT, Sabin M, Kutcher JS, and Broglio SP. No evidence for a cumulative impact effect on concussion injury threshold. *J Neurotrauma*. 2011;28(10):2079-90. doi:10.1089/neu.2011.1910.
58. Farb NA, Grady CL, Strother S, Tang-Wai DF, Masellis M, Black S, Freedman M, Pollock BG, Campbell KL, Hasher L, and Chow TW. Abnormal network connectivity in frontotemporal dementia: evidence for prefrontal isolation. *Cortex*. 2013;49(7):1856-73. doi:10.1016/j.cortex.2012.09.008.

59. Feinberg DA, Moeller S, Smith SM, Auerbach E, Ramanna S, Glasser MF, Miller KL, Ugurbil K, and Yacoub E. Multiplexed Echo Planar Imaging for Sub-Second Whole Brain fMRI and Fast Diffusion Imaging. *PLOS ONE*. 2010;5(12):e15710. doi:10.1371/journal.pone.0015710.
60. Ford JH, Giovanello KS, and Guskiewicz KK. Episodic Memory in Former Professional Football Players with a History of Concussion: An Event-Related Functional Neuroimaging Study. *Journal of Neurotrauma*. May 2013:130516071626007. doi:10.1089/neu.2012.2535.
61. Formisano E, De Martino F, and Valente G. Multivariate analysis of fMRI time series: classification and regression of brain responses using machine learning. *Magnetic Resonance Imaging*. 2008;26(7):921-934. doi:10.1016/j.mri.2008.01.052.
62. Fox MD, Corbetta M, Snyder AZ, Vincent JL, and Raichle ME. Spontaneous neuronal activity distinguishes human dorsal and ventral attention systems. *Proc Natl Acad Sci U S A*. 2006;103(26):10046-51. doi:10.1073/pnas.0604187103.
63. Fox PT, and Raichle ME. Focal physiological uncoupling of cerebral blood flow and oxidative metabolism during somatosensory stimulation in human subjects. *Proc Natl Acad Sci U S A*. 1986;83(4):1140-4.
64. Fréchède B, and McIntosh AS. Numerical reconstruction of real-life concussive football impacts. *Med Sci Sports Exerc*. 2009;41(2):390-8. doi:10.1249/MSS.0b013e318186b1c5.
65. Funk JR, Duma SM, Manoogian SJ, and Rowson S. Biomechanical risk estimates for mild traumatic brain injury. *Annu Proc Assoc Adv Automot Med*. 2007;51:343-61.

66. Funk JR, Rowson S, Daniel RW, and Duma SM. Validation of concussion risk curves for collegiate football players derived from HITS data. *Ann Biomed Eng.* 2012;40(1):79-89. doi:10.1007/s10439-011-0400-8.
67. Gessel LM, Fields SK, Collins CL, Dick RW, and Comstock RD. Concussions among United States high school and collegiate athletes. *J Athl Train.* 2007;42(4):495-503.
68. Golland P, and Fischl B. *Permutation Tests for Classification: Towards Statistical Significance in Image-Based Studies.* Springer Berlin Heidelberg; 2003:330-341. doi:10.1007/978-3-540-45087-0_28.
69. Gosselin N, Bottari C, Chen JK, Petrides M, Tinawi S, de Guise E, and Ptito A. Electrophysiology and functional MRI in post-acute mild traumatic brain injury. *J Neurotrauma.* 2011;28(3):329-41. doi:10.1089/neu.2010.1493.
70. Greenwald RM, Gwin JT, Chu JJ, and Crisco JJ. Head impact severity measures for evaluating mild traumatic brain injury risk exposure. *Neurosurgery.* 2008;62(4):789-98; discussion 798. doi:10.1227/01.neu.0000318162.67472.ad.
71. Greicius MD, Krasnow B, Reiss AL, and Menon V. Functional connectivity in the resting brain: a network analysis of the default mode hypothesis. *Proc Natl Acad Sci U S A.* 2003;100(1):253-8. doi:10.1073/pnas.0135058100.
72. Gurdjian ES, Lissner HR, Hodgson VR, and Patrick LM. Mechanism of head injury. *Clinical neurosurgery.* 1964;12:112.
73. Guskiewicz KM, Mihalik JP, Viswanathan S, Marshall SW, Crosswell DH, Oliaro SM, Ciocca MF, and Hooker DN. Measurement of Head Impacts in Collegiate Football Players: Relationship Between Head Impact Biomechanics and Acute Clinical Outcome

After Concussion. *Neurosurgery*. 2007;61(6):1244-53.

doi:10.1227/01.NEU.0000280146.37163.79.

74. Gysland SM, Mihalik JP, Register-Mihalik JK, Trulock SC, Shields EW, and Guskiewicz KM. The relationship between subconcussive impacts and concussion history on clinical measures of neurologic function in collegiate football players. *Ann Biomed Eng*. 2012;40(1):14-22. doi:10.1007/s10439-011-0421-3.

75. Hanlon EM, and Bir CA. Real-time head acceleration measurement in girls' youth soccer. *Med Sci Sports Exerc*. 2012;44(6):1102-1108.

doi:10.1249/MSS.0b013e3182444d7d.

76. Harpham JA, Mihalik JP, Littleton AC, Frank BS, and Guskiewicz KM. The Effect of Visual and Sensory Performance on Head Impact Biomechanics in College Football Players. *Annals of Biomedical Engineering*. 2014;42(1):1-10. doi:10.1007/s10439-013-0881-8.

77. Haufe S, Meinecke F, Görgen K, Dähne S, Haynes JD, Blankertz B, and Bießmann F. On the interpretation of weight vectors of linear models in multivariate neuroimaging. *Neuroimage*. 2014;87:96-110. doi:10.1016/j.neuroimage.2013.10.067.

78. Hootman JM, Dick R, and Agel J. Epidemiology of collegiate injuries for 15 sports: summary and recommendations for injury prevention initiatives. *J Athl Train*. 2007;42(2):311-319.

79. Huang X, Huang P, Li D, Zhang Y, Wang T, Mu J, Li Q, and Xie P. Early brain changes associated with psychotherapy in major depressive disorder revealed by resting-state fMRI: evidence for the top-down regulation theory. *Int J Psychophysiol*.

2014;94(3):437-44. doi:10.1016/j.ijpsycho.2014.10.011.

80. Huber PJ. The behavior of maximum likelihood estimates under nonstandard conditions. In: *Proceedings of the Fifth Berkeley Symposium on Mathematical Statistics and Probability*. 1. ; 1967:221-233.
81. Hu XF, Zhang JQ, Jiang XM, Zhou CY, Wei LQ, Yin XT, Li J, Zhang YL, and Wang J. Amplitude of low-frequency oscillations in Parkinson's disease: a 2-year longitudinal resting-state functional magnetic resonance imaging study. *Chin Med J (Engl)*. 2015;128(5):593-601. doi:10.4103/0366-6999.151652.
82. Hwang S, Ma L, Kawata K, Tierney R, and Jeka J. Vestibular Dysfunction following Sub-Concussive Head Impact. *Journal of Neurotrauma*. February 2016. doi:10.1089/neu.2015.4238.
83. Itahashi T, Yamada T, Watanabe H, Nakamura M, Ohta H, Kanai C, Iwanami A, Kato N, and Hashimoto R. Alterations of local spontaneous brain activity and connectivity in adults with high-functioning autism spectrum disorder. *Mol Autism*. 2015;6:30. doi:10.1186/s13229-015-0026-z.
84. Jadischke R, Viano DC, Dau N, King AI, and McCarthy J. On the accuracy of the Head Impact Telemetry (HIT) System used in football helmets. *Journal of Biomechanics*. 2013;46(13):2310-2315. doi:10.1016/j.jbiomech.2013.05.030.
85. Jantzen KJ, Anderson B, Steinberg FL, and Kelso JA. A prospective functional MR imaging study of mild traumatic brain injury in college football players. *AJNR Am J Neuroradiol*. 2004;25(5):738-45.
86. Jenkinson M, Beckmann CF, Behrens TE, Woolrich MW, and Smith SM. FSL. *NeuroImage*. 2012;62(2):782-790. doi:10.1016/j.neuroimage.2011.09.015.

87. Jing B, Liu CH, Ma X, Yan HG, Zhuo ZZ, Zhang Y, Wang SH, Li HY, and Wang CY. Difference in amplitude of low-frequency fluctuation between currently depressed and remitted females with major depressive disorder. *Brain Res.* 2013;1540:74-83. doi:10.1016/j.brainres.2013.09.039.
88. Johnson B, Zhang K, Gay M, Horovitz S, Hallett M, Sebastianelli W, and Slobounov S. Alteration of brain default network in subacute phase of injury in concussed individuals: Resting-state fMRI study. *NeuroImage.* 2012;59(1):511 - 518. doi:10.1016/j.pmrj.2010.06.002<http://www.sciencedirect.com/science/article/pii/S1053811911008767>.
89. Johnson BD. Sports-Related Subconcussive Head Trauma. In: *Concussions in Athletics*. Springer New York; 2014:331-344. doi:10.1007/978-1-4939-0295-8_19.
90. Johnson BD, Neuberger T, Gay M, Hallett M, and Slobounov S. Effects of Subconcussive Head Trauma on the Default Mode Network of the Brain. *Journal of Neurotrauma.* 2014;31(23):140710103819004. doi:10.1089/neu.2014.3415.
91. Kanayama G, Takeda M, Niigawa H, Ikura Y, Tamii H, Taniguchi N, Kudo T, Miyamae Y, Morihara T, and Nishimura T. The effects of repetitive mild brain injury on cytoskeletal protein and behavior. *Methods Find Exp Clin Pharmacol.* 1996;18(2):105-15.
92. Kawata K, Rubin LH, Lee JH, Sim T, Takahagi M, Szwanki V, Bellamy A, Darvish K, Assari S, Henderer JD, Tierney R, and Langford D. Association of Football Subconcussive Head Impacts With Ocular Near Point of Convergence. *JAMA Ophthalmology.* May 2016. doi:10.1001/jamaophthalmol.2016.1085.

93. Kendall M, and Gibbons JDR. *Correlation Methods*. Oxford, England: Oxford University Press; 1990.
94. Kerr ZY, Yeargin SW, Valovich McLeod TC, Mensch J, Hayden R, and Dompier TP. Comprehensive Coach Education Reduces Head Impact Exposure in American Youth Football. *Orthopaedic Journal of Sports Medicine*. 2015;3(10). doi:10.1177/2325967115610545http://ojs.sagepub.com/cgi/content/abstract/3/10/2325967115610545.
95. King D, Hume P, Gissane C, Brughelli M, and Clark T. The Influence of Head Impact Threshold for Reporting Data in Contact and Collision Sports: Systematic Review and Original Data Analysis. *Sports Medicine*. 2016;46(2):151-169. doi:10.1007/s40279-015-0423-7.
96. Klein A, and Tourville J. 101 Labeled Brain Images and a Consistent Human Cortical Labeling Protocol. *Front. Neurosci*. 2012;6. doi:10.3389/fnins.2012.00171.
97. Koerte IK, Ertl-Wagner B, Reiser M, Zafonte R, and Shenton ME. White Matter Integrity in the Brains of Professional Soccer Players Without a Symptomatic Concussion. *JAMA: The Journal of the American Medical Association*. 2012;308(18):1859-1861. doi:10.1001/jama.2012.13735.
98. Kontos AP, Elbin RJ, Fazio-Sumrock VC, Burkhart S, Swindell H, Maroon J, and Collins MW. Incidence of Sports-Related Concussion among Youth Football Players Aged 8-12 Years. *Journal of Pediatrics*. June 2013. doi:10.1016/j.jpeds.2013.04.011.
99. Krivitzky LS, Roebuck-Spencer TM, Roth RM, Blackstone K, Johnson CP, and Gioia G. Functional magnetic resonance imaging of working memory and response inhibition

in children with mild traumatic brain injury. *J Int Neuropsychol Soc.* 2011;17(6):1143-52. doi:10.1017/S1355617711001226.

100. Lee MH, Smyser CD, and Shimony JS. Resting-State fMRI: A Review of Methods and Clinical Applications. *AJNR Am J Neuroradiol.* August 2012. doi:10.3174/ajnr.A3263.

101. Lehman EJ, Hein MJ, Baron SL, and Gersic CM. Neurodegenerative causes of death among retired National Football League players. *Neurology.* 2012;79(19):1970-1974. doi:10.1212/WNL.0b013e31826daf50.

102. Lempel R, and Moran S. Rank-Stability and Rank-Similarity of Link-Based Web Ranking Algorithms in Authority-Connected Graphs. *Information Retrieval.* 2005;8(2):245-264. doi:10.1007/s10791-005-5661-0.

103. Liang MJ, Zhou Q, Yang KR, Yang XL, Fang J, Chen WL, and Huang Z. Identify changes of brain regional homogeneity in bipolar disorder and unipolar depression using resting-state FMRI. *PLoS One.* 2013;8(12):e79999. doi:10.1371/journal.pone.0079999.

104. Lincoln AE, Caswell SV, Almquist JL, Dunn RE, and Hinton RY. Video incident analysis of concussions in boys' high school lacrosse. *Am J Sports Med.* 2013;41(4):756-61. doi:10.1177/0363546513476265.

105. Lincoln AE, Caswell SV, Almquist JL, Dunn RE, Norris JB, and Hinton RY. Trends in concussion incidence in high school sports: a prospective 11-year study. *Am J Sports Med.* 2011;39(5):958-63. doi:10.1177/0363546510392326.

106. Lipton ML, Kim N, Zimmerman ME, Kim M, Stewart WF, Branch CA, and Lipton RB. Soccer Heading Is Associated with White Matter Microstructural and Cognitive Abnormalities. *Radiology.* 2013;268(3):850-857. doi:10.1148/radiol.13130545.

107. Liu CH, Ma X, Wu X, Fan TT, Zhang Y, Zhou FC, Li LJ, Li F, Tie CL, Li SF, Zhang D, Zhou Z, Dong J, Wang YJ, Yao L, and Wang CY. Resting-state brain activity in major depressive disorder patients and their siblings. *J Affect Disord.* 2013;149(1-3):299-306. doi:10.1016/j.jad.2013.02.002.
108. Liu H, Liu Z, Liang M, Hao Y, Tan L, Kuang F, Yi Y, Xu L, and Jiang T. Decreased regional homogeneity in schizophrenia: a resting state functional magnetic resonance imaging study. *Neuroreport.* 2006;17(1):19-22.
109. Liu J, Zhu YS, Khan MA, Brunk E, Martin-Cook K, Weiner MF, Cullum CM, Lu H, Levine BD, Diaz-Arrastia R, and Zhang R. Global brain hypoperfusion and oxygenation in amnesic mild cognitive impairment. *Alzheimers Dement.* 2014;10(2):162-70. doi:10.1016/j.jalz.2013.04.507.
110. Liu Y, Wang K, Yu C, He Y, Zhou Y, Liang M, Wang L, and Jiang T. Regional homogeneity, functional connectivity and imaging markers of Alzheimer's disease: a review of resting-state fMRI studies. *Neuropsychologia.* 2008;46(6):1648-56. doi:10.1016/j.neuropsychologia.2008.01.027.
111. Logothetis NK. The neural basis of the blood-oxygen-level-dependent functional magnetic resonance imaging signal. *Philos Trans R Soc Lond B Biol Sci.* 2002;357(1424):1003-37. doi:10.1098/rstb.2002.1114.
112. Longhi L, Saatman KE, Fujimoto S, Raghupathi R, Meaney DF, Davis J, McMillan A, Conte V, Laurer HL, Stein S, Stocchetti N, and McIntosh TK. Temporal Window of Vulnerability to Repetitive Experimental Concussive Brain Injury. *Neurosurgery.* 2005;56(2):364. doi:10.1227/01.NEU.0000149008.73513.44.

113. Lord LD, Allen P, Expert P, Howes O, Broome M, Lambiotte R, Fusar-Poli P, Valli I, McGuire P, and Turkheimer FE. Functional brain networks before the onset of psychosis: A prospective fMRI study with graph theoretical analysis. *Neuroimage Clin.* 2012;1(1):91-8. doi:10.1016/j.nicl.2012.09.008.
114. De Luca M, Beckmann CF, De Stefano N, Matthews PM, and Smith SM. fMRI resting state networks define distinct modes of long-distance interactions in the human brain. *Neuroimage.* 2006;29(4):1359-67. doi:10.1016/j.neuroimage.2005.08.035.
115. Lynall RC, Clark MD, Grand EE, Stucker JC, Littleton AC, Aguilar AJ, Petschauer MA, Teel EF, and Mihalik JP. Head Impact Biomechanics in Women's College Soccer. *Med Sci Sports Exerc.* May 2016. doi:10.1249/MSS.0000000000000951.
116. Mahmoudi A, Takerkart S, Regragui F, Boussaoud D, and Brovelli A. Multivoxel pattern analysis for FMRI data: a review. *Comput Math Methods Med.* 2012;2012:961257. doi:10.1155/2012/961257.
117. Malonek D, and Grinvald A. Interactions between electrical activity and cortical microcirculation revealed by imaging spectroscopy: implications for functional brain mapping. *Science.* 1996;272(5261):551-4.
118. Manoogian S, McNeely D, Duma S, Brolinson G, and Greenwald R. Head acceleration is less than 10 percent of helmet acceleration in football impacts. *Biomed Sci Instrum.* 2006;42:383-8.
119. Marar M, McIlvain NM, Fields SK, and Comstock RD. Epidemiology of concussions among United States high school athletes in 20 sports. *Am J Sports Med.* 2012;40(4):747-55. doi:10.1177/0363546511435626.

120. Martini D, Eckner J, Kutcher J, and Broglio SP. Subconcussive head impact biomechanics: comparing differing offensive schemes. *Med Sci Sports Exerc.* 2013;45(4):755-61. doi:10.1249/MSS.0b013e3182798758.
121. Martland H. Punch drunk. *JAMA.* 1928;91:1103-7.
122. Mayer AR, Mannell MV, Ling J, Gasparovic C, and Yeo RA. Functional connectivity in mild traumatic brain injury. *Hum Brain Mapp.* 2011;32(11):1825-35. doi:10.1002/hbm.21151.
123. McAllister TW, Saykin AJ, Flashman LA, Sparling MB, Johnson SC, Guerin SJ, Mamourian AC, Weaver JB, and Yanofsky N. Brain activation during working memory 1 month after mild traumatic brain injury: a functional MRI study. *Neurology.* 1999;53(6):1300-8.
124. McAllister TW, Sparling MB, Flashman LA, Guerin SJ, Mamourian AC, and Saykin AJ. Differential working memory load effects after mild traumatic brain injury. *Neuroimage.* 2001;14(5):1004-12. doi:10.1006/nimg.2001.0899.
125. McCaffrey MA, Mihalik JP, Crowell DH, Shields EW, and Guskiewicz KM. Measurement of head impacts in collegiate football players: clinical measures of concussion after high- and low-magnitude impacts. *Neurosurgery.* 2007;61(6):1236-43; discussion 1243. doi:10.1227/01.neu.0000306102.91506.8b.
126. McCuen E, Svaldi D, Breedlove K, Kraz N, Cummiskey B, Breedlove EL, Traver J, Desmond KF, Hannemann RE, Zanath E, Guerra A, Leverenz L, Talavage TM, and Nauman EA. Collegiate Women's Soccer Players Suffer Greater Cumulative Head Impacts than their High School Counterparts. *Journal of Biomechanics.* 2015;48(13):3729-32. doi:10.1016/j.jbiomech.2015.08.003.

127. McKee AC, Cantu RC, Nowinski CJ, Hedley-Whyte ET, Gavett BE, Budson AE, Santini VE, Lee HS, Kubilus CA, and Stern RA. Chronic traumatic encephalopathy in athletes: progressive tauopathy after repetitive head injury. *J Neuropathol Exp Neurol*. 2009;68(7):709-35. doi:10.1097/NEN.0b013e3181a9d503.
128. McKee AC, Daneshvar DH, Alvarez VE, and Stein TD. The neuropathology of sport. *Acta Neuropathologica*. 2013;127(1):1-23. doi:10.1007/s00401-013-1230-6.
129. Meier TB, Bellgowan PSF, and Mayer AR. Longitudinal assessment of local and global functional connectivity following sports-related concussion. *Brain Imaging and Behavior*. January 2016:1-12. doi:10.1007/s11682-016-9520-y.
130. Meier TB, Desphande AS, Vergun S, Nair VA, Song J, Biswal BB, Meyerand ME, Birn RM, and Prabhakaran V. Support vector machine classification and characterization of age-related reorganization of functional brain networks. *NeuroImage*. 2012;60(1):601-613. doi:10.1016/j.neuroimage.2011.12.052.
131. Mihalik JP, Bell DR, Marshall SW, and Guskiewicz KM. Measurement of head impacts in collegiate football players: an investigation of positional and event-type differences. *Neurosurgery*. 2007;61(6):1229-1235. doi:10.1227/01.neu.0000306101.83882.c8.
132. Militana AR, Donahue MJ, Sills AK, Solomon GS, Gregory AJ, Strother MK, and Morgan VL. Alterations in default-mode network connectivity may be influenced by cerebrovascular changes within 1 week of sports related concussion in college varsity athletes: a pilot study. *Brain Imaging Behav*. May 2015. doi:10.1007/s11682-015-9407-3.
133. Moeller S, Yacoub E, Olman CA, Auerbach E, Strupp J, Harel N, and Uğurbil K. Multiband multislice GE-EPI at 7 tesla, with 16-fold acceleration using partial parallel

- imaging with application to high spatial and temporal whole-brain fMRI. *Magnetic Resonance in Medicine*. 2010;63(5):1144-1153. doi:10.1002/mrm.22361.
134. Mourão-Miranda J, Bokde AL, Born C, Hampel H, and Stetter M. Classifying brain states and determining the discriminating activation patterns: Support Vector Machine on functional MRI data. *NeuroImage*. 2005;28(4):980-995.
doi:10.1016/j.neuroimage.2005.06.070.
135. Müller K-R, Mika S, Rätsch G, Tsuda K, and Schölkopf B. An introduction to kernel-based learning algorithms. *Neural Networks, IEEE Transactions on*. 2001;12(2):181-201.
136. Nathan DE, Wang BQ, Wolfowitz RD, Liu W, Yeh PH, Graner JL, Harper J, Pan H, Oakes TR, and Riedy G. Examining intrinsic thalamic resting state networks using graph theory analysis: implications for mTBI detection. *Conf Proc IEEE Eng Med Biol Soc*. 2012;2012:5445-8. doi:10.1109/EMBC.2012.6347226.
137. Naunheim RS, Standeven J, Richter C, and Lewis LM. Comparison of impact data in hockey, football, and soccer. *J Trauma*. 2000;48(5):938-41.
138. Newman JA, Shewchenko N, and Welbourne E. A proposed new biomechanical head injury assessment function - the maximum power index. *Stapp Car Crash J*. 2000;44:215-47.
139. Nowinski C, and Ventura J. *Head Games : Football's Concussion Crisis From the NFL to Youth Leagues*. East Bridgewater, MA: Drummond Pub. Group; 2007.
140. Omalu BI, DeKosky ST, Hamilton RL, Minster RL, Kamboh MI, Shakir AM, and Wecht CH. Chronic traumatic encephalopathy in a national football league player: part II.

Neurosurgery. 2006;59(5):1086-92; discussion 1092-3.

doi:10.1227/01.NEU.0000245601.69451.27.

141. Omalu BI, DeKosky ST, Minster RL, Kamboh MI, Hamilton RL, and Wecht CH. Chronic traumatic encephalopathy in a National Football League player. *Neurosurgery*. 2005;57(1):128-34; discussion 128-34.

142. Ommaya AK, Goldsmith W, and Thibault L. Biomechanics and neuropathology of adult and paediatric head injury. *Br J Neurosurg*. 2002;16(3):220-42.

143. Orrù G, Pettersson-Yeo W, Marquand AF, Sartori G, and Mechelli A. Using Support Vector Machine to identify imaging biomarkers of neurological and psychiatric disease: A critical review. *Neuroscience & Biobehavioral Reviews*. 2012;36(4):1140-1152. doi:10.1016/j.neubiorev.2012.01.004.

144. Paakki JJ, Rahko J, Long X, Moilanen I, Tervonen O, Nikkinen J, Starck T, Remes J, Hurtig T, Haapsamo H, Jussila K, Kuusikko-Gauffin S, Mattila ML, Zang Y, and Kiviniemi V. Alterations in regional homogeneity of resting-state brain activity in autism spectrum disorders. *Brain Res*. 2010;1321:169-79. doi:10.1016/j.brainres.2009.12.081.

145. Pardini JE, Pardini DA, Becker JT, Dunfee KL, Eddy WF, Lovell MR, and Welling JS. Postconcussive symptoms are associated with compensatory cortical recruitment during a working memory task. *Neurosurgery*. 2010;67(4):1020-7; discussion 1027-8. doi:10.1227/NEU.0b013e3181ee33e2.

146. Pellman EJ. Background on the National Football League's research on concussion in professional football. *Neurosurgery*. 2003;53(4):797-8.

147. Pellman EJ, Viano DC, and National Football League's Committee on Mild Traumatic Brain Injury. Concussion in professional football: summary of the research

conducted by the National Football League's Committee on Mild Traumatic Brain Injury.

Neurosurg Focus. 2006;21(4):E12.

148. Pellman EJ, Viano DC, Tucker AM, and Casson IR. Concussion in professional football: location and direction of helmet impacts-Part 2. *Neurosurgery*.

2003;53(6):1328-40; discussion 1340-1.

149. Pellman EJ, Viano DC, Tucker AM, Casson IR, and Waeckerle JF. Concussion in professional football: reconstruction of game impacts and injuries. *Neurosurgery*.

2003;53(4):799-812; discussion 812-4.

150. Pereira F, Mitchell T, and Botvinick M. Machine learning classifiers and fMRI: A tutorial overview. *NeuroImage*. 2009;45(1):S199-S209.

doi:10.1016/j.neuroimage.2008.11.007.

151. Power JD, Cohen AL, Nelson SM, Wig GS, Barnes KA, Church JA, Vogel AC, Laumann TO, Miezin FM, Schlaggar BL, and Petersen SE. Functional network organization of the human brain. *Neuron*. 2011;72(4):665-78.

doi:10.1016/j.neuron.2011.09.006.

152. Premi E, Cauda F, Gasparotti R, Diano M, Archetti S, Padovani A, and Borroni B. Multimodal FMRI resting-state functional connectivity in granulin mutations: the case of fronto-parietal dementia. *PLoS One*. 2014;9(9):e106500.

doi:10.1371/journal.pone.0106500.

153. Queen RM, Weinhold PS, Kirkendall DT, and Yu B. Theoretical study of the effect of ball properties on impact force in soccer heading. *Med Sci Sports Exerc*.

2003;35(12):2069-76. doi:10.1249/01.MSS.0000099081.20125.A5.

154. Rack-Gomer AL, Liao J, and Liu TT. Caffeine reduces resting-state BOLD functional connectivity in the motor cortex. *Neuroimage*. 2009;46(1):56-63. doi:10.1016/j.neuroimage.2009.02.001.
155. Reed N, Taha T, Keightley M, Duggan C, McAuliffe J, Cubos J, Baker J, Faught B, McPherson M, and Montelpare W. Measurement of head impacts in youth ice hockey players. *Int J Sports Med*. 2010;31(11):826-33. doi:10.1055/s-0030-1263103.
156. Reynolds BB, Patrie J, Henry EJ, Goodkin HP, Broshek DK, Wintermark M, and Druzgal TJ. Practice Type Effects on Head Impact in Collegiate Football. *Journal of Neurosurgery*. 2016;124(2):501-510.
157. Robinson ME, Shenk TE, Breedlove EL, Leverenz LJ, Nauman EA, and Talavage TM. The Role of Location of Subconcussive Head Impacts in fMRI Brain Activation Change. *Developmental Neuropsychology*. May 2015. doi:10.1080/87565641.2015.1012204.
158. Rosenbaum SB, and Lipton ML. Embracing chaos: the scope and importance of clinical and pathological heterogeneity in mTBI. *Brain Imaging Behav*. 2012;6(2):255-82. doi:10.1007/s11682-012-9162-7.
159. Rowson S, and Duma SM. Brain Injury Prediction: Assessing the Combined Probability of Concussion Using Linear and Rotational Head Acceleration. *Ann Biomed Eng*. January 2013. doi:10.1007/s10439-012-0731-0.
160. Rowson S, and Duma SM. The Virginia Tech Response. *Ann Biomed Eng*. October 2012. doi:10.1007/s10439-012-0660-y.

161. Rowson S, Beckwith JG, Chu JJ, Leonard DS, Greenwald RM, and Duma SM. A Six Degree of Freedom Head Acceleration Measurement Device for Use in Football. *Journal of Applied Biomechanics*. 2011;27:8-14.
162. Rowson S, Brolinson G, Goforth M, Dietter D, and Duma S. Linear and angular head acceleration measurements in collegiate football. *J Biomech Eng*. 2009;131(6):061016. doi:10.1115/1.3130454.
163. Schnebel B, Gwin JT, Anderson S, and Gatlin R. In vivo study of head impacts in football: a comparison of National Collegiate Athletic Association Division I versus high school impacts. *Neurosurgery*. 2007;60(3):490-495. doi:10.1227/01.NEU.0000249286.92255.7F.
164. Schrouff J, Cremers J, Garraux G, Baldassarre L, Mourao-Miranda J, and Phillips C. Localizing and Comparing Weight Maps Generated from Linear Kernel Machine Learning Models. *IEEE Xplore*. June 2013:124-127. doi:10.1109/PRNI.2013.40.
165. Schrouff J, Rosa MJ, Rondina JM, Marquand AF, Chu C, Ashburner J, Phillips C, Richiardi J, and Mourão-Miranda J. PRoNTTo: pattern recognition for neuroimaging toolbox. *Neuroinformatics*. 2013;11(3):319-37. doi:10.1007/s12021-013-9178-1.
166. Schulz MR, Marshall SW, Mueller FO, Yang J, Weaver NL, Kalsbeek WD, and Bowling JM. Incidence and risk factors for concussion in high school athletes, North Carolina, 1996-1999. *Am J Epidemiol*. 2004;160(10):937-44. doi:10.1093/aje/kwh304.
167. Seeley WW, Menon V, Schatzberg AF, Keller J, Glover GH, Kenna H, Reiss AL, and Greicius MD. Dissociable intrinsic connectivity networks for salience processing and executive control. *J Neurosci*. 2007;27(9):2349-56. doi:10.1523/JNEUROSCI.5587-06.2007.

168. Shehzad Z, Kelly AM, Reiss PT, Gee DG, Gotimer K, Uddin LQ, Lee SH, Margulies DS, Roy AK, Biswal BB, Petkova E, Castellanos FX, and Milham MP. The resting brain: unconstrained yet reliable. *Cereb Cortex*. 2009;19(10):2209-29. doi:10.1093/cercor/bhn256.
169. Shenk TE, Robinson ME, Svaldi DO, Abbas K, Breedlove KM, Leverenz LJ, Nauman EA, and Talavage TM. fMRI of visual working memory in high school football players. *Dev Neuropsychol*. 2015;40(2):63-8. doi:10.1080/87565641.2015.1014088.
170. Shen T, Qiu M, Li C, Zhang J, Wu Z, Wang B, Jiang K, and Peng D. Altered spontaneous neural activity in first-episode, unmedicated patients with major depressive disorder. *Neuroreport*. 2014;25(16):1302-7. doi:10.1097/WNR.0000000000000263.
171. Shukla DK, Keehn B, and Müller RA. Regional homogeneity of fMRI time series in autism spectrum disorders. *Neurosci Lett*. 2010;476(1):46-51. doi:10.1016/j.neulet.2010.03.080.
172. Shultz SR, MacFabe DF, Foley KA, Taylor R, and Cain DP. Sub-concussive brain injury in the Long-Evans rat induces acute neuroinflammation in the absence of behavioral impairments. *Behavioural Brain Research*. 2012;229(1):145-152. doi:10.1016/j.bbr.2011.12.015.
173. Shumskaya E, Andriessen TM, Norris DG, and Vos PE. Abnormal whole-brain functional networks in homogeneous acute mild traumatic brain injury. *Neurology*. 2012;79(2):175-82. doi:10.1212/WNL.0b013e31825f04fb.
174. Slobounov SM, Gay M, Zhang K, Johnson B, Pennell D, Sebastianelli W, Horovitz S, and Hallett M. Alteration of brain functional network at rest and in response to YMCA

physical stress test in concussed athletes: RsfMRI study. *Neuroimage*. 2011;55(4):1716-27. doi:10.1016/j.neuroimage.2011.01.024.

175. Slobounov SM, Zhang K, Pennell D, Ray W, Johnson B, and Sebastianelli W. Functional abnormalities in normally appearing athletes following mild traumatic brain injury: a functional MRI study. *Exp Brain Res*. 2010;202(2):341-54. doi:10.1007/s00221-009-2141-6.

176. Smith SM, Fox PT, Miller KL, Glahn DC, Fox PM, Mackay CE, Filippini N, Watkins KE, Toro R, Laird AR, and Beckmann CF. Correspondence of the brain's functional architecture during activation and rest. *Proc Natl Acad Sci U S A*. 2009;106(31):13040-5. doi:10.1073/pnas.0905267106.

177. Smits M, Dippel DW, Houston GC, Wielopolski PA, Koudstaal PJ, Hunink MG, and van der Lugt A. Postconcussion syndrome after minor head injury: brain activation of working memory and attention. *Hum Brain Mapp*. 2009;30(9):2789-803. doi:10.1002/hbm.20709.

178. Snyder AZ, and Raichle ME. A brief history of the resting state: The Washington University perspective. *Neuroimage*. 2012;62(2):902-10. doi:10.1016/j.neuroimage.2012.01.044.

179. Sripada CS, Kessler D, Welsh R, Angstadt M, Liberzon I, Phan KL, and Scott C. Distributed effects of methylphenidate on the network structure of the resting brain: A connectomic pattern classification analysis. *NeuroImage*. 2013;81:213-221. doi:10.1016/j.neuroimage.2013.05.016.

180. Stein TD, Alvarez VE, and McKee AC. Chronic traumatic encephalopathy: a spectrum of neuropathological changes following repetitive brain trauma in athletes and military personnel. *Alzheimers Res Ther.* 2014;6(1):4. doi:10.1186/alzrt234.
181. Stern RA, Riley DO, Daneshvar DH, Nowinski CJ, Cantu RC, and McKee AC. Long-term consequences of repetitive brain trauma: chronic traumatic encephalopathy. *PM R.* 2011;3(10 Suppl 2):S460-7. doi:10.1016/j.pmrj.2011.08.008.
182. Stevens MC, Lovejoy D, Kim J, Oakes H, Kureshi I, and Witt ST. Multiple resting state network functional connectivity abnormalities in mild traumatic brain injury. *Brain Imaging Behav.* 2012;6(2):293-318. doi:10.1007/s11682-012-9157-4.
183. Stoffers D, Diaz BA, Chen G, den Braber A, van 't Ent D, Boomsma DI, Mansvelder HD, de Geus E, Van Someren EJ, and Linkenkaer-Hansen K. Resting-State fMRI Functional Connectivity Is Associated with Sleepiness, Imagery, and Discontinuity of Mind. *PLoS One.* 2015;10(11):e0142014. doi:10.1371/journal.pone.0142014.
184. Stulemeijer M, Vos PE, van der Werf S, van Dijk G, Rijpkema M, and Fernández G. How mild traumatic brain injury may affect declarative memory performance in the post-acute stage. *J Neurotrauma.* 2010;27(9):1585-95. doi:10.1089/neu.2010.1298.
185. Svaldi DO, McCuen EC, Joshi C, Robinson ME, Nho Y, Hannemann R, Nauman EA, Leverenz LJ, and Talavage TM. Cerebrovascular reactivity changes in asymptomatic female athletes attributable to high school soccer participation. *Brain Imaging and Behavior.* January 2016:1-15. doi:10.1007/s11682-016-9509-6.
186. Swartz EE, Broglio SP, Cook SB, Cantu RC, Ferrara MS, Guskiewicz KM, and Myers JL. Early Results of a Helmetless-Tackling Intervention to Decrease Head Impacts in Football Players. *J Athl Train.* December 2015. doi:10.4085/1062-6050-51.1.06.

187. Talavage TM, Nauman E, Breedlove EL, Yoruk U, Dye AE, Morigaki K, Feuer H, and Leverenz LJ. Functionally-Detected Cognitive Impairment in High School Football Players Without Clinically-Diagnosed Concussion. *J Neurotrauma*. 2010;31(4):327-338. doi:10.1089/neu.2010.1512.
188. Tang L, Ge Y, Sodickson DK, Miles L, Zhou Y, Reaume J, and Grossman RI. Thalamic resting-state functional networks: disruption in patients with mild traumatic brain injury. *Radiology*. 2011;260(3):831-40. doi:10.1148/radiol.11110014.
189. Tomasi D, and Volkow ND. Resting functional connectivity of language networks: characterization and reproducibility. *Mol Psychiatry*. 2012;17(8):841-54. doi:10.1038/mp.2011.177.
190. Tsushima WT, Geling O, Arnold M, and Oshiro R. Are There Subconcussive Neuropsychological Effects in Youth Sports? An Exploratory Study of High- and Low-Contact Sports. *Applied Neuropsychology: Child*. March 2016. doi:10.1080/21622965.2015.1052813.
191. Urban JE, Davenport EM, Golman AJ, Maldjian JA, Whitlow CT, Powers AK, and Stitzel JD. Head impact exposure in youth football: high school ages 14 to 18 years and cumulative impact analysis. *Ann Biomed Eng*. 2013;41(12):2474-2487. doi:10.1007/s10439-013-0861-z.
192. Vapnik V. *The Nature of Statistical Learning Theory*. Springer Science & Business Media; 2013.
193. Vapnik V. *The Nature of Statistical Learning Theory*. Springer Science & Business Media; 2013.

194. Viano DC, and Pellman EJ. Concussion in professional football: biomechanics of the striking player--part 8. *Neurosurgery*. 2005;56(2):266-80; discussion 266-80.
195. Viano DC, Casson IR, and Pellman EJ. Concussion in professional football: biomechanics of the struck player--part 14. *Neurosurgery*. 2007;61(2):313-27; discussion 327-8. doi:10.1227/01.NEU.0000279969.02685.D0.
196. Viano DC, Casson IR, Pellman EJ, Bir CA, Zhang L, Sherman DC, and Boitano MA. Concussion in professional football: comparison with boxing head impacts--part 10. *Neurosurgery*. 2005;57(6):1154-72; discussion 1154-72.
197. Viano DC, Casson IR, Pellman EJ, Zhang L, King AI, and Yang KH. Concussion in professional football: brain responses by finite element analysis: part 9. *Neurosurgery*. 2005;57(5):891-916; discussion 891-916.
198. Viano DC, Pellman EJ, Withnall C, and Shewchenko N. Concussion in professional football: performance of newer helmets in reconstructed game impacts--Part 13. *Neurosurgery*. 2006;59(3):591-606; discussion 591-606. doi:10.1227/01.NEU.0000231851.97287.C2.
199. Vincent JL, Kahn I, Snyder AZ, Raichle ME, and Buckner RL. Evidence for a frontoparietal control system revealed by intrinsic functional connectivity. *J Neurophysiol*. 2008;100(6):3328-42. doi:10.1152/jn.90355.2008.
200. Voss MW, Weng TB, Burzynska AZ, Wong CN, Cooke GE, Clark R, Fanning J, Awick E, Gothe NP, Olson EA, McAuley E, and Kramer AF. Fitness, but not physical activity, is related to functional integrity of brain networks associated with aging. *NeuroImage*. 2016;131:113-125. doi:10.1016/j.neuroimage.2015.10.044.

201. Wang X, Jiao Y, Tang T, Wang H, and Lu Z. Altered regional homogeneity patterns in adults with attention-deficit hyperactivity disorder. *Eur J Radiol.* 2013;82(9):1552-7. doi:10.1016/j.ejrad.2013.04.009.
202. White H. A heteroskedasticity-consistent covariance matrix estimator and a direct test for heteroskedasticity. *Econometrica: Journal of the Econometric Society.* 1980;48(4):817-838.
203. Wilcox BJ, Beckwith JG, Greenwald RM, Raukar NP, Chu JJ, McAllister TW, Flashman LA, Maerlender AC, Duhaime A, and Crisco JJ. Biomechanics of head Impacts associated with diagnosed concussion in female collegiate ice hockey Players. *Journal of Biomechanics.* April 2015. doi:10.1016/j.jbiomech.2015.04.005.
204. Winkler AM, Ridgway GR, Webster MA, Smith SM, and Nichols TE. Permutation inference for the general linear model. *Neuroimage.* 2014;92:381-97. doi:10.1016/j.neuroimage.2014.01.060.
205. Withnall C, Shewchenko N, Gittens R, and Dvorak J. Biomechanical investigation of head impacts in football. *Br J Sports Med.* 2005;39 Suppl 1:i49-57. doi:10.1136/bjism.2005.019182.
206. Wong RH, Wong AK, and Bailes JE. Frequency, Magnitude, and Distribution of Head Impacts in Pop Warner Football: The Cumulative Burden. *Clinical Neurology and Neurosurgery.* 2014;118(0):1-4. doi:10.1016/j.clineuro.2013.11.036<http://www.sciencedirect.com/science/article/pii/S030384671300509X>.
207. Wong RH, Wong AK, and Bailes JE. Frequency, Magnitude, and Distribution of Head Impacts in Pop Warner Football: The Cumulative Burden. *Clinical Neurology and*

Neurosurgery. 2014;118(0):1-4.

doi:10.1016/j.clineuro.2013.11.036<http://www.sciencedirect.com/science/article/pii/S030384671300509X>.

208. Wu LC, Nangia V, Bui K, Hammor B, Kurt M, Hernandez F, Kuo C, and Camarillo DB. In Vivo Evaluation of Wearable Head Impact Sensors. *Ann Biomed Eng*. August 2015. doi:10.1007/s10439-015-1423-3.

209. Xia S, Foxe JJ, Sroubek AE, Branch C, and Li X. Topological organization of the "small-world" visual attention network in children with attention deficit/hyperactivity disorder (ADHD). *Front Hum Neurosci*. 2014;8:162. doi:10.3389/fnhum.2014.00162.

210. Xu J, Moeller S, Auerbach EJ, Strupp J, Smith SM, Feinberg DA, Yacoub E, and Uğurbil K. Evaluation of slice accelerations using multiband echo planar imaging at 3T. *NeuroImage*. 2013;83:991-1001. doi:10.1016/j.neuroimage.2013.07.055.

211. Yard EE, and Comstock RD. Injuries sustained by pediatric ice hockey, lacrosse, and field hockey athletes presenting to United States emergency departments, 1990-2003. *J Athl Train*. 2006;41(4):441-9.

212. Yeo RA, Gasparovic C, Merideth F, Ruhl D, Doezema D, and Mayer AR. A longitudinal proton magnetic resonance spectroscopy study of mild traumatic brain injury. *J Neurotrauma*. 2011;28(1):1-11. doi:10.1089/neu.2010.1578.

213. Yuh EL, Hawryluk GW, and Manley GT. Imaging concussion: a review. *Neurosurgery*. 2014;75 Suppl 4:S50-63. doi:10.1227/NEU.0000000000000491.

214. Yu R, Hsieh MH, Wang HL, Liu CM, Liu CC, Hwang TJ, Chien YL, Hwu HG, and Tseng WY. Frequency dependent alterations in regional homogeneity of baseline brain

activity in schizophrenia. *PLoS One*. 2013;8(3):e57516.

doi:10.1371/journal.pone.0057516.

215. Zang Y, Jiang T, Lu Y, He Y, and Tian L. Regional homogeneity approach to fMRI data analysis. *NeuroImage*. 2004;22(1):394-400. doi:10.1016/j.neuroimage.2003.12.030.

216. Zang YF, He Y, Zhu CZ, Cao QJ, Sui MQ, Liang M, Tian LX, Jiang TZ, and Wang YF. Altered baseline brain activity in children with ADHD revealed by resting-state functional MRI. *Brain Dev*. 2007;29(2):83-91. doi:10.1016/j.braindev.2006.07.002.

217. Zhang K, Johnson B, Gay M, Horovitz SG, Hallett M, Sebastianelli W, and Slobounov S. Default mode network in concussed individuals in response to the YMCA physical stress test. *J Neurotrauma*. 2012;29(5):756-65. doi:10.1089/neu.2011.2125.

218. Zhang K, Johnson B, Pennell D, Ray W, Sebastianelli W, and Slobounov S. Are functional deficits in concussed individuals consistent with white matter structural alterations: combined FMRI & DTI study. *Exp Brain Res*. 2010;204(1):57-70.

doi:10.1007/s00221-010-2294-3.

219. Zhang L, Yang KH, and King AI. Comparison of brain responses between frontal and lateral impacts by finite element modeling. *J Neurotrauma*. 2001;18(1):21-30.

doi:10.1089/089771501750055749.

220. Zhang L, Yang KH, and King AI. A proposed injury threshold for mild traumatic brain injury. *J Biomech Eng*. 2004;126(2):226-36.

221. Zhang MR, Red SD, Lin AH, Patel SS, and Sereno AB. Evidence of cognitive dysfunction after soccer playing with ball heading using a novel tablet-based approach. *PLoS One*. 2013;8(2):e57364. doi:10.1371/journal.pone.0057364.

222. Zhan J, Gao L, Zhou F, Bai L, Kuang H, He L, Zeng X, and Gong H. Amplitude of Low-Frequency Fluctuations in Multiple-Frequency Bands in Acute Mild Traumatic Brain Injury. *Front Hum Neurosci*. 2016;10:27. doi:10.3389/fnhum.2016.00027.
223. Zhan J, Gao L, Zhou F, Kuang H, Zhao J, Wang S, He L, Zeng X, and Gong H. Decreased Regional Homogeneity in Patients With Acute Mild Traumatic Brain Injury: A Resting-State fMRI Study. *J Nerv Ment Dis*. September 2015. doi:10.1097/NMD.0000000000000368.
224. Zhou Y, Lui YW, Zuo XN, Milham MP, Reaume J, Grossman RI, and Ge Y. Characterization of thalamo-cortical association using amplitude and connectivity of functional MRI in mild traumatic brain injury. *J Magn Reson Imaging*. 2014;39(6):1558-1568. doi:10.1002/jmri.24310.
225. Zhou Y, Milham MP, Lui YW, Miles L, Reaume J, Sodickson DK, Grossman RI, and Ge Y. Default-mode network disruption in mild traumatic brain injury. *Radiology*. 2012;265(3):882-92. doi:10.1148/radiol.12120748.
226. Zhou Y, Yu F, Duong TQ, and Alzheimer's Disease Neuroimaging Initiative. White matter lesion load is associated with resting state functional MRI activity and amyloid PET but not FDG in mild cognitive impairment and early Alzheimer's disease patients. *J Magn Reson Imaging*. 2015;41(1):102-9. doi:10.1002/jmri.24550.
227. Zou QH, Zhu CZ, Yang Y, Zuo XN, Long XY, Cao QJ, Wang YF, and Zang YF. An improved approach to detection of amplitude of low-frequency fluctuation (ALFF) for resting-state fMRI: fractional ALFF. *J Neurosci Methods*. 2008;172(1):137-41. doi:10.1016/j.jneumeth.2008.04.012.

228. Zuckerman SL, Kerr ZY, Yengo-Kahn A, Wasserman E, Covassin T, and Solomon GS. Epidemiology of Sports-Related Concussion in NCAA Athletes From 2009-2010 to 2013-2014. *The American Journal of Sports Medicine*. September 2015:0363546515599634. doi:10.1177/0363546515599634.